Institut für Physik
Arbeitsgruppe Nichtlineare Dynamik

Manipulations of spike trains and their impact on synchrony analysis

Dissertation
zur Erlangung des akademischen Grades
"doctor rerum naturalium"
(Dr. rer. nat.)
in der Wissenschaftsdisziplin "Theoretische Physik"

Eingereicht an der
Mathematisch-Naturwissenschaftlichen Fakultät
der Universität Potsdam

von
Antonio Pazienti

Postdam, den 28.11.2007

Elektronisch veröffentlicht auf dem
Publikationsserver der Universität Potsdam:
http://opus.kobv.de/ubp/volltexte/2008/1744/
urn:nbn:de:kobv:517-opus-17447
[http://nbn-resolving.de/urn:nbn:de:kobv:517-opus-17447]

Summary

The interaction between neuronal cells can be identified as the computing mechanism of the brain. Neurons are complex cells with a rich dynamics. However, they do not operate in isolation, but constantly exchange information through modulation of the emission of action potentials and formation of synchronous ensembles. By jointly increasing their firing rate, groups of neurons compute sensorial information more reliably than single cells individually. However, there is strong evidence that also the precise timing (i.e. in the millisecond scale) of action potentials emitted by different neurons plays a major role. This mechanism has been shown to explain e.g. stimulus expectancy. Time dependencies (referred to as *correlations*) between neurons seem to be a key mechanism for information processing. This challenging hypothesis predicts that assemblies of synchronized neurons may ultimately explain brain functions at all levels.

In order to answer the challenging question of how the brain computes, a fundamental methodological step is constituted by recording large sets of single neurons in parallel. Techniques that allow this task, such as arrays of extracellular electrodes, have become available in the last couple of decades, and are meanwhile widely employed. They allow the simultaneous recording of tens to hundreds of neurons. Such technological improvements yet need to be accompanied by analogous advancements in the pre-processing of the large volumes of acquired data and in data analysis techniques. Major issues in the analysis of correlation between multiple parallel recordings involve the correct isolation and identification of individual neurons –a procedure referred to as *spike sorting*. Spike sorting is a fundamental step in the treatment of extracellular electrophysiological data, however it is subject to errors whose effects are poorly studied. Another important issue is the availability of distributions for assessing statistical significance. Making assumptions on the statistics of spike trains requires long recordings and repeated measurements, but neurophysiological data often do not fulfill these requirements. Algorithms are used for creating surrogate distributions by selectively destroying some features of the data while preserving their main structure. However the effectiveness of algorithms in generating surrogates yet needs to be ultimately established.

In this dissertation I present my theoretical work that approaches these problems by answering the following questions: how is the correlation analysis of multiple neuronal processes affected by spike sorting errors? What kind of strategies can be followed to reduce the drawbacks of spike sorting and obtain more reliable results? How effective are methods for generating surrogate data in destroying correlations? The two complementary strategies I followed are both founded on the manipulation of point processes under rigorous analytical control. In an extensive study I modeled the effect of spike sorting on correlated spike trains by corrupting them with realistic failures. Analytical expressions were derived to compare the outcomes of two different correlation analyses on the original and on the corrupted processes. The statistical model of spike sorting errors I propose is of general application, and can be used to evaluate and improve other data analysis methods. In another study I investigated the effectiveness of methods for creating surrogate distributions for statistical significance. These methods destroy correlations in the data by displacing coincident spikes around their original position (referred to as dithering). I contrasted different strategies of spike dithering (namely dithering 1 or both neurons)

against two established methods of counting coincident patterns: by partitioning the temporal axis in disjunct bins (Disjunct Binning), and by integrating the coincidence count over multiple relative shifts of the spike trains (Multiple Shift).

My results show that coincidence patterns of multiple parallel spike trains are severely affected by spike sorting. Synchronization analyses underestimate in most cases the underlying correlation due to spike sorting errors. This holds true even when only false positive errors –i.e. spikes assigned to a neuron although they belong to other neurons or they are noise artifacts– affect the data. However, false negative errors –i.e. erroneously un- or mis-classified spikes– have a more severe impact on the significance than false positive errors. This result suggests that sorting strategies characterized by classifying only "good" spikes (conservative strategies) are prone to more inaccurate estimations than "tolerant" strategies. Furthermore, the effectiveness of spike dithering in creating surrogate data strongly depends on the dithering method and on the method of counting coincidences. I provide analytical expressions of the probability of coincidence detection after dithering. These expressions reduce to simple closed forms for the case where the dithering window equals the coincidence detection window. Under these constraints I derived limit values for the effectiveness of dithering in destroying correlations. The intuition that in such a case the 50% of the coincidences are destroyed is confirmed only for the case of 1-neuron dithering and disjunct binning. For 2-neuron dithering and the multiple shift method only less than 25% of coincidences can be destroyed, while 2-neuron dithering with disjunct binning achieves the best results with $\sim 60\%$ of the coincidences destroyed.

This work provides new insights into the methodologies to identify correlations in large-scale neuronal recordings and to evaluate their statistical significance. The rigorous conclusions of this work provide practical guidelines for the study of synchrony as a computing mechanism of the brain.

Zusammenfassung

Die Informationsverarbeitung im Gehirn erfolgt maßgeblich durch interaktive Prozesse von Nervenzellen. Nervenzellen zeigen eine komplexe Dynamik ihrer chemischen und elektrischen Eigenschaften. Die Informationsweiterleitung erfolgt jedoch nicht aufgrund des Wirkens isolierter Neurone, sondern als Ergebnis der Interaktion vieler Neurone durch den Austausch von elektrischen Aktionspotentialen, den sogenannten *Spikes*. Das Konzept der Populationskodierung postuliert, dass Gruppen von Neuronen durch die simultane Erhöhung ihrer Feuerraten sensorische Informationen mit weitaus höherer Geschwindigkeit und Zuverlässigkeit übertragen und somit eine schnellere und tiefere Verarbeitung der Informationen ermöglichen. Es gibt aber auch deutliche Hinweise darauf, dass das Gehirn eine zusätzliche Art der Informationskodierung nutzt. Nach der Theorie der zeitlich präzisen Koordination von Aktionspotentialen unterschiedlicher Zellen im Gehirn formieren sich funktionale Gruppen, sogenannte Zellverbände (cell assemblies), indem sie ihre Aktionspotentiale mit einer sehr hohen zeitlichen Genauigkeit von nur wenigen Millisekunden synchronisieren. So konnte z. B. empirisch gezeigt werden, dass dieser Mechanismus mit dem Ereignis der einem Stimulus vorausgehende Erwartung in Zusammenhang steht. Die zeitlich präzise Korrelation der Aktivität von Neuronen scheint also ein Schlüsselmechanismus der Informationsverarbeitung zu sein. Aus diesem Befund lässt sich die Hypothese ableiten, dass mit Hilfe von Gruppen synchronisierter Neurone letztlich die Funktionsweise des Gehirns auf allen Ebenen erklärt werden kann.

Um die schwierige Frage nach der genauen Funktionsweise des Gehirns zu beantworten, ist es daher notwendig, die Aktivität vieler Neuronen gleichzeitig zu messen. Die technischen Voraussetzungen hierfür sind in den letzten Jahrzehnten geschaffen worden, insbesondere durch die Entwicklung und Optimierung von elektrophysiologischen Meßmethoden, z. B. Multielektrodensyteme, die heute eine breite Anwendung finden. Sie ermöglichen die simultane extrazelluläre Ableitung von bis zu mehreren hunderten Kanälen. Diese technologischen Entwicklungen stellen aber auch neue Anforderungen an die Vorverarbeitung der enorm gewachsenen Datenmengen und erfordern die Entwicklung völlig neuer Datenanalysetechniken. Die Voraussetzung für die Korrelationsanalyse von vielen parallelen Messungen ist zunächst die korrekte Erkennung und Zuordnung der Aktionspotentiale einzelner Neurone, sogenannter *single units*, ein Verfahren, das als Spikesortierung (*spike sorting*) bezeichnet wird. Die Spikesortierung stellt einen fundamentalen Schritt der weiteren statistischen Datenauswertung dar. Gleichwohl sind die hierfür verwendeten Methoden bekanntermassen anfällig für Fehler, deren Auswirkungen auf die Genauigkeit der auf ihnen aufbauenden Korrelationsanalysen nur wenig untersucht sind. Eine weitere Herausforderung ist die statistisch korrekte Bewertung von empirisch beobachteten Korrelationen. Für die Signfikanzabschätzung werden gute Modelle für die zufallsbasiert zu erwartenden Verteilungen von Korrelationen benötigt. Hierzu werden künstliche Daten erzeugt, sogenannte Surrogatdaten, in denen bestimmte statistische Eigenschaften gezielt zerstört werden, während andere erhalten bleiben. Allerdings ist die Effektifität dieser Methode bislang kaum untersucht.

Mit dieser Dissertationsschrift lege ich eine theoretische Arbeit vor, die sich der Vorverarbeitung der Daten durch Spikesortierung und ihrem Einfluss auf die Genauigkeit der statistischen Auswertungsverfahren sowie der Effektivität zur Erstellung von Surrogar-

daten für die statistische Signifikanzabschätzung auf Korrelationen widmet. Insbesondere stelle ich folgende Fragen: Wie wird die Korrelationsanalyse von multi-variaten neuronalen Punktprozessen durch Spikesortierung beeinflusst? Welche Strategien können zur Reduzierung der Nachteile von Spikesortierung aufgezeigt werden, um damit zuverlässligere Ergebnisse zu erhalten? Wie effektiv sind Surrogatmethoden zur gezielten Zerstörung von Korrelationen? Ich verwende hier zwei komplementäre Strategien, die beide auf der analytischen Berechnung von Punktprozessmanipulationen basieren. In einer ausführlichen Studie haben ich den Effekt von Spikesortierung in mit realistischen Fehlern behafteten korrelierten Spikefolgen modeliert. Zum Vergleich der Ergebnisse zweier unterschiedlicher Methoden zur Korrelationsanalyse auf den gestörten, sowie auf den ungestörten Prozessen, leitete ich die entsprechenden analytischen Formeln her. Ich präsentiere ein statistisches Modell von Spikesortierungsfehlern, das zur generellen Anwendung geeignet ist und daher auch zur Auswertung und Verbesserung von weiteren Methoden der Datenanalyse genutzt werden kann. In einer weiteren Studie untersuchte ich die Effektivität einer Surrogatmethode, das sogenannte Dithering, welches paarweise Korrelationen zerstört, in dem es koinzidente Spikes von ihrer ursprünglichen Position in einem kleinen Zeitfenster verrückt. Ich vergleiche hierzu zwei verschiedene Strategien von Dithering: die sogenannte Ein-Neuron-Dithermethode, in dem nur die Spikes eines der beiden Neurone zeitlich verschoben werden, und die Zwei-Neuronen-Dithermethode, wobei die Spikefolgen beider Neurone manipuliert werden. Anschließend werden auf jede der beiden Methoden zwei verschiedene Arten der Koinzidenzzählung angewendet: Bei der ersten wird die zeitliche Achse in disjunkte Zeitsegmente unterteilt (*Disjunct Binning*). Die zweite Methode (*Multiple Shift Methode*) basiert auf der Ermittlung der Anzahl der Koinzidenzen über mehrfache relative Verschiebungen der Spikefolgen untereinander.

Meine Ergebnisse zeigen, dass koinzidente Aktivitätsmuster multipler Spikefolgen durch Spikeklassifikation erheblich beeinflusst werden. Das ist der Fall, wenn Neuronen nur fälschlicherweise Spikes zugeordnet werden, obwohl diese anderen Neuron zugehörig sind oder Rauschartefakte sind (falsch positive Fehler). Jedoch haben falsch-negative Fehler (fälschlicherweise nicht-klassifizierte oder missklassifizierte Spikes) einen weitaus grösseren Einfluss auf die Signifikanz der Korrelationen. Dieses Ergebnis zeigt, dass eine konservative Klassifizierung (hohe Signifikanzschwelle für eine Zuordnung zu einem Neuron) zu einer ungenaueren Abschätzung führt als tolerante Strategien (niedrige Signifikanzsschwelle). Weiterhin zeige ich, dass die Effektivität von Spike-Dithering zur Erzeugung von Surrogatdaten sowohl von der Dithermethode als auch von der Methode zur Koinzidenzzählung abhängt. Für die Wahrscheinlichkeit der Koinzidenzerkennung nach dem Dithern stelle ich analytische Formeln zur Verfügung. Für den Spezialfall, in der die Größe des Ditherfensters sich mit der des Koinzidenzdetektionsfensters deckt, reduzieren sich die Gleichungen zu einfachen, geschlossenen Formen. Unter dieser Bedingung erhält man Grenzwerte für die Effektivität des Ditherns zur Korrelationszerstörung. Die intuitive Annahme, dass dabei 50 % der Koinzidenzen zerstört werden, gilt ausschließlich für die Ein-Neuronen-Dither-Methode mit disjunkten Zeitsegmenten. Beim Zwei-Neuronen-Dithern mit der Multiple Shift Methode können nur weniger als 25 % der Koinzidenzen zerstört werden, wohingegend das Zwei-Neuronen-Dithern mit disjunkten Zeitsegmenten das beste Ergebnis erzielte ($\sim 60\%$).

Die vorliegende Arbeit bietet neue Einblicke in die Methoden zur Korrelationsanalyse auf multi-variaten Punktprozessen mit einer genauen Untersuchung von unterschiedlichen statistischen Einsflüssen auf die Signifikanzabschätzung. Für die praktische Anwendung ergeben sich Leitlinien für den Umgang mit Daten zur Synchronizitätsanalyse.

Contents

Roadmap

Here is a concise description of the content of each of the sections of this dissertation. Its first part (**Sections 1-5**) is a review of the current status of theories and methodologies that deal with the investigation of neuronal synchrony. The second part of this dissertation (**Sections 6-8**) reproduce the publications that constitute my contribution to the topic.

In **Section 1** the concept of neuronal correlation is introduced and embedded in the framework of the experimental results. They show evidence of synchronization of neurons in a millisecond time scale. Current hypotheses are discussed. It is concluded that in order to test these hypotheses it is crucial to record the activity of large portions of the network simultaneously.

Section 2 and **3** give an overview of the current status of the techniques for recording multiple neurons in parallel (**Sec. 2**) and for extracting single units activity from the recordings (referred to as spike sorting, **Sec. 3**). The most common approaches and algorithms for spike sorting are reviewed, together with the related problems and the type of errors that can affect their outcomes. It is concluded that current techniques urgently need to be supported by advancements in the methods for handling the data and for correlation analysis. Major issues are in particular the correct identification of the activity of single neurons and the assessment of the significance of correlation.

Sections 4 and **5** introduce the statistical tools for spike train correlation analysis. The mathematical formalism of point processes is presented (**Sec. 4**), and methods for measuring correlations between multiple spike trains are explained (**Sec. 5**). Further methods for assessing statistical significance based on surrogate distributions are introduced as well.

In **Sections 6-8** two aspects in close relation are investigated: the relationship between pre-processing of multi-unit recordings and measuring synchrony and the issue of estimating the statistical significance of the synchrony. My work on the modification of multiple spike trains with a statistical model of sorting errors in order to study analytically the effects on different correlation methods is presented in **Sections 6** and **7**. **Section 8** is a rigorous study of the effectiveness of different algorithms in creating appropriate surrogate data for assessing statistical significance.

1 Neuronal Correlations

A neuronal cell, or neuron, is the elementary computing unit of the central nervous system. Neurons do not act in isolation, but rather it is the network composed by the neurons which is responsible for information processing (Abeles, 1991; Eggermont, 1990; Buzsáki and Draguhn, 2004). Communication exchange between neurons takes place by way of emission of action potentials (or *spikes*) that travel through the network. Many functions of neuronal networks are well known. They include e.g. the processing of sensory input, the storing and accessing of memory, and the motor output control. However, structure and dynamical properties of such networks need yet to be uncovered.

Groups of neurons are able to jointly increase their frequency of spike emission in order to undertake a task. Mountcastle (1957) introduced after his observations in the somato-sensory cortex the concept of *cortical columns*, i.e. vertically arranged and heavily interconnected groups of cells spreading all six layers of cortex. Comparable observations were made by Hubel and Wiesel (1968), who showed that in primary visual cortex a large proportion of the neurons belonging to a cortical column increases its firing rate in association with a particular property of the presented visual stimulus (referred to as preferred stimulus), e.g. to the the angle of inclination of a bar in the receptive field. Furthermore, spatially adjacent columns are tuned to complementary orientations, such that within $\sim 1\,\mathrm{mm}$ a complete representation of all orientations in the visual field is built up (orientation map). Another example of the coding performed by groups of neurons is the so-called population vector, introduced by Georgopoulos et al. (1986). Here single neurons in motor cortex, whose spiking activity was shown to be broadly enhanced for movements in different directions, when considered in combination, i.e. when the response of the *population* is taken, "predict" the actual direction of movement with much higher accuracy.

However, there is emerging evidence that populations of neurons are also able to synchronize their activity in a millisecond time scale and that *synchrony* plays a role in the information processing. In the work of Riehle et al. (1997) correlations between pairs of simultaneously recorded neurons in primary motor cortex of monkeys were observed to occur in a time scale of $1 - 5\,\mathrm{ms}$ in relation with signal expectancy and during epochs in which the firing rate did not show any significant modulation. As a consequence of these and other results, synchrony was interpreted to be related to internal (i.e. not behaviorally relevant) information computing (see e.g. Engel et al., 2001). It has also been proposed that synchrony is a relevant mechanism for another computational task, the so-called *binding problem*, i.e. the issue in vision theories of perceiving elementary distinct parts as belonging to the same object. According to this assumption, neurons are able to synchronize in a context-dependent way, such that subset of correlated neurons represent different object features at different points in time (Singer et al., 1997; Shadlen and Movshon, 1999). Since a neuron may participate in several correlated groups at once, this mechanism offers the advantage to allow perceptual grouping of features in a very time-efficient fashion.

However the role of neuronal correlations and whether they represent a complementary computing mechanism independent of the modulation of the firing rate is still a matter of debate (see discussion in Sec. 2 on the related topic of analyzing simultaneous recordings

of many neurons). Many authors debated the concept of *cell assembly*, postulated by D. Hebb as a group of

> [...] association-area cells which can act briefly as a closed system after stimulation has ceased; this prolongs the time during which the structural changes of learning can occur and constitutes the simplest instance of a representative process (image or idea) (Hebb, 1949, Ch. 4. See also Harris, 2005; Gerstein et al., 1989; Singer et al., 1997).

According to von der Malsburg (1981) "a cell assembly is a set of neurons cross-connected such that the whole set is brought to become simultaneously active upon activation of appropriate subsets which have to be sufficiently similar to the assembly to single it out from overlapping others". This idea implies that an assembly is constituted by a population of neurons that can be "ignited" by some sufficient spatio-temporal input and only then acts as a functional unit. Indeed, the common view of cell assemblies is that, in contrast with the cortical columns in visual and neuronal populations in motor cortex, where correlated populations are anatomically (i.e. topographically) well defined, the neurons participating in an assembly are not necessarily spatially co-localized in the brain. Instead, they join their activity in a function-dependent fashion to achieve the required computational task (referred to as *functional connectivity*, Vaadia et al., 1995).

A broad scenario proposed by Abeles (1991) embeds the postulation of cell assembly in the concept of *synfire chains*. Starting with the observation that neurons are connected by converging and diverging pathways, the author proposed the existence of chains of groups (sets) of neurons as a computing mechanism of the brain. Each set is composed of serially connected neurons, and each neuron belonging to a set branch out its synapses to a large number of neurons in the next set of the chain and receive many connections from neurons in the previous set. When one set is ignited by an external stimulus, the whole chain becomes active, processes the stimulus and eventually produces an outcome.

The compelling ideas discussed in this section are still matter of experimental and theoretical research in computational neuroscience. The central goal is to gain knowledge of the brain mechanisms for information processing. The sections 2-5 of this dissertation are devoted to illustrate how this task is being approached.

2 Multi-unit recordings of neuronal activity

> Recording from every neuron in the bran is an unreasonable goal. On the other hand, recording from statistically representative samples of identified neurons from several local areas while minimally interfering with brain activity is feasible with currently available and emerging technologies and indeed is a high-priority goal in system neuroscience (Buzsáki, 2004).

Neurons have shown to synchronize in the millisecond time scale in relation to experimental protocols (see e.g. Riehle et al., 1997). However, the actual mechanisms of the synchronization of large neural networks have yet to be identified. The only way to detect the signature of these mechanisms is to record simultaneously the activity of many neurons. Indeed, environment and internal brain processes condition the brain status and modify it in an uncontrollable way during experiments, making the traditional practice of measuring a single cell and pooling over different trials unjustified.

The activity of a neuron can be exactly monitored by recording it *intracellularly*, i.e. by inserting a glass micropipette into the cell soma and measuring differentially the potential inside and outside the cell's membrane. However, recording intracellularly is hard to achieve *in vivo* (i.e. with awake animals) and for long recording sessions. Furthermore, extending this technique for collecting the activity of populations of neurons is difficult, and might even be not feasible. *Extracellular* recording techniques offer the advantage of allowing i) more stable recordings in vivo without the risk of "losing" the signal and ii) the simultaneous recording of several cells in the surroundings (*multi-unit recordings*).

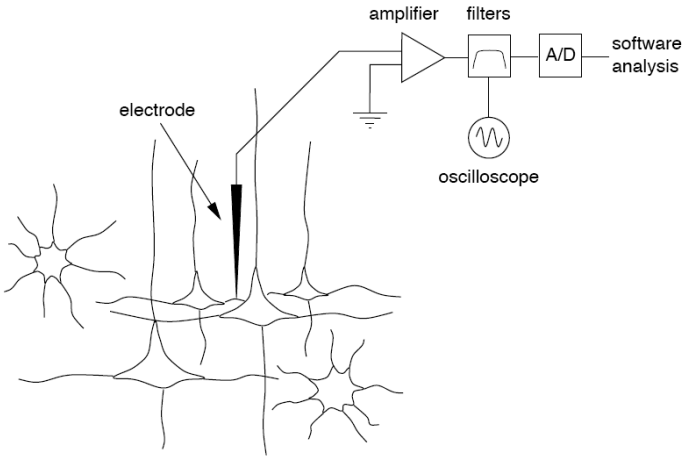

Figure 1: Schematic representation of extracellular recordings setup (from Lewicki, 1998)

The extracellular electrode consist typically of an electrically isolated wire, ending with a tip of variable size (of the order of tens of μm). When action potentials are generated and/or traverse axons or dendrites, the electrical fields generated in the extracellular medium are detected. Exact shape and size of the tip determine the volume the electrode records from. Due to the high density of the neurons (especially in the neocortex, see e.g. Abeles, 1991) up to tens of neurons can be "perceived" from a single electrode. When

action potentials are emitted by cells located in the close vicinity of the electrode tip a clear modulation of the field is observed, whereas the amplitude of spikes generated in neurons more distant from the recording site decreases with their distance, eventually contributing to the "noisiness" of the signal. This latter, due also to measurement noise and amplification stages, appears indeed quite noisy and is characterized by a complex frequency spectrum. The identification of individual neurons and the classification of the spikes are a technical challenge that requires a first data processing step, referred to as spike sorting (see Sec. 3).

Another advantage offered by recording extracellularly is the possibility of using more than one electrode at the same time, thus minimizing also damage of the tissue. Such arrays of electrodes are meanwhile in use in many laboratories, and multi-unit recordings of up to one hundred neurons can be relatively easily performed. In a typical experimental setup the inter-electrode distance is of the order of $\sim 100\mu$m. As the field generated by one neuron is assumed, given typical tip impedances, not to be detectable by two different electrodes located at this distance, individual wires of a multi-electrode array record different (groups of) cells that can be as far as a few millimeters away from each other. This technique allows to record e.g. a horizontal portion of the cortex (two dimensional arrays), or at different depths spanning all cortical layers (laminar recordings).

An issue that arises when recording with extracellular electrodes, especially when a low impedance allows to detect a large number of cells, is that spikes from different neurons may have a similar shape. To alleviate this problem one may use electrodes composed of several wires bundled together, referred to as multi-trodes. The most common examples are stereo-trodes (two recording tips) and tetrodes (four tips). The advantage in this case is that the different tips, being very close to each other, detect the fields of the same neurons, however from slightly different spatial positions. The redundant information obtained this way can be exploited for classifying spikes with similar shape more accurately. Finally, it is also possible to distribute multi-trodes in arrays and combine the advantages of multi-electrode recordings with good spike sorting performances.

We have seen in this section that it is now possible to record populations of neurons large enough to constitute a representative sample of the entire network. The next section describes the pre-processing stage needed to extract and store the activity of the different neurons from the multi-unit recordings.

3 Spike sorting

Spike sorting is a necessary step for those, who aim at reconstructing the activity of multiple single neurons from multi-unit extracellular recordings (Lewicki, 1998). Due to the difficulty of this task, the specificities of different brain areas, and although electrode arrays provide recordings of large numbers of cells (see previous section) and big amounts of data have to be processed per recording session, there is no standard way of performing spike sorting. Its outcomes are often sorter-dependent and hard to compare and/or reproduce (Harris et al., 2000). In this section we will provide a brief overview of the main approaches to spike sorting and comment on some of the issues experimenters have to deal with.

3.1 Supervised spike sorting

Spike sorting typically consists of two stages: first, spike waveforms originating from different neurons are identified and separated from the background extracellular noise; second, spikes are classified, i.e. assigned to putative neurons. The fundamental assumptions in spike sorting is that the shape of the spikes from a particular neuron is stationary (i.e. does not change in time), and that spikes from different neurons have different shapes. This is motivated by the fact that the spatial orientation and/or the distances of different detected neurons are different. This task requires computer algorithms and visualization software as well as human supervision. A variety of algorithms are meanwhile available for spike sorting (see e.g. Lewicki (1998) for the most recent review). The choice of the best algorithm for this problem depends on a number of factors, e.g. the electrode type, the brain area, the cell type of interest, etc. Additional constraints for sorting methods are reasonable computation time, available hard-disk space, compatibility with the electrophysiological setup and software, and finally also the intended subsequent data analysis.

i) Spike identification

Every electrode provides as output an analog signal, which is amplified, filtered and A/D converted. The filtering stage separates spiking waveform from low-frequency activity (referred to as local field potential), assumed to be the signature of sub-threshold membrane activity of populations of cells. The high frequency signal (typically in the band 300-500 up to 5000-10000 Hz) is referred to as spike waveform. Spikes originating in neurons located near the electrode are more likely to have a good signal-to-noise ratio. These are detected by setting a (more or less) heuristic threshold and cutting a region of the waveform around the point where the threshold is crossed. Methods for quality controls of spike identification will be discussed in Sec. 3.3.2.

ii) Spike classification

The following sections will introduce the most common techniques for spike classification. For seek of clarity we discussed them separately, however many algorithms consist actually

of a combinations of algorithms. Sec. 3.2 is reserved to the illustration of the emerging field of automatic spike sorting.

Template matching

An alternative method to thresholding algorithms is to define a *spike template* for each neuron on the basis of the available data and to compare potential spikes with this template, collecting the spikes whose shape is similar enough to the template (allowing some uncertainty). Definition of several templates allows to simultaneously identify and classify spikes to different putative neurons. This technique is quite computationally efficient, and can be performed on-line for maximal time save. A popular package is provided by the company Alpha Omega[1] (see e.g. Bar-Gad et al., 2003).

Feature extraction and cluster analysis

The most basic signature of a spike is its amplitude. However, other shape features can be measured and used for classification. Typical examples are the peak-to-trough distance and the peak width. By collecting, say, K features for every identified spike, and plotting them on the cartesian space where each axis represents one feature one obtains for every spike a point in a K-dimensional space.

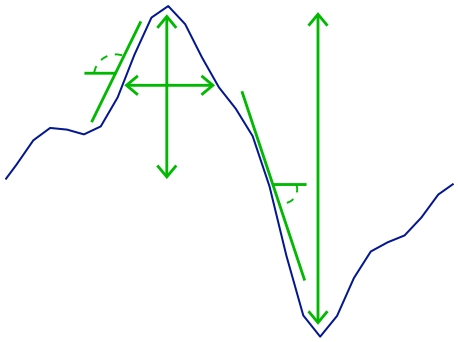

Figure 2: Schematic representation of feature extraction from a spike waveform. Blue: spike; green: examples of features.

Similar spikes (i.e. from the same neuron) will result in neighboring clusters of dots, and algorithms may then be used to i) identify the number of neurons (given by the number of separable clusters) and ii) assign the spikes to the corresponding neuron class (see e.g. Harris et al., 2000). For low-dimensional projections of the feature space, cluster separation may be done by eye inspection, but typically better results are achieved by using the complete high-dimensionality and running algorithms. Indeed, cluster separation analysis is a standard technique in statistics, and a variety of supervised or unsupervised algorithms are available (Daley and Vere-Jones, 2003). Software packages containing scripts and tools for analyzing neuronal data are e.g. MClust[2], Klusters[3] (Hazan et al.,

[1] www.alphaomega-eng.com

[2] web.ahc.umn.edu/∼redish/mclust/

[3] klusters.sourceforge.net. This is part of a bigger package containing also NeuroScope (neuroscope.sourceforge.net) and NDManager (ndmanager.sourceforge.net).

2006), Wave_Clus[4] (Quian Quiroga et al., 2004). They are all available under the GNU license and include spike pre-classification routines and the possibility of interaction by the sorter for refining the results.

A drawback of sorting by feature classification techniques is that they are sensible to outliers, in particular to overlapping spikes (see Sec. 3.3). Indeed the result of the overlap of, say, two spikes contributes as only one point in the feature space, which in addition is likely to be located outside of the clusters; thus it will either be discarded or –in the best case– assigned to one neuron only (and not to both).

Principal component analysis

Principal component analysis (PCA) is an analysis of variance of a multi-dimensional set of random variables. The analysis works in the following way. If time is divided into consecutive bins each spike occupies, say, r bins[5]. Defining A_i as the spike amplitude in bin i, PCA considers the r random variables $A_1, A_2, ..., A_r$. As spikes from different neurons have different shapes, the variables $A_1, A_2, ..., A_r$ will have some variability. PCA calculates the variance of the data in the r-dimensional space of the variables, individuates the directions of maximal variance, and organize them in a descending order; the first PC is the direction where the data vary the most, whereas the last PC points in the direction where data set shows the least variance. This basically corresponds to make a linear transformation of the coordinates and project in the new axes given by the PCs. Principal component analysis is useful to reduce the high dimensionality of the data to few components that explains most of the spike shape variability. Practically only the first couple of PCs are kept and used as features for clustering analyses. PCA is typically more effective than using as features merely geometrical attributes of the spikes. Often PCA and feature extraction are combined to provide clustering algorithms as much information as possible.

3.2 Automatic spike sorting

Improvements of the standard (and time-consuming) methods of spike sorting were motivated e.g. to make unsupervised classification and to sort in real-time, i.e. during data acquisition. This is particularly useful in case of huge amounts of data, when large arrays of independent electrodes are used. Algorithms were proposed e.g. by Quian Quiroga et al. (2004); Bar-Hillel et al. (2006); Horton et al. (2007).

Independent Component Analysis

Independent Component Analysis (ICA) is a statistical method originally introduced to solve the so-called blind source separation problem. In the context of spike sorting it is suitable to handle data recorded with tetrodes or multi-trodes (Hyvärinen and Oja, 2000). The assumption is that neurons are independent sources emitting signals that (linearly) mix together into each of the electrode tips. Exploiting the information given

[4] vis.caltech.edu/∼rodri/Wave_clus/Wave_clus_home.htm

[5] If the bin width was 1 ms the value of r would be given by the length of the spike in ms times the sampling frequency.

by the combination of the multiple tips, one can separate back the contribution of each source. Let us say that the four tips of a tetrode record the signals $x_1(t), x_2(t), x_3(t), x_4(t)$, resulting from the linear superposition of four neurons (sources) $s_1(t), s_2(t), s_3(t), s_4(t)$,

$$x_i = \sum_{j=1}^{4} a_{ij} s_j \quad , \qquad i = 1, ..., 4 \quad . \tag{1}$$

ICA algorithms find the linear combination of the signals $x_i(t)$ that "de-correlates" the most the signals $s_i(t)$, de facto inverting (1). The outcomes of ICA are temporal traces that should represent the activity of the individual neurons. Advantages of this analysis are i) the efficiency in terms of time (being unsupervised) and ii) the possibility to discriminate overlapping spikes. Limitations are on the other hand that i) no more neurons than tips can be identified and ii) the assumption of neurons being statistically independent may be considered unrealistic.

3.3 Major issues

One major problem in spike sorting is the overlap between spikes from different neurons. In order to get a basic intuition of the problem, Fig. 3 shows an "exercise" where two real spikes waveforms were summed up with all possible relative time delays. As it can be seen,

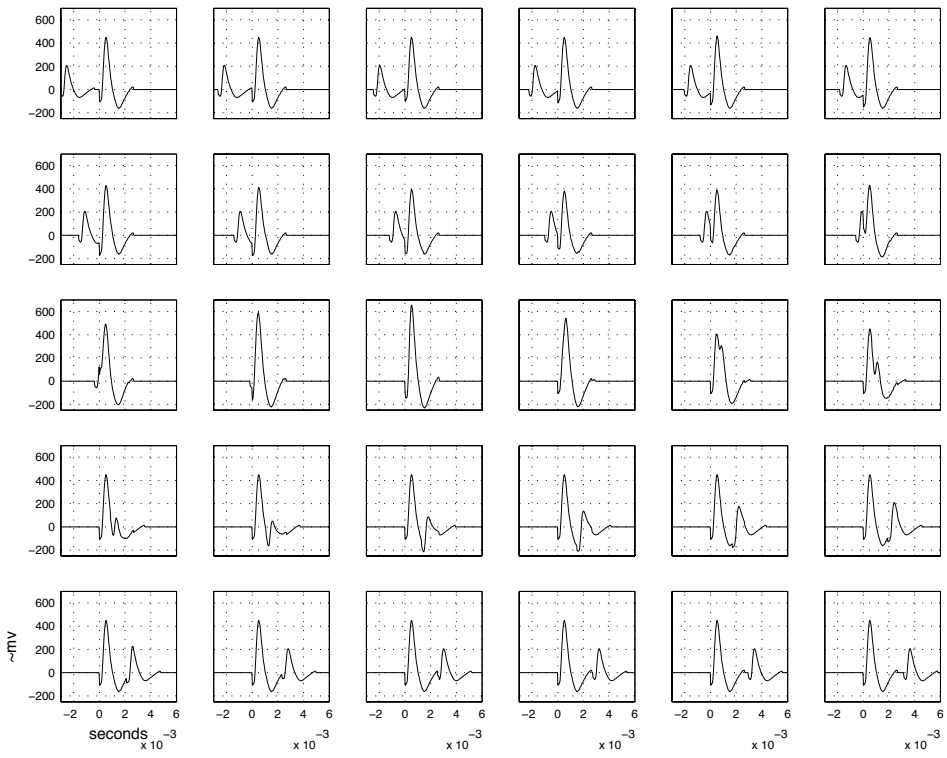

Figure 3: Overlaps of two experimental spikes with different lags (data courtesy of Uli Eggert).

in many cases the sum is again spike-shaped with very similar features; in other cases, the overlap is a bimodal shape of small amplitude. Overlapping spikes are presumably one of the major sources of spike sorting failures. Some attempts to specifically address this problem were made by Pouzat et al. (2002); Zhang et al. (2004); Wang et al. (2006).

Another major issue is the variability of the spike shape over time (Fee et al., 1996; Quirk and Wilson, 1999; Harris et al., 2000). This can be due to intrinsic signal variability, during the occurrences of bursts of spikes, or because the electrode drifts in long recording sessions. Efforts to cope with this problem were made e.g. by Pouzat et al. (2004) and Bar-Hillel et al. (2006).

3.3.1 Spike sorting errors

In both spike sorting stages of spike identification and classification failures are committed. Sorting errors can be categorized into two classes, false negative type (FN) and false positive type (FP) errors. Taking the perspective of a particular neuron, a false positive spike is a spike which is assigned to the neuron despite having originated in some other neuron or being simply noise. Conversely, a false negative spike was actually emitted by the neuron but successively unclassified (i.e. discarded) or misclassified. A few studies have quantified the amount of errors introduced by sorting. Wehr et al. (1999) and Harris et al. (2000) made use of simultaneous intracellular and extracellular recordings in vivo (from adult locust and rat hippocampus, respectively) and compared the outcome of spike sorting with the real activity of the neurons. They reported average error rates of 6.2% for FPs and 15.9% for FNs (Harris et al., 2000), and 3.5% for FPs and 2.8% for FNs (Wehr et al., 1999). In another study, Wood et al. (2004) estimated error rates of 23% FPs and 30% FNs based on simulated data.

3.3.2 Sorting quality measures

Each experimenter develops his/her own criteria to defend himself from sorting errors. However there are some standard tests that are commonly being done. One of them is to look at the inter-spike interval (ISI) histogram of the sorted neurons (cf. Sec. 4.1), i.e. at the distribution of interval lengths between successive spikes. Neurophysiology says that the firing of a neuron is prevented immediately after the emission of a spike (referred to as *refractory period*, typically $1 - 5$ ms); this implies that if the neuron is correctly identified each ISI histogram should display no spikes for very short intervals. If this is not the case, a sorter may consider to review the spike classification. Another common test is provided by the autocorrelation function, i.e. the cross-correlation of a spike train with itself (see Sec. 5.1). If the the analysis of the autocorrelation shows that a spike tends to be followed by another spike at a certain delay, the hypothesis is considered that the spike train actually contains spikes from two different neurons (which have a delayed correlation, e.g. they are synaptically connected) and possibly the spike sorting should be reexamined.

Over the last years several more objective quality controls of spike sorting have been proposed. Schmitzer-Torbert et al. (2005) have introduced two measures, L_{ratio} and Isolation Distance, with the aim of allowing comparability of results of spike sorting across laboratories. According to their simulations and application to real data the value of the

L_{ratio} tends to correlate with FN errors, whereas the Isolation Distance value with FPs. These measures may thus be useful to get hints about the amount of committed errors. Pouzat et al. (2002) have proposed several tests for assessing the quality of sorting, especially in terms of the separation of different clusters. Another measure of the goodness of clustering, the Figure of Merit, was recently introduced by Smith and Mtetwa (2007); it depends on both FN and FP failures and allows an objective quality assessment under controlled conditions.

In conclusion, the correct identification and classification of action potentials from extracellular recordings is a fundamental stage of data pre-processing, however still subject to failures that affect the outcomes. Improvements in spike sorting techniques and estimation of the influence of errors on data analysis are still an open field of research. In the next section we will introduce the mathematical formalism used to represent spike trains, in order to prepare the ground for the correlation analysis of multiple neurons.

4 Spike trains and point processes

Neurons convey information through trains of spikes. As we have seen in the previous section, even spikes from the same neuron may display variability in shape; however, they are typically assumed to be identical. In such a view, spike trains can be represented using only the time of spike occurrence, i.e. as *point processes*. A train of n action potentials occurring in a time window $(0, T]$ is thus defined by the the times t_i with $i = 1, ..., n$. The spike sequence can be seen as a sum of infinitesimally narrow Dirac δ functions (Dayan and Abbott, 2001)

$$\rho(t) = \sum_{i=1}^{n} \delta(t - t_i) \quad , \tag{2}$$

where $\rho(t)$ is the neural response function. The number of spikes occurring in the time window $(0, T]$, also called spike count, is the integral of $\rho(t)$ up to time T,

$$\int_0^T \rho(\tau) d\tau = n \quad . \tag{3}$$

Because the neuronal response is not identical from trial to trial, it has to be treated probabilistically. We will refer to the time varying firing rate $\lambda(t)$ for some small time window Δt as the number of spikes occurring between the times t and $t + \Delta t$ averaged over many trials (with identical stimulus) and divided by Δt,

$$\lambda(t) = \frac{1}{\Delta t} \int_t^{t+\Delta t} \langle \rho(\tau) \rangle d\tau \quad , \tag{4}$$

where $\langle \cdot \rangle$ represents the trial average. $\lambda(t)$ is therefore the average number of spikes occurring within $[t, \Delta t]$. If this window is small enough so that at most one spike can occur, $\lambda(t)$ represents also the fraction of the trials containing a spike in this time interval. The probability of firing in the time interval Δt follows from (4) and is defined as $p(t) = \lambda(t)\Delta t$. If the probability of firing at any instant of time is known the activity of the neuron is then completely determined. However, often this probability cannot be exactly derived experimentally, and needs to be estimated. When the spiking process can be reasonably assumed to be stationary in time the average firing rate $\overline{\lambda}$ is used,

$$\overline{\lambda} = \frac{1}{T} \int_0^T \langle \rho(\tau) \rangle d\tau \quad . \tag{5}$$

We will refer to this quantity indifferently with the symbols $\overline{\lambda}$ or simply λ (without explicit time dependence) and to the stationary probability of firing as $\lambda \Delta t = p$.

As we mentioned it is convenient to treat spike trains probabilistically, that is to consider the firing activity of neurons a stochastic process with associated rate $\lambda(t)$. A point process is a stochastic process which generates series of events, such as action potentials. In general the probability of occurrence of an event may depend on the history

of the process - i.e. on the times of all preceding events. In such a case, in order to characterize the process it is necessary to know the probability of occurrence of events for all times between the origin of the process and its end.

However, it is often methodologically convenient to make hypotheses on the process that, if finally accepted, would allow the use of well-known statistical tools. If for example the occurrence of an event depends only on the timing from the preceding event, the process is called *renewal process* (Cox and Lewis, 1966). If in addition the occurrence of each event is statistically independent of the occurrence of *any* other events in the history, the process is a *Poisson process*. Renewal –and in particular Poisson– processes are often very reasonable approximations of the spike trains. We will review in the following sections some of their properties.

4.1 Renewal processes

Consider the sequence of events $x_k, k = 0, ..., n$ and the corresponding times of occurrence t_k, ordered such that $t_k > t_{k-1}$ and $t_0 = 0$. Let us call I_k the time interval between two consecutive events x_k and x_{k-1}, $I_k = t_k - t_{k-1}$ where now $k = 1, ..., n$. The process is called renewal if the random variables I_k are independently and identically distributed. We also define the *survivor function* $R(t)$ as the probability for an interval to last longer than t,

$$R(t) = Prob(I_k > t) \quad , \tag{6}$$

whereas $F(t)$ and $f(t)$ are the probability distribution and density function of the intervals, respectively. The following relations apply:

$$R(t) \quad = \quad 1 - F(t) = \int_t^\infty f(\tau) d\tau \tag{7}$$

$$f(t) \quad = \quad \frac{dF}{dt} = \frac{dS}{dt} \quad . \tag{8}$$

Thus $f(t)dt$ represents the probability for the length of an interval to be within t and $t + dt$. Commonly used is also the so-called *hazard function* $z(t)$, defined such that $z(t)dt$ is the conditional probability for an interval to be at the same time longer than t and terminate between t and dt,

$$z(t) = \frac{f(t)}{R(t)} = \frac{d}{dt} \left[\log R(t)\right] = -\frac{d}{dt} \left\{\log \left[1 - F(t)\right]\right\} \quad . \tag{9}$$

Examples of stationary renewal processes

The *Weibull*, *gamma* and *log normal* distributions are defined respectively by

$$z(t) = \beta\lambda t^{\beta-1} \quad \text{with } R(t) = e^{-\lambda t^{\beta}} \quad (\lambda > 0, \beta > 0) \tag{10}$$

$$f(t) = \frac{\lambda^{\alpha} t^{\alpha-1} e^{-\lambda t}}{\Gamma(\alpha)} \quad \text{with } \alpha, \lambda > 0 \tag{11}$$

$$f(t) = \frac{e^{-[(\log t - \mu)/\sigma]^2/2}}{\sigma t\sqrt{2\pi}} \ , \tag{12}$$

where $\Gamma(\alpha) = \int_0^{\infty} t^{\alpha-1} e^{-t} dt$ is the gamma function. Especially the class of gamma processes is often used to model spike train intervals. In fact, the Poisson process (see next section) is a special case of gamma process for $\alpha = 1$. The parameters (λ, α) in (11) allow to model the rate and also the regularity of the process. For $\alpha > 1$ the process is more regular than the Poisson process; that is by increasing α the intervals become more and more of uniform length. On the contrary, for $\alpha < 1$ the process increases its irregularity. The mean and variance of the interval distribution are respectively

$$\langle I_k \rangle = \int_0^{\infty} t \frac{\lambda^{\alpha} t^{\alpha-1} e^{-\lambda t}}{\Gamma(\alpha)} dt = \frac{\alpha}{\lambda} \tag{13}$$

$$\sigma_I^2 = \int_0^{\infty} t^2 \frac{\lambda^{\alpha} t^{\alpha-1} e^{-\lambda t}}{\Gamma(\alpha)} dt - \frac{\alpha^2}{\lambda^2} = \frac{\alpha}{\lambda^2} \ , \tag{14}$$

where $\langle \cdot \rangle$ in this case the time average. One advantage of the gamma process (11) as compared to Poisson in modeling neurons is that the parameters can be chosen such that the probability of short intervals is almost zero; this is an elegant way to model the refractory period of real neurons.

4.2 Homogeneous poisson process

As discussed, in renewal processes the intervals I_k between events are independently and identically distributed. That is the occurrence of an event x_k is dependent only on the time since the previous (and only the previous) event x_{k-1}. When in addition the occurrence of an event is independent of the occurrence of *any* other previous events the process is called Poisson process. We will consider here homogeneous Poisson processes. Survivor function, probability distribution, probability density function and hazard function of the intervals for a stationary Poisson process are respectively

$$R(t) = e^{-\lambda t} \tag{15}$$

$$F(t) = 1 - e^{-\lambda t} \tag{16}$$

$$f(t) = \lambda e^{-\lambda t} \tag{17}$$

$$z(t) = \lambda \ , \tag{18}$$

where $t > 0$. In a Poisson process the inter-event intervals follow the exponential distribution (16), and the hazard function is a constant. The mean and variance of the interval distributions are respectively

$$\langle I_k \rangle = \int_0^\infty \lambda t e^{-\lambda t} dt \quad = \quad \frac{1}{\lambda} \tag{19}$$

$$\sigma_I^2 = \int_0^\infty \lambda t^2 e^{-\lambda t} dt - \frac{1}{\lambda^2} \quad = \quad \frac{1}{\lambda^2} \ , \tag{20}$$

It can be shown that the distribution of number of events n_i occurring in time windows $(a_i, b_i], i = 1, ..., K$ follows the Poisson distribution

$$P(n_i) = \prod_{i=1}^{K} \frac{[\lambda(b_i - a_i)]^{n_i}}{n_i!} \cdot e^{-\lambda(b_i - a_i)} \ , \tag{21}$$

where $a_i < b_i \leq a_{i+1}$, that is the time windows are disjoint. Eq. 21 is an alternative definition of a Poisson process as counting process. It embodies also some important features of Poisson processes:

i) the number of events in each finite interval $(a_i, b_i]$ has a Poisson distribution;

ii) the number of events in disjoint intervals are independent random variables;

iii) the distribution of number of events is stationary and depends only on the length of the intervals $b_i - a_i$.

Consequence of Eq. 21 is that the mean and the variance of the number of events n occurring in an interval $(a, b]$ are identical,

$$\mathrm{E}[n] = \lambda(b - a) = \mathrm{Var}(n) \ ; \tag{22}$$

the parameter λ can be thus interpreted as the *mean rate* of the process. Another consequence is that for the time window $(0, t]$ the probability of having no events is $P(0) = e^{-\lambda t}$. This can be seen as the probability of an interval between events to extend for a length t, i.e. the survivor function of the process $R(t)$ (cf. Eq. 15).

The inter-spike interval (ISI) probability density function (17) of a homogeneous Poisson process is a exponential function of time. That is the most likely intervals are short ones, and long intervals have a probability that falls exponentially as a function of their duration. Looking at the ISI distribution (of a stationary process) is a straightforward test to determine if the Poisson hypothesis can be accepted.

A feature of Poisson processes is that their superposition is again a Poisson process (Cox, 1962). The same holds true also when the inverse operation is performed, the so-called *thinning*, consisting in randomly removing spikes from a Poisson process. However, recent studies showed that the superposition of spike trains generally does *not* result in a Poisson process (Lindner, 2006; Câteau and Reyes, 2006).

4.3 Variability measures of point processes

We briefly introduce in the following two of the statistical measures that can be used to characterize the variability of point processes. They can be used e.g. for evaluating whether or not an experimental spike train can be modeled by the Poisson process.

The first measure is the index of dispersion, or *Fano Factor* FF (Fano, 1947). It is defined as the ratio between the variance and the mean of the spike count,

$$\mathsf{FF} = \frac{\mathrm{Var}(n)}{\mathrm{E}[n]} \quad . \tag{23}$$

For a homogeneous Poisson process this takes the value 1, independently of the counting time T. For deviations of FF from the value 1 the process is either more regular or more irregular than Poisson. Similar considerations, but for interval variability, apply to the *coefficient of variation* $\mathsf{C_V}$ defined as

$$\mathsf{C_V^2} = \frac{\sigma_I^2}{\langle I_k \rangle^2} \quad , \tag{24}$$

where, again, for homogeneous Poisson processes $\mathsf{C_V^2} = 1$. The coefficient of variation $\mathsf{C_V^2}$ is a measure of the interval variability in the observation time T, and for non stationary processes can capture the interval variability in short periods of time *within* the trial. The Fano Factor instead quantifies the variability of the counts *across* trials. However, these two measure are not independent: variability of intervals affects also variability of counts. For stationary renewal processes and the limit of long observation time it holds in particular

$$\mathsf{C_V^2} = \mathsf{FF} \tag{25}$$

A deviation from this equality indicates deviation from the hypothesis of stationary renewal processes (Nawrot et al., 2007).

In conclusion, the theory of point processes provides a rigorous framework to model neural activity. In the next section I will introduce statistical measures that, using this framework, allow to quantify the correlations between neurons.

5 Characterizing neuronal correlations

The signature of the activity of single neurons is the sequence of the spike waveforms. To conveniently visualize the activity of multiple units recorded in parallel the *dot display* is widely used (Fig. 4, see Eggermont, 1990). In this representation each row contains the activity of one neuron, and for each spike a tick mark indicates the point in time at which the spike occurred. Thus, the shape information of individual spikes is discarded (cf. Sec. 3.3) and the neuronal activity is treated as the outcome of a point process (cf. Sec. 4). The dot display gives a convenient overview of the firing rate modulations and of the

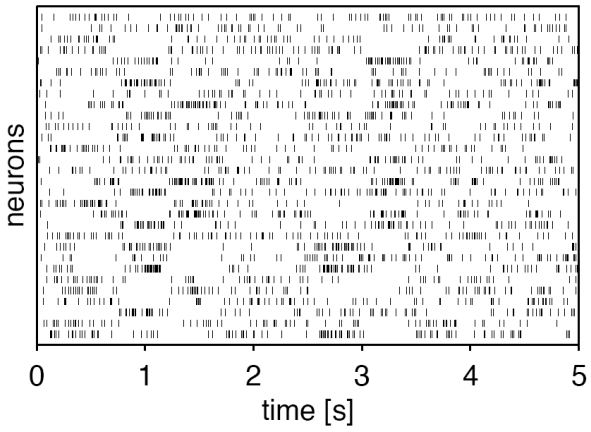

Figure 4: Dot display (courtesy from Nawrot, 2003).

synchronous activity of the whole set of neurons. Although the identification of trends in the joint activity involving several cells is in principle possible by visual inspection, this is often a hard task. Indeed, patterns of coincidences can be "hidden" in the dot display, especially when the units involved are not graphically adjacent. Therefore, to identify the correlated activity of multiple neurons a number of methods were developed. In this section we will briefly review some of the relevant ones (Brown et al., 2004).

5.1 Cross-correlation function

If $\rho_{i,j}(t)$ is the neural response function of neurons $i, j = 1, ..., n$ (Eq. 2), the raw cross-correlation function (Perkel et al., 1967a,b) is defined as

$$CCF_{i,j}^{\text{raw}}(\tau) = \frac{1}{T} \int_0^T \rho_i(t) \cdot \rho_j(t-\tau) dt \quad , \tag{26}$$

and is a function of the time delay τ between the occurrence of spikes on the first and on the second spike train. Let us now discretize the time axis into disjoint bins and represent each spike train as a sequence of zeros (no spike in the bin) and ones (one or more spikes in the bin). The raw CCF can be then computed by counting the synchronous spikes between neurons i and j (delay $\tau = 0$), then shift the spike train j of one bin with respect of the spike train i and count again all synchronous spikes ($\tau = 1$) and

so on, for positive and negative values of τ up to a certain maximal value. The cross-correlation histogram, obtained by plotting the number of spikes occurring for each value of τ, provides information about the exact as well as the delayed joint-firing between two neurons. If the two processes are firing in an uncorrelated manner the histogram will result flat. Copious epochs of coincident firing will result instead in the central peak ($\tau = 0$). If neuron j tends to fire $t^\star$ ms after neuron i the cross-correlation histogram will present a peak at the bin that includes the time $t^\star$.

It is possible to correct the raw CCF for the individual activity of the neurons by subtracting the product of the average firing rates. For stationary processes

$$\begin{aligned} CCF_{i,j}(\tau) &= CCF_{i,j}^{\text{raw}}(\tau) - \overline{\lambda}_i \cdot \overline{\lambda}_j \\ &= \frac{1}{T}\int_0^T (\rho_i(t) - \overline{\lambda}_i)(\rho_j(t-\tau) - \overline{\lambda}_j)dt \quad , \end{aligned} \tag{27}$$

which also corresponds to the covariance of the processes. Thus, if the processes are statistically independent the CCF will be randomly distributed around zero. By dividing the value of the CCF at lag $\tau = 0$ by the product of the standard deviations of the processes one obtains the *cross-correlation coefficient*,

$$CC_{i,j} = \frac{CCF_{i,j}(0)}{\sigma_i \cdot \sigma_j} \quad , \tag{28}$$

a standard measure of the deviation of the covariation from the null-hypothesis of independence.

5.2 Joint Peri-Stimulus Time Histogram

The cross-correlation function does not allow investigation of the time dynamics of correlated firing during the experimental task. For this purpose the *JointPSTH* was proposed (Aertsen et al., 1989). The basic idea is to combine cross-correlation and Peri Stimulus Time Histogram (PSTH), a standard tool that estimates the average firing rate of one neuron. The PSTH is constructed by counting and summing up the spikes occurring at each instant of time over different trials of the same experiment. Indeed it is commonly assumed that by repeating an experiment with identical external stimulus the response of the neurons can be averaged.

The JointPSTH is a scatter diagram, in which the position of each dot (x, y) displays the joint spike count at time x from stimulus onset for neuron 1 and y for neuron 2. The JointPSTH appears thus as a two dimensional "matrix" and contains information about joint firing between the neurons at any delay. Various ways of normalizing the JointPSTH were proposed (Aertsen et al., 1989; Ventura et al., 2005), e.g. by subtracting the product of the average firing rate and divide the result by the standard deviations of the processes. This avoids artifactual peaks of correlation due to the individual firing rates, and represents a test of the null-hypothesis of independent firing.

5.3 Unitary events

Unitary event analysis (UE) measures the significance of joint-spike events occurring amongst multiple, simultaneously recorded neurons (Grün et al., 2002a,b). When their synchronization exceeds the chance level by a significant amount, the coincident patterns are called unitary events. UE analysis evaluates the significance based on the null-hypothesis of independent firing. Having N binned processes, a pattern $\underline{v}^{\xi}(t)$ of complexity degree ξ is defined as the N-dimensional vector of zeros and ones representing the firing/not firing activity at time t. The complexity ξ refers to the number of synchronous spikes, and for the ith neuron $v_i^{\xi} = 1$ for a spike and $v_i^{\xi} = 0$ for no spike. In the case of Poisson and statistically independent spike trains, the probability distribution of the number of patterns can be analytically derived and equals the binomial distribution. For spike trains deviating from Poisson or non-stationary methods for correction have been suggested (Grün et al., 2003b; Pipa et al., 2003; Pipa and Grün, 2003). Here we briefly introduce UE analysis for stationary and Poissonian spike trains, i.e. the situation described in (Grün et al., 2002a,b). Under the null-hypothesis of statistically independent firing of the neurons, the probability of a pattern $\underline{v}^{\xi}$ is

$$\begin{aligned} P_{v^{\xi}} &= \prod_{i=1}^{N} P(v_i^{\xi}) \qquad (29) \\ P(v_i^{\xi}) &= \begin{cases} P(v_i^{\xi}=1) & \text{if } v_i^{\xi}=1 \\ 1-P(v_i^{\xi}=1) & \text{if } v_i^{\xi}=0 \end{cases} \end{aligned}$$

The probability distribution for the pattern $\underline{v}^{\xi}$ to occur exactly m times can be approximated, for number of bins T and $P_{v^{\xi}}$ such that $P_{v^{\xi}} \cdot T$ stays finite, by a Poisson distribution (for a derivation see Grün et al., 2002a):

$$\psi(n; P_{v^{\xi}}; T) = \frac{(P_{v^{\xi}} T)^n}{n!} \cdot e^{-P_{v^{\xi}} T} \quad . \qquad (30)$$

The mean defines the *expected number of coincidences* $x(\xi, N) = P_{v^{\xi}} \cdot T$. Methodologically, the *empirical* number of coincidences $n(\xi, N)$ is compared to the corresponding predicted value $x(\xi, N)$ using the distribution (30). Significant deviations from the expected value are estimated by the joint-p-value, obtained through the cumulative probability of having $n(\xi, N)$ or more coincident events (see Grün et al., 2002a for details) The significance is expressed as a non-linear (log-)transformation of the joint-p-value Ψ, resulting in the significance measure given by the *joint surprise*

$$js(\Psi_{\xi}) = js_{\xi}\left(n(\xi, N) | x(\xi, N)\right) = log \frac{1 - \Psi_{\xi}}{\Psi_{\xi}} \quad , \qquad (31)$$

with

$$\Psi_{\xi}\left(n(\xi, N) | x(\xi, N)\right) = \sum_{m=n(\xi,N)}^{\infty} \frac{[x(\xi, N)]^m}{m!} e^{-x(\xi,N)} \quad . \qquad (32)$$

When the value of js_{ξ} exceeds an a priori threshold js_{α} the synchronization is considered significant.

Unlike the cross-correlation function and the JointPSTH, unitary event analysis allows study of correlation of complexity higher than two. However, a critic to this method is that the null-hypothesis of statistical independence is not necessarily justified when estimating higher-order correlations (see e.g. discussion in Brown et al., 2004).

5.4 Likelihood methods

Likelihood methods aim to estimate unknown parameters of the processes based on the observed outcomes. These methods are based on maximum likelihood estimation of the free parameters of experimental neuronal activities based on a probability model. If the probability model is a good approximation of the processes, likelihood methods represent the optimal way of solving the problem (Brown et al., 2004). Examples of use of these methods to analyze neuronal data are available in the literature (Brillinger, 1988; Kass and Ventura, 2001). The key point of this approach is to define a model that accurately represents the spike trains, and to design efficient algorithms for fitting.

5.5 Information theory

We briefly mention that measures like entropy and mutual information, which offer the chance to investigate the information processing of the brain and are used in analysis of neuronal data. One example is the study by Reich et al. (2001).

5.6 Significance estimation through surrogate data

Statistical measures of neuronal data require hypotheses for assessing significance that are often hard to formulate without knowledge of the underlying processes. One widely used approach to circumvent this difficulty is to create distributions of "surrogate data" obtained with the method of the bootstrap (Efron and Tibshirami, 1993). Let us say that we have n independent observations $(x_1, x_2, ..., x_n) = \underline{x}$ originating from the unknown distribution $F : F \rightarrow \underline{x}$ and want to estimate a statistic of the distribution $\eta = s(F)$. An estimate of the statistic η is obtained by applying it on the observations $x_1, x_2, ..., x_n$, i.e. $\hat{\eta} = s(\underline{x})$. A bootstrap sample $\underline{x}^\star = (x_1^\star, x_2^\star, ..., x_n^\star)$ is obtained by randomly sampling n times, with replacement, from the original data points $x_1, x_2, ..., x_n$. If $\hat{F}$ is the empirical distribution of F, the bootstrap sample $\underline{x}^\star$ is defined as a random sample drawn from $\hat{F}$, $F \rightarrow \underline{x}^\star$. The *bootstrap replication* of the statistic η is obtained from the bootstrap sample, $\hat{\eta}^\star = s(\underline{x}^\star)$. The bootstrap algorithm generates a large set of independent bootstrap samples $\underline{x}_1^\star, \underline{x}_2^\star, ..., \underline{x}_B^\star$, each of size n, where B is typically of the order of hundreds to thousands. This procedure allows to obtain the estimate $\hat{F}$ of the true distribution F. Bootstrap methods are made possible via the use of computers, and have the advantage to be very easy to implement.

In the handling of neuronal data, these methods are very useful for assessing confidence intervals to the experimental estimate $\hat{\eta}$, that is to associate to $\hat{\eta}$ an estimate of its standard error $\hat{\sigma}$ without having to make hypotheses about the true distribution. Bootstrap methods can be useful for example for assessing the significance of the synchronization between the neurons when the data can not be reasonably assumed to follow a Poisson distribution (Ventura et al., 2005).

5.6.1 Permutation tests and spike dithering

A subclass of the bootstrap methods is the family of the permutation tests, introduced in their theoretical form well before the modern computers by Sir Ronald Fisher in the early 1920's. Permutation tests are typically used for addressing the so-called *two-sample problem*. Two independent sets of observations $y_1, y_2, ..., y_n$ and $z_1, z_2, ..., z_m$ are drawn from different probability distributions F and G,

$$\begin{aligned} F &\rightarrow \underline{y} = (y_1, y_2, ..., y_n) \\ G &\rightarrow \underline{z} = (z_1, z_2, ..., z_n) \ . \end{aligned}$$

We wish to test the *null-hypothesis* H_0 of no difference between F and G,

$$H_0 : F = G \ . \tag{33}$$

If the hypothesis H_0 is accepted the two distributions are identical, whereas if it is rejected one can say that the two sets of observations $\underline{y}$ and $\underline{z}$ originate from two independent distributions. This is a formal way of deciding whether or not the data decisively reject H_0. The permutation test takes a sample m and a sample n randomly from the combination of the $m + n$ observations and compare the two novel sets. By repeating this many times one infers about the difference between the two distributions.

To test the correlation between neurons the null-hypothesis H_0 is that the observations $\underline{y}$ arise from the activity of independent neurons. If one had then a set of observations $\underline{z}$ that are known to be independent, a test of H_0 would serve to accept or reject the hypothesis of synchronization between the processes. An example for obtaining a distribution like this is given by *spike dithering*. With this method the correlation structure of the processes is destroyed while other features, like the rate profile, are maintained. Dithering methods will be introduced in Sec. 8 (see also Gerstein, 2004).

On the approach of manipulating the spike train statistics

We have reviewed in the previous sections the state-of-the-art of theories and methodologies of investigation of neuronal correlations as the computing mechanism of the brain. The remaining sections of this dissertation present my contribution to the topics. Two studies address the issue of the influence of spike sorting on correlation methods. They constitute the **Sections 6** and **7**. A third study deals with tools for statistical significance evaluation in correlation analysis, and is reproduced in **Section 8**.

The common point of these studies is the approach of challenging established methods of investigation with spike trains whose statistics was manipulated. Working in an analytical framework allowed me to rigorously test the methods with respect to their power, their robustness and their limitations.

Note about section and equation numbering

In the following sections, for maximal conformity with both the published version of the manuscripts and the structure and readability of this dissertation, I use a slightly different notation for numbering subsections and formulae.

For subsection titles, the section number (assigned in this dissertation) is shown in square parentheses and is followed by the number found in the published version of the manuscript. For example Sec. [6].2 is the second section as found in the scientific journal, but belongs to the sixth section of this dissertation. Similarly, for formulae the number as in the published version of the manuscript follows the section number, i.e. Eq. 6.27.

6 Robustness of the significance of spike synchrony with respect to sorting errors

Antonio Pazienti and Sonja Grün

This section is published as

Pazienti A, Grün S (2006)
Robustness of the significance of spike synchrony with respect to sorting errors.
J Comput Neurosci 21(3): 329-342.

Abstract

The aim of spike sorting is to reconstruct single unit spike times from extracellular multi-unit recordings. Failure in the identification of a spike (false negative) or assignment of a spike to a wrong unit (false positive) are typical examples of sorting errors. Their influence on cross-correlation measures has been addressed and it has been shown that correlation analysis of multi-unit signals may lead to incorrect interpretations. We formulate a model to study the influence of sorting errors on the significance of synchronized spikes, and thus are able to study if and how the significance changes in case of imperfect sorting. Here we explore the case of two simultaneously recorded neurons. Interestingly, a decrease in the significance is observed in the presence of false positives, as well as for false negatives. Furthermore, false negative errors reduce the significance of synchronized spikes more strongly than false positives. Thus, conservative sorting strategies have a stronger tendency to lead to a loss of the significance of synchronization. We demonstrate that a detailed understanding of sorting techniques and their possible effects on subsequent data analyses is important in order to rule out inconsistencies in the interpretation of results.

[6].1 Introduction

In the field of electrophysiology, spike sorting is the procedure of extracting single unit activity from a recorded extracellular "multi-unit" signal. Multiple single-unit recordings offer the chance to detect assembly activities, and to identify the network composition and functions. The spike sorting procedure typically consists of two stages: first, spike waveforms originating from different neurons are identified and separated from the background "extra-cellular noise", which is presumably composed of weaker neural signals and measurement noise (Lewicki, 1998); second, spikes are then classified, i.e. assigned, to putative neurons. Spike sorting failures may occur in any of these two stages.

A variety of techniques and algorithms are meanwhile available for spike sorting (see e.g. Lewicki (1998) for the most recent review). The choice of the best algorithm for

this problem depends on a number of factors, like e.g. the type electrode, the brain area, the cell type of interest, etc. Additional constraints for sorting methods are reasonable computation time, available hard-disk space, compatibility with the recording setup and software, and finally also the intended subsequent data analysis. For offline sorting, standard approaches to the classification problem are cluster cutting in a feature space (see e.g. Harris et al., 2000). Unsupervised (at least partially) statistical algorithms are available, such as independent component analysis (ICA, Hyvärinen and Oja, 2000) for multitrode (stereotrodes, tetrodes, etc) recordings, and superparamagnetic clustering (Quian Quiroga et al., 2004) for independent multi-electrode recordings. For resolving more neurons than available electrodes in the multi-trode, Takahashi et al. (2003a) suggested to combine ICA and k-means clustering. However, also less sophisticated techniques, but with the advantage of online applicability, like threshold crossing, window discrimination, or multiple-point template-matching procedures are in use. Major problems in spike sorting are the difficulty to resolve spikes from different neurons which overlap in time, and the variability of the spike waveform (Fee et al., 1996; Quirk and Wilson, 1999; Harris et al., 2000). A solution for spike sorting for the latter problem was suggested by Pouzat et al. (2004), solutions for the problem of overlapping spikes had been suggested by Pouzat et al. (2002) and Zhang et al. (2004).

As this wide interest in finding the "ultimate" algorithm suggests, there is not a unique solution and all existing ones are subject to errors. Objective controls for sorting quality have been proposed by Pouzat et al. (2002) and recently by Schmitzer-Torbert et al. (2005), with the aim to allow for comparability of sorting results from the different methods.

Sorting errors appear either as failures in the identification of spikes, or as assignments of spikes to wrong units, referred to as false negative errors (FN) or false positive errors (FP), respectively. Taking the perspective of a particular neuron, a false positive spike is a spike which is assigned to that neuron despite having originated from another neuron or from extra-cellular noise. Conversely, a false negative spike was emitted by the neuron and successively unclassified or assigned to another neuron. A few studies have quantitatively shown the amount of errors introduced by sorting. Wehr et al. (1999) and Harris et al. (2000) made use of simultaneous intracellular and extracellular recordings in vivo (from adult locust and rat hippocampus, respectively). They reported average error rates of 6.2% for FPs and 15.9% for FNs (Harris et al., 2000), and 3.5% for FPs and 2.8% for FNs (Wehr et al., 1999). Wood et al. (2004) estimated average error rates of 23% FP and 30% FN based on simulated data.

However, studies on how such errors affect subsequent analyses of these data are surprisingly lacking. Bedenbaugh and Gerstein (1997) and Gerstein (2000) investigated the consequences of unresolved spike trains on cross-correlation analysis, and found that the correlation coefficients calculated between spike trains that contain wrongly assigned spikes can be strongly biased, depending on the degree of mixing spike trains and also depending on correlation structures between local and/or remote groups of neurons. In contrast, Bar-Gad et al. (2001b) concentrated on the influence of correlated false negative spikes on the cross-correlation analysis. They also found that the cross-correlation function can be heavily biased due to the errors. Quirk and Wilson (1999) showed for the case of neuronal bursting activity that spikes occurring later in the burst may be assigned to

another neuron due a change in its spike shapes. The cross-correlation analysis between such neurons also revealed a strong bias by indicating artificial delayed coincidences.

Here we present a study that combines the occurrence of FN and FP sorting errors and that evaluates their influence on unitary events (UE; Grün et al., 1999; Grün et al., 2002a,b). UE analysis detects the presence of conspicuous spike coincidences in multiple parallel spike recordings and evaluates their statistical significance. The UE method enabled to study the relation between spike synchronization and behavioral events (Riehle et al., 1997, 2000; Grün et al., 2002b) for the case of two simultaneously recorded neurons.

A brief introduction to the method is provided in Section [6].2.1. In Section [6].2.2 we introduce a simple statistical model for spike sorting errors, which allows us to study how FP and FN errors influence the significance of joint-spike events, as well as the measures entering the significance estimation (Section [6].3.1). On the basis of the derived analytical expressions and numerical simulations, we demonstrate that the firing rates and the number of coincidences (empirical as well as expected) may be increased or decreased depending on the error rate combination, but the resulting significance is always reduced irrespective of the error type. A rigorous analysis reveals that the origin of significance reduction is different for the two error types. In Section [6].3.2 we illustrate that variation of physiological parameters, such as firing rates of the neurons and their coincidence rate, influence the resulting significance only weakly as compared to the error rates. Finally we discuss our results and further steps (Section [6].4).

[6].2 Methods

[6].2.1 Unitary event analysis

Unitary event analysis, introduced by Grün et al. (2002a), measures the significance of joint-spike events occurring amongst multiple, simultaneously recorded neurons. When their synchronization exceeds the chance level by a significant amount, the coincident patterns are called unitary events. UE analysis evaluates the significance based on the null-hypothesis of independent firing. In the case of Poissonian spike trains, the probability distribution of the number of coincident patterns can be analytically derived. For the case of spike trains deviating from Poisson or non-stationary data we suggested methods for correction (Grün et al., 2003b; Pipa et al., 2003; Pipa and Grün, 2003). Here we restrict ourselves to the assumptions of stationary and Poissonian spike trains, i.e. the situation described in Grün et al. (2002a), which we briefly introduce below.

Let us consider a stationary process (of rate λ) in the observed time window T containing $N = T/\delta$ bins (with δ the bin width in seconds). The probability of neuron i to fire within the time interval of bin size δ is

$$p_i = \lambda_i \delta \quad , \tag{6.1}$$

here for neurons $i = 1, 2$. Under the null-hypothesis of statistically independent firing of the neurons, we derive the probability of joint-firing in one bin as $P = p_1 \cdot p_2$. The probability distribution of the coincident events can be approximated by a Poisson distribution (for a derivation see Grün et al., 2002a):

$$\psi(n; p_i; N) = \frac{(n_{\text{pred}})^n}{n!} \cdot e^{n_{\text{pred}}} \quad , \tag{6.2}$$

with n_{pred} being the expected number of coincidences, given the firing rates:

$$n_{\text{pred}} = p_1 p_2 N = \lambda_1 \lambda_2 \delta^2 N \quad . \tag{6.3}$$

The empirically found number of coincidences n_{emp} is then compared to the predicted value n_{pred} using the Poisson distribution (Eq. 7.31). Significant deviation from the expected value is estimated by the joint-p-value, i.e. the cumulative probability of having n_{emp} or even more coincident events (gray area from n_{emp} to ∞ under the probability density curve in Fig. 5a, middle distribution). For better visibility of the relevant significance values we express the significance as a non-linear (log-)transformation of the joint-p-value Ψ, resulting in the significance measure 'joint-surprise' js:

$$js(\Psi) \quad = \quad log\frac{1-\Psi}{\Psi} \quad , \tag{6.4}$$

with

$$\Psi\left(n_{\text{emp}}|n_{\text{pred}}\right) = \sum_{n=n_{\text{emp}}}^{\infty} \frac{(n_{\text{pred}})^n}{n!} e^{-n_{\text{pred}}} \quad . \tag{6.5}$$

When the value of js exceeds an a priori threshold, e.g. 1% or 5%, the synchrony is classified as significant.

[6].2.2 Statistical model of spike sorting errors

We shall now formulate a statistical model on how spike sorting errors may affect neuronal spike trains. Given simultaneous spike trains of two neurons (Fig. 5b, top), we assume a uniformly distributed probability for spikes to be missed as false negatives, or that spikes may be added with uniform probability as false positives to the spike trains (for illustration see Fig. 5b, bottom). Both error types are applied independently to each neuron. Effectively we assume the neurons to be recorded from different electrodes, such that neuronal activity of one neuron may only be registered at one electrode, and that errors do not interact across electrodes. Thus, for a single neuron the different errors are assumed to be applied independently, however excluding the unrealistic case that an introduced FP spike is considered as FN.

Errors are expressed as fractions σ_i^+ for FPs and σ_i^- for FNs of the original firing rates of neuron $i = 1, 2$. As a result, the firing rate of neuron i after sorting (λ_i^σ) is the sum of three terms, i.e. the original rate (λ_i), the FP rate and the FN rate:

$$\lambda_i \longrightarrow \lambda_i^\sigma = \lambda_i + \lambda_i \cdot \sigma_i^+ - \lambda_i \cdot \sigma_i^- = \lambda_i \cdot \left(1 + \sigma_i^+ - \sigma_i^-\right) \quad . \tag{6.6}$$

Thus sorting errors alter the original firing rates λ_i by contaminating the spike trains. False negatives reduce the rate, whereas false positives enhance the rate, and they may

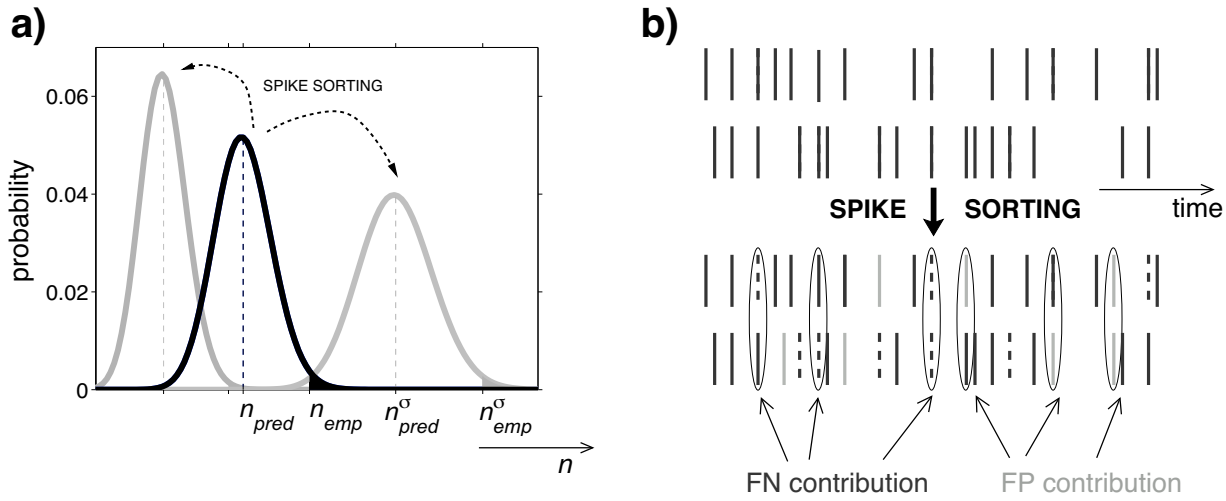

Figure 5: (a) Probability density function of number of coincident events before and after spike sorting. The distribution in the middle illustrates the density function for the original case before sorting. Its mean n_{pred} is the expected number of coincidences based on the firing rates of the original spike trains. The empirical number of coincidences n_{emp} is shown to be higher than expected, i.e. on the tail of the distribution. The black area represents the p-value for significance estimation. The two gray distributions to the left and to the right, show examples of coincidence distributions, whose mean n^{σ}_{pred} is derived from the firing rates after sorting. The distribution on the left mimicks the case of more FN errors than FP ($\sigma^{+} < \sigma^{-}$), and the one on the right the case for more FP than FN ($\sigma^{+} > \sigma^{-}$). The number of coincidences after sorting (n^{σ}_{emp}) does not necessarily generate the same p-value (gray area) as n_{emp}. (b) Sketch of the spike sorting model. (Top) Original spiking activity of two neurons before sorting. Each time a spike occurred is marked by a black line. (Bottom) The spike trains after having experienced sorting errors. Black solid lines show the original and correctly classified spikes. Black dashed spikes are missed (FNs), whereas gray spikes are falsely assigned (FPs). Marked coincidences indicate all possible coincidence error types (FN and FP coincidences) entering the number of coincidences after sorting (n^{σ}_{emp}).

compensate for equal error rates. Thus, the resulting firing rate after sorting may be larger or smaller than the original rate depending on the relative contributions of errors.

In the following, the index σ will indicate a variable after sorting. For simplifying reasons we define the variable σ_i for the combined influence of errors as:

$$\sigma_i = \sigma_i^- - \sigma_i^+ \quad . \tag{6.7}$$

Inserting Eq. 6.6 and using Eq. 6.7 in Eq. 6.1, we similarly get new values for the firing probability per time bin:

$$p_i \longrightarrow p_i^\sigma = p_i \cdot (1 + \sigma_i^+ - \sigma_i^-) = p_i \cdot (1 - \sigma_i) \quad . \tag{6.8}$$

[6].2.3 Simulations

For understanding the influence of spike sorting errors on significance estimation by the unitary events method, we make use of two approaches: analytical derivation and numerical simulations. For the simulations we follow the approach introduced in Grün et al. (1999). Neuronal spiking activities are realized as a combination of independent background activity and correlated spiking activities. The background activity is generated as realizations of stationary Poisson processes with rate λ_i' for each neuron $i = 1, 2$. Correlations between the neurons are introduced by inserting coincident events of rate λ_c simultaneously to both processes. Then the total rate of the neurons reads

$$\lambda_i = \lambda_c + \lambda_i', \qquad i = 1, 2 \quad . \tag{6.9}$$

As a result, each of the simultaneous spike trains contain intermixed independent background spikes and correlated spikes. The consecutively applied sorting errors affect spikes irrespective of their origin.

[6].3 Results

This section presents results for the expected and empirical number of coincidences after sorting as functions of the unperturbed ("original") values and of the error rates (Sections [6].3.1.1 and [6].3.1.2) and under variation of physiological parameters, i.e. firing rates of the neurons and degree of correlation (Sections [6].3.2.1 and [6].3.2.2). These results find entry in the evaluation of the significance of joint-spike events. The influence of sorting onto the latter is explored in Sections [6].3.1.3 and [6].3.2.3.

Analytical descriptions serve to derive the expected and empirical number of coincidences after sorting given the original values and to evaluate their effects on the significance. In addition, numerical simulations of simultaneous spike trains of controllable firing rates and degree of correlation allow to study the influence of physiological parameters on the various measures under sorting errors.

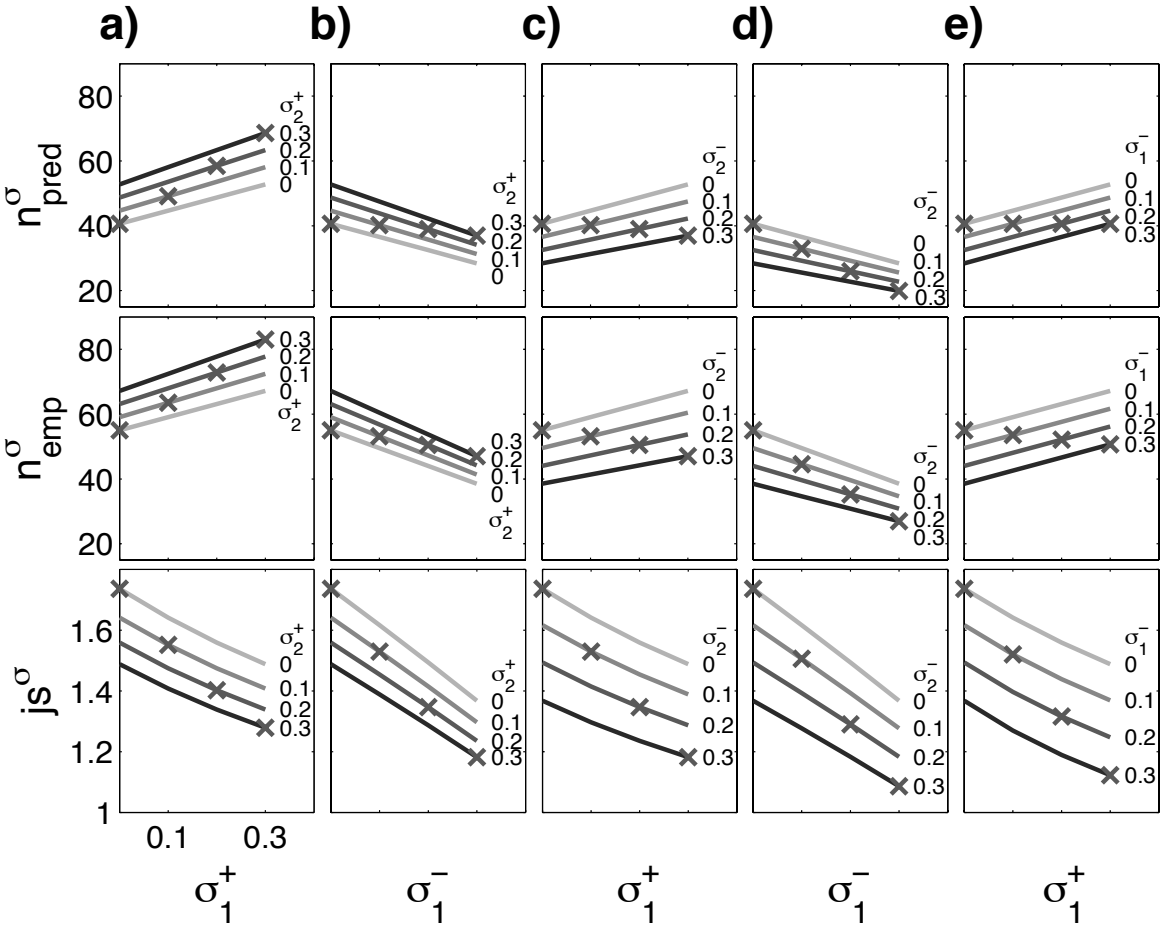

Figure 6: Number of coincidences and resulting significance as a function of various combinations of error rates. Number of expected (top row) and empirical (middle row) coincidences after sorting and joint-surprise after sorting (bottom row), as a function of errors applied to neuron 1 (either FPs (σ_1^+) or FNs (σ_1^-)) in combination with different error types and rates applied to neuron 2 (a-d, either FPs (σ_2^+) or FNs (σ_2^-)). (e) neuron 1 experiences the two different types of errors, while neuron 2 is perfectly sorted (no errors). For each curve the second error rate is constant. Curves for n^{σ}_{pred} (top), n^{σ}_{emp} (middle) and js^{σ} (bottom) with the same gray level correspond to the same parameters. In each of the cases, only two error types (out of four possible) are applied, the other two are set to zero. Crosses show the symmetrical cases where the two applied errors are of equal absolute amount. Additional parameters are the same for all cases and set to $\lambda_1' = \lambda_2' = 20\,\text{Hz}, \lambda_c = 2\,\text{Hz}, T = 100$ seconds, bin size $\delta = 1\,\text{ms}$.

[6].3.1 Dependence on error rates

[6].3.1.1 Number of expected coincidences

In the following we derive the relation between the expected number of coincidences before (n_{pred}, original value) and after sorting (n^{σ}_{pred}). Their relation results directly from the sorting model introduced in Section [6].2.2. By substituting in the expression for the original expected number of coincidences (Eq. 7.15) the expression for the firing probabilities after sorting (Eq. 6.8), we obtain for the expected number of coincidences after sorting:

$$n_{\text{pred}} \quad \longrightarrow \quad n^{\sigma}_{\text{pred}} = (1-\sigma_1)p_1 \cdot (1-\sigma_2)p_2 \cdot N = n_{\text{pred}} \cdot \left(1+\sigma_1^+ - \sigma_1^-\right) \cdot \left(1+\sigma_2^+ - \sigma_2^-\right) \quad . \tag{6.10}$$

The expected number of coincidences after sorting n^{σ}_{pred} is proportional to the expected number of coincidences before sorting, multiplied by scaling factors that contains the error rates σ_i^+ and σ_i^-. In Fig. 6 (top) it can be seen that the predicted number of coincidences after sorting n^{σ}_{pred} is an increasing function of σ_1^+ and σ_2^+ and a decreasing function of σ_1^- and σ_2^-. Thus, depending on their relative amounts, n^{σ}_{pred} may be larger (for $\sigma_i^+ > \sigma_i^-$, $i = 1, 2$) or smaller than n_{pred} (for $\sigma_i^+ < \sigma_i^-$, $i = 1, 2$) as a direct consequence of the sorting errors onto the firing rates (Eq. 6.6). This in turn leads to a different position of the probability distribution used for significance estimation (cf. Fig. 5a).

[6].3.1.2 Number of empirical coincidences

The empirical number of coincidences after sorting is not a mere function of altered firing rates as the expected number of coincidences, but is also a function of changes in the number of joint-events across neurons. New coincidences may be created and/or deleted by sorting:

$$n_{\text{emp}} \quad \longrightarrow \quad n^{\sigma}_{\text{emp}} = n_{\text{emp}} - n^{\mathsf{FN}} + n^{\mathsf{FP}} \quad . \tag{6.11}$$

As illustrated in Fig. 5b (bottom) the number of coincidences deleted by false negative spikes (n^{FN}) may be composed by three contributions: spikes originally involved in coincidences may be deleted from neuron 1, or from neuron 2, or simultaneously from both neurons. This is expressed as:

$$n^{\mathsf{FN}} = n_{\text{emp}} \cdot \left[\sigma_1^- \left(1-\sigma_2^-\right) + \sigma_2^- \left(1-\sigma_1^-\right) + \sigma_1^- \cdot \sigma_2^-\right] \quad . \tag{6.12}$$

On the other hand, wrongly assigned spikes may lead to false positive coincidences (n^{FP}). By inserting spikes either in one or in the other neuron at the very same time when the corresponding other neuron contributes with an original spike, or inserting two false positive spikes in the two neurons coincidently in time, new coincidences are created:

$$n^{\mathsf{FP}} = n_{\text{pred}} \cdot \left[\sigma_1^+ \left(1-\sigma_2^-\right) + \sigma_2^+ \left(1-\sigma_1^-\right) + \sigma_1^+ \cdot \sigma_2^+\right] \quad , \tag{6.13}$$

(see appendix for a formal derivation of Equations 6.12 and 6.13). Inserting these expressions in Eq. 6.11 and rearranging the terms, leads to the following relation for the empirical number of coincidences after sorting:

$$n^{\sigma}_{\text{emp}} = \left(1-\sigma_1^-\right)\left(1-\sigma_2^-\right) \cdot [n_{\text{emp}} - n_{\text{pred}}] + \left(1+\sigma_1^+ - \sigma_1^-\right)\left(1+\sigma_2^+ - \sigma_2^-\right) \cdot n_{\text{pred}} \quad . \tag{6.14}$$

As a result, the empirical number of coincidences n^{σ}_{emp} after sorting can be expressed as a function of the original expected and empirical number of coincidences, multiplied by factors containing the error rates. The first term consists of the difference of the empirical and the expected number of coincidences, i.e. the original "excess" coincidences, multiplied by a factor consisting of false negative errors only. The more false negatives occur, the more the factor is deviating from 1 to smaller values in a nonlinear fashion. Thus, excess coincidences may only be reduced due to sorting errors. The second term is actually the expected number after sorting (cf. Eq. 6.10). Interestingly, only here false positive errors enter the expression for the empirical number of coincidences after sorting. As discussed in Section [6].3.1.1, the errors may –depending on the relation of the errors rates– compensate to 0, or may lead to a factor larger or smaller than 1.

Two important results may be extracted from this discussion of Eq. 6.14 and are depicted in Fig. 6 (middle row):

- False positive spikes contribute to chance coincidences only and increase them.
- False negatives are the only error type that affects excess coincidences and may only lead to a reduction of their number.

[6].3.1.3 Significance

In the previous two sections we learned that the empirical as well as the expected number of coincidences are affected by both types of sorting errors. These two measures enter the significance estimation of the empirically found number of coincidences given the number of coincidences expected by chance (Eq. 7.33), i.e. we obtain now a value js^{σ}, as a function of n^{σ}_{emp} and n^{σ}_{pred} :

$$js^{\sigma} = js(n^{\sigma}_{\text{emp}}, n^{\sigma}_{\text{pred}}) \quad , \tag{6.15}$$

where n^{σ}_{pred} defines the mean of the distribution that enters the significance measure (Eq. 7.31). In addition, this number also affects the shape of the distribution: the larger the mean, the wider the distribution (a feature of the Poisson distribution, Fig. 5a), and thus the larger the empirical number of coincidences required for significance. Since the errors enter both the empirical and the expected number, it is not obvious how the significance measure is affected.

Fig. 6 (bottom row) shows that the value of the joint-surprise after sorting js^{σ} is always decreasing, irrespective of the combination of error types applied to the two neurons. If only one error rate is modified, the offset of the decreasing joint-surprise is higher (light gray lines) than if another error is also applied (darker lines). Identical levels of the error rates are marked additionally by crosses. Their slope is always steeper than for non-identical levels (i.e. when one neuron experiences less errors), indicating an even stronger effect for identical error levels. Therefore we restrict ourselves in the following to the worst case scenario, i.e. to the case $\sigma_1^- = \sigma_2^- = \sigma^-$ and $\sigma_1^+ = \sigma_2^+ = \sigma^+$, without loss of generality but thereby lightening the formalism.

In order to investigate more deeply where the overall decrease of significance originates from, we jointly observe n^{σ}_{pred}, n^{σ}_{emp} and js^{σ} as functions of (symmetrical) false negatives and false positives error rates (Fig. 7). As expected (Eq. 6.14 and Eq. 6.10 and Fig. 6

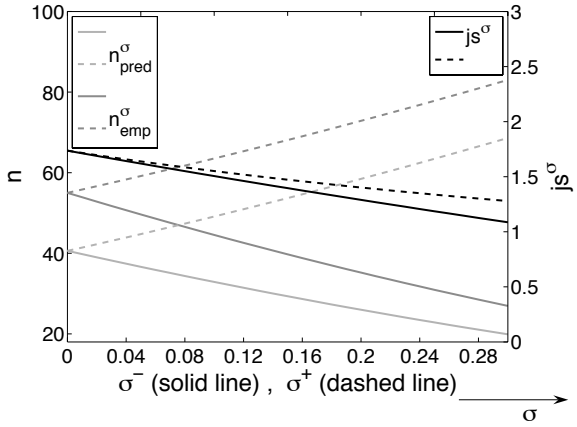

Figure 7: Number of coincidences and resulting significance as a function of error rates. Two situations: increase of σ^- while $\sigma^+ = 0$ (solid lines), and increase of σ^+ while $\sigma^- = 0$ (dashed lines). For each of the situations, the empirical (n^σ_{emp}, dark gray) and the expected number of coincidences (n^σ_{pred}, light gray), as well as the resulting joint-surprise (js^σ, black) are shown. Both $js^\sigma(\sigma^-)$ and $js^\sigma(\sigma^+)$ decrease with error increase, although for increasing σ^+ the underlying number of coincidences increases. Parameters: $\lambda'_1 = \lambda'_2 = 20\,\text{Hz}, \lambda_c = 0.15\,\text{Hz}, 100$ seconds, bin size 1 ms.

(bottom)), both measures decrease with σ^-, however n^σ_{emp} reduces more rapidly with increasing σ^- than n^σ_{pred} (solid gray lines). As a result, the significance also decreases with increasing σ^- (solid black line). For FPs only ($\sigma^- = 0$ and increasing σ^+), i.e. adding chance coincidences only, n^σ_{emp} and n^σ_{pred} increase in parallel (dashed gray lines). Again, the joint-surprise decreases with increasing errors (dashed black line), however for a different reason. Although the difference of the empirical and the expected number stays constant, due to increasing the mean and thus the width of the distribution the empirical number becomes less significant. As a consequence, both types of errors tend to reduce the significance of the observed coincidences after sorting, although the absolute number of coincidences may even increase with false positive errors.

Fig. 8a illustrates the relation of the joint-suprise after sorting in relation to the original value. Interestingly, this ratio (js^σ/js) is always smaller than 1, and decreases with increasing sorting errors, irrespective of error type. For false positive errors only (dashed line), the significance is less drastically reduced than for the same amount of false negative errors (solid line). This is particularly surprising, since in case of FP errors new coincidences are created and no coincidences are deleted.

Fig. 8b shows the same curves as in panel a) but for different combinations of error rates: instead of the respective other error to be set to 0, here it is set to 0.08. Now both curves start at values lower than 1, and cross each other. The crossing point is exactly at $\sigma^- = \sigma^+$. It is worth noticing that although the case $\sigma^- = \sigma^+$ balances the effect of errors on the firing rates (Eq. 6.6), it still affects (and reduces) the significance after sorting. The inset shows that for the part of the curves always being largest (black line) holds the condition $\sigma^+ > \sigma^-$, again indicating that FNs reduce the joint-surprise more strongly than FPs do.

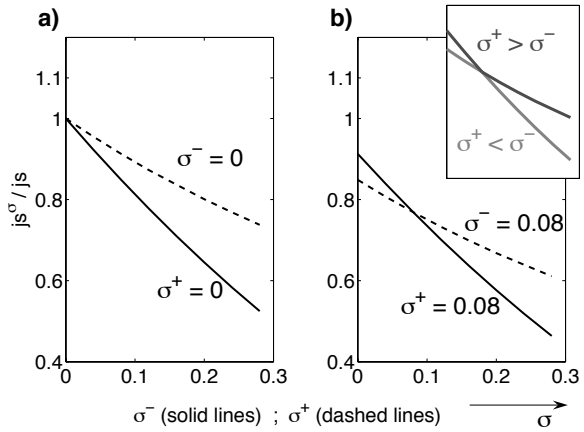

Figure 8: Underestimation of significance of synchronization after spike sorting. The ratio between the joint-surprise after sorting js^σ and the original significance js is shown under variation of σ^+ for fixed values of σ^- (dashed lines) and under variation of σ^- while σ^+ has a fixed value (solid lines). (a) $\sigma^- = 0$ (dashed) and $\sigma^+ = 0$ (solid); (b) $\sigma^- = 0.08$ (dashed) and $\sigma^+ = 0.08$ (solid). (b, inset) Same data and parameters as in b), but now colored according to the relation of the error rates. Portions of the curves for which holds $\sigma^+ < \sigma^-$ are marked in light gray, for the condition $\sigma^+ > \sigma^-$ they are marked in dark gray.

[6].3.2 Dependence on Physiological Parameters

In this section we evaluate the dependencies of the various measures on physiological parameters, such as background rates λ_i' of the neurons $i = 1, 2$ and injected coincidence rate λ_c. We shall make use of simulations as introduced in Section [6].2.3. Since we are interested in the change of the coincidence numbers after sorting in relation to before sorting, we again express them as ratios. Also here, we only consider symmetrical error rates and use now Eq. 6.10 and Eq. 6.14 in which we have replaced $\sigma_1^- = \sigma_2^-$ by σ^- and $\sigma_1^+ = \sigma_2^+$ by σ^+.

[6].3.2.1 Expected Coincidences

The relation of the expected number of coincidences after sorting in relation to before sorting is given by Eq. 6.10 divided by n_{pred}:

$$\frac{n_{\text{pred}}^\sigma}{n_{\text{pred}}} = \left(1 + \sigma^+ - \sigma^-\right)^2 \quad . \tag{6.16}$$

Thus, $n_{\text{pred}}^\sigma / n_{\text{pred}}$ does not show any dependence on rates, but only a quadratic dependence on error rates.

[6].3.2.2 Empirical Coincidences

We analyse here the ratio between n_{emp}^σ (Eq. 6.14) and n_{emp}. As introduced by Grün et al. (2002b) the latter can be expressed as the expected number given the uncorrelated neuronal activity plus the additionally injected coincidences (of rate λ_c):

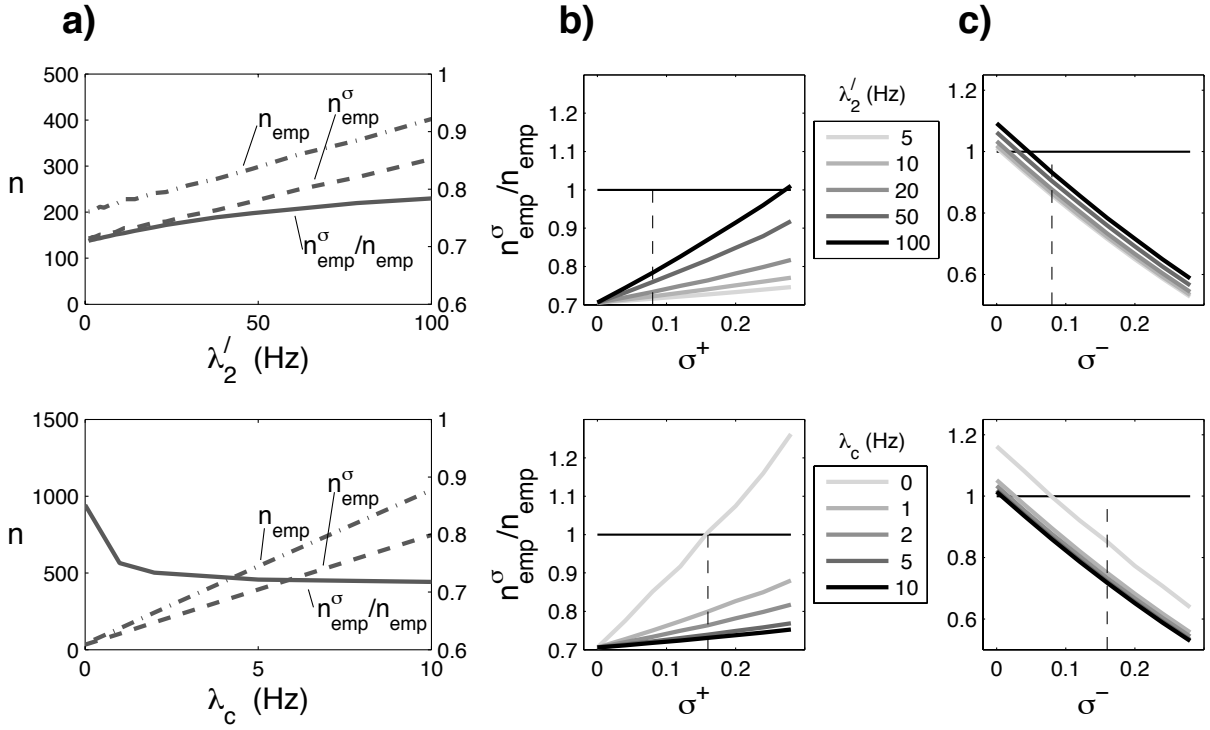

Figure 9: Influence of firing, coincidence and error rates on the number of coincidences. (a) Empirical number of coincidences before (n_{emp}, dashed-dotted line) and after sorting (n^{σ}_{emp}, dashed line) and their relation $n^{\sigma}_{\text{emp}}/n_{\text{emp}}$ (solid line; corresponding axis on the right) as a function of backgound firing rate $\lambda_2^{'}$ (top) and of injected coincidence rate λ_c (bottom). Values of error rates: $\sigma^+ = 0.08, \sigma^- = 0.16$. (b,c) $n^{\sigma}_{\text{emp}}/n_{\text{emp}}$ as a function of error rates, in b) as a function of σ^+, and in c) as a function of σ^-. In the top row, the background rate of neuron 2 is varied (see legend) while $\lambda_c = 2$ Hz. In the bottom row, the coincidence rate is varied (see legend) while $\lambda_2^{'} = 20$ Hz. In all plots (a,b,c) $\lambda_1^{'} = 20$ Hz. The thin black line depicts for reference the identity relation $\frac{n^{\sigma}_{\text{emp}}}{n_{\text{emp}}} = 1$. The dashed thin lines mark the parameters used in a). The values chosen for σ^+ and σ^- in a) are (about) the average error rates extracted by Harris et al. (2000).

$$n_{\text{emp}} = (\lambda_c \delta + \lambda_1' \delta \cdot \lambda_2' \delta) \cdot N \quad . \tag{6.17}$$

For the expression of the expected number of coincidences we replace in Eq. 7.15 the rates by Eq. 6.9:

$$n_{\text{pred}} = (\lambda_c + \lambda_1')\, \delta \cdot (\lambda_c + \lambda_2' \delta) \cdot N \quad . \tag{6.18}$$

Inserting Eq. 6.17 and Eq. 6.18 into Eq. 6.14 and rearranging leads to:

$$\frac{n^{\sigma}_{\text{emp}}}{n_{\text{emp}}} = (1-\sigma^-)^2 + (2\sigma^+ - 2\sigma^-\sigma^+ + \sigma^{+2}) \frac{n_{\text{pred}}}{n_{\text{emp}}} \tag{6.19}$$

$$= (1-\sigma^-)^2 + (2\sigma^+ - 2\sigma^-\sigma^+ + \sigma^{+2}) \frac{(\lambda_c^2 + \lambda_1'\lambda_c + \lambda_2'\lambda_c + \lambda_1'\lambda_2')\delta^2}{(\lambda_c \delta + \lambda_1'\lambda_2'\delta^2)}. \tag{6.20}$$

Fig. 9a illustrates the two variables and their relation ($n^{\sigma}_{\text{emp}}/n_{\text{emp}}$) as a function of firing rate (top) and as a function of coincident firing rate (bottom) for fixed error rates. The graph shows that both, n^{σ}_{emp} and n_{emp}, increase with coincidence rate as well as with firing rate, with n^{σ}_{emp} always being lower than n_{emp}. For increasing λ_c (bottom), n^{σ}_{emp} increases with smaller slope than n_{emp}. As a consequence, the relation $n^{\sigma}_{\text{emp}}/n_{\text{emp}}$ decreases rapidly with λ_c. An increase in firing rate (top) leads to a slightly smaller increase of n^{σ}_{emp} as compared to n_{emp}, such that $n^{\sigma}_{\text{emp}}/n_{\text{emp}}$ grows rather slowly.

Fig. 9b shows the dependence on error rates. $n^{\sigma}_{\text{emp}}/n_{\text{emp}}$ increases with σ^+ approximately linearly, with changes in firing and coincidence rates. Increasing firing rate increases the slope (top), whereas increasing coincidence rate decreases it (bottom). Taking the dashed line (corresponding to the parameters used in (a)) as a reference, we notice that the slope varies non-linearly with firing and coincidence rates. $n^{\sigma}_{\text{emp}}/n_{\text{emp}}$ decreases approximately linearly with σ^- (Fig. 9c). Here, changes in rate or coincidence rate do not influence the slope of the relation but rather the intersection with the vertical axis, again in a non-linear way. With increase in rate the vertical offset of $n^{\sigma}_{\text{emp}}/n_{\text{emp}}$ slightly increases, with increasing coincidence rate it slightly decreases. Note that the ratio may be larger than 1 for high firing rates or low coincidence rates, i.e. after sorting the empirical number of coincidences may be increased.

[6].3.2.3 Significance

Here we analyze how the significance of synchronized spikes changes due to sorting errors in combination with the changes of physiological parameters explored in the forgoing subsections. We have seen above that the empirical number of coincidences may increase or decrease depending on the specific parameter combinations. The change of the predicted numbers depends only on the error rates, i.e. no dependence on firing and coincidence rate is present. Now it needs to be evaluated how the significance of empirical coincidences given the predicted numbers changes with sorting. Fig. 10a illustrates the changes of the joint-suprise relation js^{σ}/js as a function of firing rate (top) and coincidence rate (bottom). With increasing $\lambda_2^{'}$, both components decrease. js^{σ} is always smaller than js, but js decreases faster and thus the relation of the two decreases. Although both components

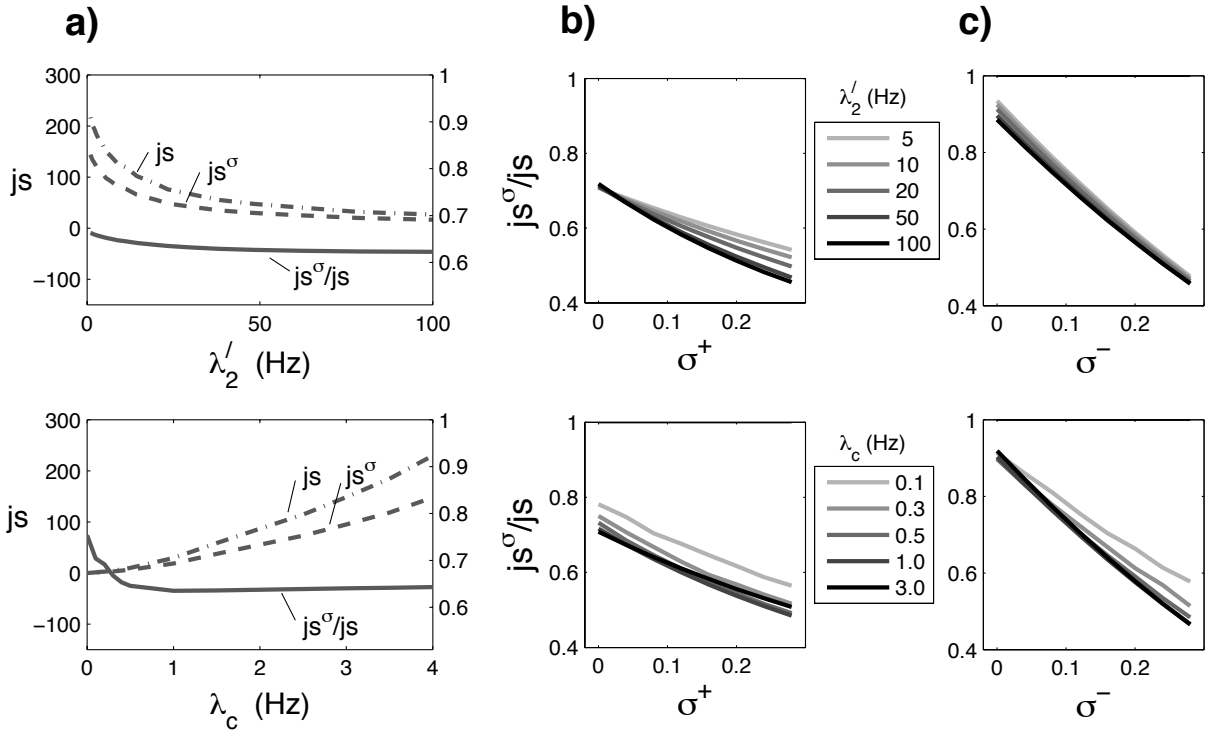

Figure 10: Significance of synchronization: before and after spike sorting and their relation. Same parameters as in Fig. 9. (a) Joint-surprise before (js, dashed-dotted line) and after sorting (js^σ, dashed line) and their ratio (js^σ/js, axis on the right) as a function of backgound firing rate $\lambda_2^{'}$ (top) and of injected coincidence rate λ_c (bottom). (b) js^σ/js as a function of σ^+ and (c) as a function of σ^-, both for different $\lambda_2^{'}$ (top) and λ_c (bottom).

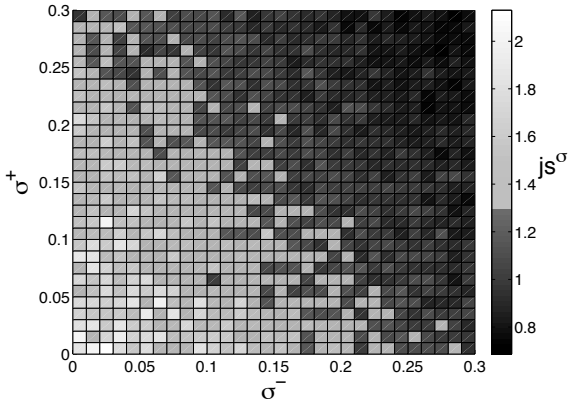

Figure 11: Example of loss of significance due to sorting errors. Two simultaneous spike trains are simulated with background rates $\lambda_1' = \lambda_2' = 20$ Hz and a coincident rate of $\lambda_c = 0.15$ Hz. Duration of the simulation $T = 10^5$ ms, time resolution $\delta = 1$ ms and 50 repetitions for each parameter setting of the error rates. Each bin in the matrix corresponds to a set of parameters σ^- (horizontal axis) and σ^+ (vertical axis), both varied from 0 to 0.3 in steps of 0.01. The original joint-surprise value without any sorting errors (bottom left corner) is $\bar{js} = 1.9 \pm 1.2$, i.e. well above the 5% level which corresponds to a value of $js = 1.28$ (switch dark to light in color bar). Increasing levels of sorting errors cause the significance js^σ to progressively decrease (from left to right and bottom to top). Light values represent js^σ above, dark values below significance threshold of 5%.

increase with increasing λ_c, the ratio also decreases, since js^σ is always smaller than js and does not increase as much as js.

Fig. 10b,c shows the dependence of the ratio js^σ/js on the error rates (in b) for σ^+, in c) for σ^-) under variation of the firing rate (top) and variation of the coincidence rate (bottom). As already shown in Fig. 8, the relation decreases with error rates, and we see here that the firing and coincidence rates are only slightly modifying the slopes. The dominating parameters are the error rates.

In summary, as a general result we observe that sorting errors always reduce the significance, irrespective of the error type, and mostly independent of the physiological parameters. Fig. 11 shows an example where the originally significant synchronization is changed due to the sorting errors to an unsignificant result.

[6].4 Discussion

[6].4.1 Sorting errors reduce significance of spike synchrony

We studied the influence of spike sorting errors on the analysis of unitary events. Our statistical model of spike sorting is based on the assumptions that false positive and false negative errors are likely to occur at any instant in time and independently for the two neurons. As a consequence, sorting errors lead to erroneous statistical rate estimations, as well as to erroneous coincidence counts and erroneous significance of the latter. In order

to understand the influence of these errors on the significance estimation of coincident spikes, we derived analytically the predicted and the empirical number of coincidences after sorting as compared to their original values before sorting. In addition we also tested, both analytically and through simulations, the influence of physiological parameters like the firing rate of the neurons and the coincidence rate. We showed that the joint-surprise reduces with error rates, finally leading to a loss of significance of originally significant spike synchronization. It turned out, that the significance of spike synchronization is always reduced by sorting errors irrespective of the error type. This also holds for non-symmetrical combinations of error rates experienced by the two neurons, however with less strong reduction of the significance as compared to the symmetrical case. The reduction of significance is mainly due to the "normalization" of the observed coincidence counts by comparison to their expected number. However, the reason for significance reduction is different for the different error types.

False positive spikes lead to an increase of the empirical as well as of the expected number of coincidences. Most interestingly they even increase by the same absolute amount, which is due to additional chance coincidences only. The difference between the two measures are the "excess coincidences", whose relative amount reduces, thus leading to a decrease in significance.

Missing spikes (FNs) reduce the number of expected coincidences as well as the empirical number. The expected number is reduced due to decreased firing rates. The empirical number in addition experiences a reduction of the excess coincidences (first term in Eq. 6.14). Therefore the significance reduces (Fig. 7, solid lines). The impact of FNs on synchronized spikes is strong (for error rates found by Harris et al. (2000) the joint-surprise may be reduced by 40%, cf. also Fig. 8), which is explained by the fact that the loss of only one spike of a synchronized event already leads to the loss of the coincidence. Furthermore, the higher the coincidence rate, the larger the chance to miss a spike, and thus the larger the reduction of the empirical coincidences (see Fig. 9a,b, bottom). In summary, a conservative sorting strategy, i.e. rather missing a spike than capturing a wrong one, might lead to a stronger loss of detectability of originally existing significant synchronization.

Co-occurrence of both error types may lead to partial (for $\sigma^- \neq \sigma^+$) or even to full cancellation (for $\sigma^- = \sigma^+$) of change of the expected number of coincidences after sorting. Depending on the net excess of errors the expected number may be increased (for $\sigma^- < \sigma^+$) or decreased (for $\sigma^- > \sigma^+$). For the empirical number, the errors may not cancel in respect to the number of excess coincidences. Excess coincidences may be deleted by FNs, but cannot be created by FPs, since newly created coincidences enter as chance coincidences only. In addition, the probability for generating chance coincidences is much smaller than the impact of injected coincidences (cf. Eq. 6.17 and 6.18), and thus the effects on the significance are not canceled in case $\sigma^- = \sigma^+$ (see also Fig. 8). Interestingly, the available literature on the relative amounts of both errors documented a tendency towards higher values of FNs as compared to FPs (Harris et al., 2000; Wood et al., 2004), indicating a preference for conservative strategies. Thus one may conclude that neural synchronization is typically underestimated.

[6].4.2 Relation to cross-correlation

The cross-correlogram is a widely used method for estimating the correlation between the spiking activities of two neurons (Perkel et al., 1967b). The method allows to study zero-lag and delayed coincidences. The unitary event analysis method concentrates on zero-lag (or near-coincident) events and may be directly compared to the zero-lag (or near-by) bins of the cross-correlogram. Cross-correlograms are often used without any normalization and just provide the empirical coincidence counts (raw cross-correlation). In addition, normalization procedures are availabe, that account for the expected number of coincidences given the firing rates of the neurons (cross-covariance) by subtracting the latter from the empirical counts. Normalizing this number to the product of the variances of the single processes yields the correlation coefficient (for an extensive discussion and comparison of such measures see Aertsen et al., 1989). Thus, the zero-bin correlation coefficient in our variables reads $r = \frac{n_{\mathrm{emp}} - n_{\mathrm{pred}}}{\sqrt{\delta \cdot \lambda_1}\sqrt{\delta \cdot \lambda_2}}$. This measure behaves very similarly to the joint-surprise, however with different abolute numbers.

Let us emphasize that correlation analyses which only consider the raw (i.e. empirical) coincidence counts, e.g. like in an uncorrected cross-correlogram, would find increased synchronization in the case of FPs. However relating the observed number of coincidences to the expected ones, as done in the UE analysis (Grün et al., 2002a,b; Grün et al., 1999) or by the correlation coefficient, corrects for that.

[6].4.3 Experimental situations that violate UE assumptions

Inherent assumptions of the unitary event analysis are stationary Poisson processes. However, experimental data typically do not fulfill these assumptions and methods to account for non-stationary (Grün et al., 2002b; Grün et al., 2003b) and non-Poisson processes (Pipa et al., 2003; Pipa and Grün, 2003; Pipa, 2001, 2006) have been worked out.

In case of non-stationary processes in time the solution to avoid false positives is to perform the analysis in sliding window fashion to account for the change in rate (Grün et al., 2002b). In case of non-stationarity across trials, the expected number of coincidences is calculated within the sliding window in a trial-by-trial manner and then summed yields the correct estimate for the expected number of coincidences (Grün et al., 2003b). By doing that we account for non-stationary firing rates. A change in brain state or different behavioral variables could lead to coherent change of neuronal firing rates, e.g. by a common increase in the membrane potentials as discussed in Brody (1998). In the same way as the firing rates co-vary the amount of chance coincidences do: the larger the firing rates the more chance coincidences. As discussed before such a case is well treated by the unitary event method which is specifically designed to evaluate the degree of excess synchrony as compared to chance synchrony and to estimate its significance, also under non-stationary conditions.

Sorting errors like the loss of coincident spikes due to an overlap of the spike waveforms, would trivially covary with covariation of the rates. However, treating the data in segments of stationary firing rates, we are per segment in a stationary situation which is discussed below (Section [6].4.4.2).

In Grün et al. (2002a) we have shown that the unitary event analysis method reacts robustly to non-Poissonian point processes that were simulated as Gamma processes.

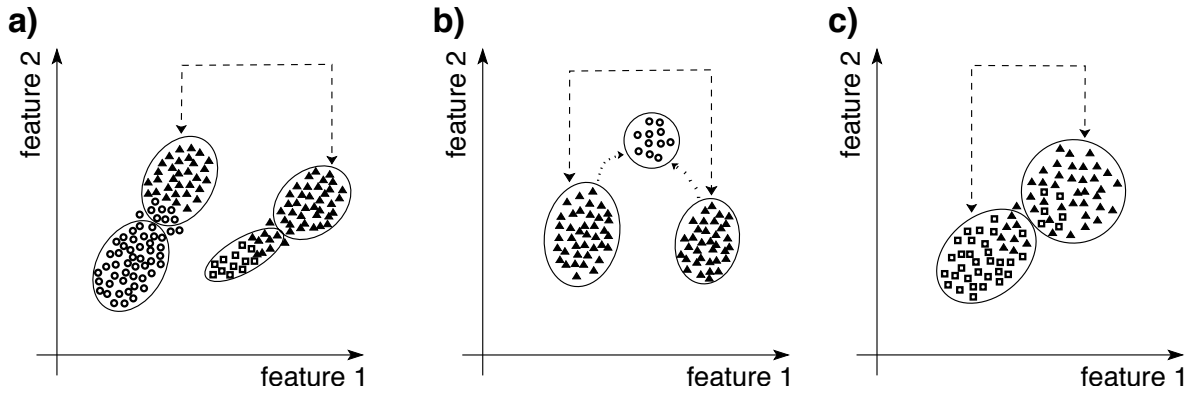

Figure 12: Experimentally relevant cases of spike sorting. Sketch of possible origins of spike sorting errors due to specific cluster configurations in the space of two spike-waveform features. Triangles, squares and circles represent spikes, contours represent putative clusters, and dashed lines indicate the two neurons whose correlation is analyzed. a) Due to the presence of other neurons they may erroneously provide (FP error; circles in upper left cluster) or "steal" (FN error; triangles in lower right cluster) spikes to/from the neurons under consideration. b) Ghost cluster. A significant amount of overlapping spikes originating from the two neurons under consideration for correlation analysis, gives rise to a ghost cluster (middle cluster containing circles), which "steals" coincident spikes from the two neurons. c) Correlated errors. The neurons being analyzed are recorded from the same electrode and their cluster separation is poor, indicated by squares from the left cluster mixing with triangles in the right cluster, and vice versa. Therefore a number of spikes are assigned from one neuron to the other and vice versa, resulting in false negatives of one neuron that become false positives in the other.

Although the auto-correlation structure of the spike trains affects the shape of the coincidence distribution, it turned out that assuming a Poisson distribution -as analytically derived for Poisson spike trains (Grün et al., 2002a)- leads to conservative estimates for experimentally found ranges of the shape factor (Pipa, 2001, 2006).

We also performed the analysis for the dependence of FN and FP sorting errors for the case of Gamma processes (not shown here) and found no differences in the results. FN and FP errors applied to Gamma processes also lead to a reduction of the sigificance as in the case of Poisson spike trains.

[6].4.4 Typical errors in sorting

Now we shall relate our considerations to typical experimental cases, thus eventually abandoning the model hypotheses of independent errors and neurons recorded from different electrodes. Furthermore we will also discuss this in the framework of cluster analysis in spike-waveform feature space.

[6].4.4.1 Independent sorting errors

Here we investigate the correlation between two neurons, each of which experiences FN or FP errors from other, unrelated neurons. This is the case if we consider two neurons that were recorded and sorted from two different electrodes. It may also be the case for two

neurons that are recorded from the same electrode and are well sorted, but one or both neurons experience errors due to yet other neurons (see Fig. 12a). This is actually the case we studied in the framework of our statistical sorting model, and learned that irrespective of the error type the resulting significance is reduced. The reduction is strongest for the case that both neurons experience the same degree of errors, but not as pronounced if one of the neurons experiences a smaller amount of errors than the other. If only one neuron is exposed to errors, the reduction of significance is even smaller (Fig. 6, all upper joint-surprise curves).

In the case of a rather conservative sorting strategy, i.e. if one tries to catch as little FPs as possible thereby accepting the danger of loosing spikes (i.e. having more FNs), the significance is more reduced than for the case of a rather tolerant sorting strategy. The latter would represent the case if one tries to catch as many spikes as possible while accepting false positives. In the cluster space of a given sorting algorithm, a conservative sorting strategy would correspond to accepting only spikes from within a radius smaller than the outer bound of the cluster of points, whereas a tolerant sorting strategy would take spikes from a radius catching all the points in the cluster of points. Schmitzer-Torbert et al. (2005) suggested measures for cluster quality. The L_{ratio} measures the amount of noise observed in the vicinity of the cluster. The authors showed that a high value of the L_{ratio} correlates with a high number of FNs, the case we would call conservative sorting.

Directly related to our study is the work by Bedenbaugh and Gerstein (1997) and Gerstein (2000) who evaluated the correlation coefficient as a measure for synchrony between unresolved multi-neuron recordings. They assumed the activities recorded on each of the two electrodes to be mixtures of spiking activities of up to three neurons which may fire independently or include correlations. The focus is on the resulting correlation between the multi-neuron recordings from two electrodes as functions of the original correlation of neurons across electrodes and as functions of correlations between neurons at a single electrode. Thus mixtures of spikes trains are studied which in our scenario may be interpreted as false positives, but the framework neglects the problem of missing spikes. Under specific parameter settings, Gerstein's (2000) results are directly comparable to ours. He also found that the resulting correlation between spike trains that experienced contamination with uncorrelated spikes is reduced as compared to the original, distant correlation between two neurons.

[6].4.4.2 Overlapping spikes

Another relevant situation in spike sorting is that coincident spikes of two neurons recorded at the same electrode may overlap in time such that the resulting waveform may result in the formation of a ghost cluster (Fig. 12b, cluster that includes circles). As a result, the simultaneous spikes are systematically removed from the two spike trains under consideration.

The work by Bar-Gad et al. (2001b) studied the influence of missing coincident spikes onto the cross-correlation measure, under the specific condition that a spike is followed by a noticable dead time, and neurons have high firing rates. Under these conditions they found that the shape of the cross-correlation function alters: zero-delay coincidences were lacking, but close delayed coincidences were enhanced as compared to background. Corrections for expectancy were not performed. Thus, in our words, they studied the

influence of false negative coincidences and found for the case of zero-delayed coincidences a reduction in their numbers.

In our framework this case can be represented as a specific deletion of coincident spikes. As a consequence, the empirical number of coincidences is reduced by a fraction σ^-_{coinc}: $n^{\sigma}_{\text{emp}} = \left(1 - \sigma^-_{\text{coinc}}\right) \cdot n_{\text{emp}}$. Compared to the case where FN errors are independently applied to both neurons, case which leads to quadratic dependence on σ^-_{coinc} (substitute in Eq. 6.14 σ^-_i by σ^-_{coinc} and set $\sigma^+_i = 0, i = 1, 2$), here the deletion of coincident events leads also to a reduction of the empirical coincidences, but with a slope that is less steep. On the other hand, with increasing σ^-_{coinc} the expected number is also decreased, however by a smaller amount as compared to independently applied FN errors (Eq. 6.10), since here only spikes that are involved in coincidences may be deleted. The expected number of coincidences then reads: $n^{\sigma}_{\text{pred}} = (\lambda_1 - \lambda_{\text{del}}) \cdot (\lambda_2 - \lambda_{\text{del}}) \cdot \delta^2 \cdot N$, with $\lambda_{\text{del}} = \frac{n_{\text{emp}} \cdot \sigma^-_{\text{coinc}}}{T}$ the spike reduction rate. As a result, also in the case of a joint deletion of coincident spikes, the joint-surprise decreases, even with a similar slope as for the case of independent FN errors.

[6].4.4.3 Overlapping clusters

Another problem that may arise if different neurons are recorded and sorted from the same electrode is, that spikes from one neuron may be assigned to another neuron. Quirk and Wilson (1999) discussed such a case for bursting neurons, where late spikes in a burst were different in shape and thus were wrongly assigned to the other neuron. Using cross-correlation analysis for the identification of correlation between the spiking activities of the two neurons, they found artificially increased delayed coincidences. Although their case does not apply to zero-bin correlations, the case that spikes of one neuron are assigned to another is of general interest.

This type of correlation errors can be expressed in our framework as FNs of one neuron become FPs of the other. The empirical number of the coincidences will stay the same, since coincidences will not be created by moving spikes to the other spike train, nor will spikes of coincidences be moved to the other neuron since that would correspond to another waveform (overlapping spikes). Thus, only the expected number of coincidences is influenced: $n^{\sigma}_{\text{pred}} = (1 - \sigma^1)\lambda_1 \cdot (1 + \sigma^1)\lambda_2 \cdot \delta^2 \cdot N$, with σ^1 the probability of assigning spikes to a wrong cluster. This leads to a decrease of the expected number of coincidences, and consequently the significance of the empirical coincidences increases with error rate.

A related case is if waveforms lead to overlapping clusters of entries in the feature space (Fig. 12c), a case indicated as of bad separation of clusters using the isolation distance measure suggested by Schmitzer-Torbert et al. (2005). If anyway spikes are assigned to distinct clusters, there is a high likelyhood to get false negative and false positive errors. Spikes from one cluster may be assigned to the other, i.e. FNs of the first become FPs of the other, and also vice versa. Thus errors will occur in both directions. The empirical number of coincidences will not be affected by that, for the same reasons as discussed for the one-way case above. However, the expression for the expected number of coincidences will get additional terms expressing the probability for FNs from the second cluster becoming FPs in the first (via σ^2): $n^{\sigma}_{\text{pred}} = (1 - \sigma^1 + \sigma^2)\lambda_1 \cdot (1 + \sigma^1 - \sigma^2)\lambda_2 \cdot \delta^2 \cdot N$. As a result the error rates may partly compensate each other and thereby leading to a

less strong increase of the resulting joint-surprise as compared to the one-way case.

In summary, correlated errors specifically may occur if different neurons are recorded and sorted from a single electrode. Overlapping spikes may be assigned to a third cluster, thereby leading to a loss of empirical coincidences. As a consequence the measured significance is reduced and the underlying existing correlation between neurons may be overseen. Correlation analysis of the activities of two neurons that experienced wrong assignments of spikes from one neuron to the other (and/or vice versa) is dangerous. The detected significance is prone to indicate false positive correlation. Specifically the case when only one of the neurons is giving spikes to other.

[6].4.5 Conclusions

Spike sorting introduces two types of errors into the coincidence count: false positive and false negatives. If errors were experienced independently, they both lead to a reduction of the measured significance as compared to the original correlation between the two neurons. The reason for the reduction is different for the two cases. False negatives simply partly delete correlated spikes. However, false positives may increase the correlation, and correlation measures that do not correct for expectation by chance may conclude false positive correlation.

If spike trains are sorted from a single electrode, also correlated sorting errors may occur, e.g. coincident spikes that are ignored due to overlapping waveforms, or spikes that are assigned from one neuron to another. In particular the latter is problematic if one is interested to detect spike correlation between the two neurons involved, since there is the danger of detecting false positive correlation. Therefore we rather suggest to avoid correlating neuronal spiking activity recorded from the same electrode combined with low quality of cluster separation. However, for errors resulting from a neuron not considered, this scenario leads to a reduction of significance and thus rather to an underestimation of the underlying correlation.

One main aspect is guiding our future work in this context. The unitary event analysis was designed to allow for the detection of neuronal assemblies and thus for correlation analysis of more than two neurons at a time. As a consequence we aim to understand how spike sorting errors influence the analysis of higher-order spike patterns. This includes to evaluate systems with more than two simultaneous recordings, which involves a combinatorial increase of cases to consider.

In conclusion, if one is interested in neuronal interaction in the brain, the activities of single units need to be simultaneously observed and analyzed for correlated activity. Therefore spike sorting is an important, intermediate statistical analysis for extracting the single unit activities. Subsequent analysis may be considerably influenced by sorting errors, and may arrive at wrong conclusions. In this work we have shown that for the unitary event analysis, independent sorting errors lead to reduced significance, but not to artificial correlation.

Acknowledgments

Supported in part by the Volkswagen Foundation, the Stifterverband für die Deutsche Wissenschaft and the BMBF Bernstein Center for Computational Neuroscience Berlin (grant 01GQ0413). We also thank Markus Diesmann for useful comments on an earlier version of the manuscript. Also we thank the anonymous reviewer for useful comments for further improvements of the manuscript.

Appendix

Rewriting Eq. 6.14 yields:

$$n^{\sigma}_{\text{emp}} = \left(1-\sigma_1^-\right)\left(1-\sigma_2^-\right)\cdot[n_{\text{emp}}-n_{\text{pred}}]+\left(1+\sigma_1^+-\sigma_1^-\right)\left(1+\sigma_2^+-\sigma_2^-\right)\cdot n_{\text{pred}} \quad . \tag{6.14}$$

After sorting, the experimental spike trains contain FP and miss FN spikes (cf. Fig. 5b, bottom). The former occupy bins that were empty, whereas a fraction of currently empty bins was previously occupied by the latter. We introduce the probability $p_i(+)$ to find a FP spike in a bin and the joint probability $p_i(-,\text{spike})$ to miss a spike as FN:

$$\begin{aligned} p_i(+) &= \sigma_i^+ \cdot \lambda_i \delta \\ p_i(-,\text{spike}) &= \sigma_i^- \cdot \lambda_i \delta \quad , \end{aligned}$$

where λ_i are the original firing rates of neuron i and δ the bin width. We will refer to the two neurons through the indices i, j, where $i \neq j$. These expressions are not symmetrical because they refer to intrinsically different generating processes: insertion of *new* spikes (FPs) versus deletion of *already existing* spikes (FNs). In the following we also need the expression for the conditional probability of missing a given spike $p_i(-|\text{spike})$. Using Bayes theorem we obtain $p_i(-|\text{spike}) = \frac{p_i(-,\text{spike})}{p_i(\text{spike})} = \sigma_i^-$. It follows that the probability for a (given) spike not to be missed equals $(1-p_i(-|\text{spike})) = 1-\sigma_i^-$.

The number of coincidences after sorting can be expressed as the sum of the original number of coincidences plus two additional terms, which correct for the erroneously missed and produced coincidences due to sorting:

$$n^{\sigma}_{\text{emp}} = n_{\text{emp}} - n^{\mathsf{FN}} + n^{\mathsf{FP}} \quad . \tag{6.A1}$$

The first of these additional terms is composed of three contributions. The first two are given by the probability that either one of the two coincident spikes is missed: $p_i(-|\text{spike})\cdot(1-p_j(-|\text{spike})) = \sigma_i^-\left(1-\sigma_j^-\right)$. The last term is the probability that both spikes are missed as FNs: $p_i(-|\text{spike})p_j(-|\text{spike}) = \sigma_i^-\sigma_j^-$. This results in:

$$n^{\mathsf{FN}} = n_{\text{emp}} \cdot \left[\sigma_i^-\left(1-\sigma_j^-\right) + \sigma_j^-\left(1-\sigma_i^-\right) + \sigma_i^- \cdot \sigma_j^-\right] \quad . \tag{6.A2}$$

Similarly, the number of false coincidences introduced by sorting errors (n^{FP}) receives contributions from three terms. Again, the first two terms are given by the probability that a FP is synchronous to an already existing spike, i.e. the product of the probability of a false positive in neuron i ($p_i(+)$) and the probability that in neuron j an original spike existed and survived

$$p_j^{\sigma^-} = p_j\left(1-p_j(-|\text{spike})\right) = \lambda_j\delta(1-\sigma_j^-) \quad ,$$

with p_i defined in Eq. 6.1. This yields: $p_i(+)p_j^{\sigma^-} = \lambda_i\lambda_j\delta^2\sigma_i^+\left(1-\sigma_j^-\right)$. The last term consists of the probability of a coincidence of FP spikes: $p_i(+)p_j(+) = \lambda_i\lambda_j\delta^2\sigma_i^+\sigma_j^+$. In total we obtain:

$$n^{\mathsf{FP}} = n_{\text{pred}} \cdot \left[\sigma_i^+ \left(1 - \sigma_j^-\right) + \sigma_j^+ \left(1 - \sigma_i^-\right) + \sigma_i^+ \cdot \sigma_j^+\right] \quad , \tag{6.A3}$$

We notice here that $\lambda_i \lambda_j \delta^2 N = n_{\text{pred}}$ (Eq. 7.15) and that the factor at the right-hand side of Eq. 6.A3 can be expressed as:

$$\sigma_i^+ \sigma_j^+ + \sigma_i^+ \left(1 - \sigma_j^-\right) + \sigma_j^+ \left(1 - \sigma_i^-\right) = (1 - \sigma_i)(1 - \sigma_j) - \left(1 - \sigma_i^-\right)\left(1 - \sigma_j^-\right) \quad , \tag{6.A4}$$

where we used again $\sigma_i = \sigma_i^- - \sigma_i^+$. After substituting Equations 6.A2 and 6.A3 in Eq. 6.A1 and rearranging we obtain the relation for n_{emp}^{σ} in Eq. 6.14.

7 Transition between spike patterns induced by spike sorting errors in multi-unit recordings

Antonio Pazienti and Sonja Grün

The manuscript constituting this section is going to be submitted for publication.

[7].1 Introduction

In neurophysiological multi-unit recordings the activity of a set of neurons is recorded by means of arrays of electrodes. This technique has become widely utilized over the last decade. Indeed, it has become clear that in order to identify the brain's network composition and its functions multiple cells have to be recorded in parallel, to detect temporal features of the signals and dependences between neurons (Buzsáki, 2004).

Spike sorting is a necessary intermediate step for those, who aim at identifying the single-unit activity, i.e. the activity of single cells (Lewicki, 1998). The spike activity is embedded in a large noise-like signal of rich and complex frequency content, presumably consisting of the activity of more distant cells and of extracellular- and measurement-noise (Lewicki, 1998). Spike sorting typically consists of two stages: first, spike waveforms originating from different neurons are identified and separated from the background extracellular noise; second, spikes are classified, i.e. assigned to putative neurons. In both these stages, due to the intrinsic difficulty of the task, imperfect identification and/or classification of the original spikes emitted by the neurons may occur. Failures are of two types: false negative (FN) and false positive (FP) errors. Taking the perspective of a particular neuron, a false positive spike is a spike which is assigned to that neuron despite having originated in another neuron or being extracellular noise. Conversely, a false negative spike was emitted by the neuron and successively unclassified or misclassified. Furthermore, due also to the specificities of different brain tissues, and although current electrode arrays provide recordings from tens to hundreds of cells, and thus big amounts of data have to be processed per recording's day, there is no standard way of performing spike sorting. The results are often sorter-dependent and hard to compare and/or reproduce (Harris et al., 2000).

A variety of techniques and algorithms are available for spike sorting (see e.g. Lewicki (1998) for the most recent review). They range from traditional (partly) supervised methods (Harris et al., 2000; Takahashi et al., 2003b,a, 2002) to fully automatic algorithms (Bar-Hillel et al., 2006; Horton et al., 2007; Hyvärinen and Oja, 2000; Quian Quiroga et al., 2004). The choice of the best algorithm for this task depends on a number of factors, like e.g. the electrode, the brain area, cell type of interest, etc. Additional constraints for sorting methods are reasonable computation time, available hard-disk space, compatibility with the recording setup and software, and finally also the intended subsequent data analysis. Major problems in spike sorting are e.g. the difficulty to resolve overlapping

spikes and the variability of the spike waveform (Fee et al., 1996; Quirk and Wilson, 1999; Harris et al., 2000). Attempts to solve some of them have been documented in the recent literature (Pouzat et al., 2002; Zhang et al., 2004; Pouzat et al., 2004; Bar-Hillel et al., 2006; Wang et al., 2006). A few studies have quantitatively shown the amount of FN and FP errors introduced by sorting (Wehr et al., 1999; Harris et al., 2000). Average error rates of 6.2% for FPs and 15.9% for FNs (Harris et al., 2000), and 3.5% for FPs and 2.8% for FNs (Wehr et al., 1999) were reported. Wood et al. estimated average error rates of 23% FPs and 30% FNs based on simulated data (Wood et al., 2004). To address the problem of the comparability of the results, a number of objective controls of the spike sorting have been proposed over the last years (Pouzat et al., 2002; Schmitzer-Torbert et al., 2005; Smith and Mtetwa, 2007).

The aim of this work is to evaluate the effect of spike sorting errors on spike correlation measures. The question we will answer is: how robustly and reliably is the significance of correlated neuronal activity estimated when spike sorting errors are affecting the data? For this purpose we developed a model that introduces FN and FP failures in a realistic fashion into multiple point processes containing correlations, thus mimicking the effect of spike sorting on simultaneously recorded spike trains. In our study we distinguish between the *order* ω of the correlations and their *complexity* ξ. The order of the correlation refers to the size of the subset of neurons containing a priori known correlated activity. In particular, the processes are modeled in the following way: 1) in a subset of ω out of the N neurons we inserted exactly coincident spikes (patterns of order ω); 2) the remaining $N-\omega$ processes are statistically independent; 3) all processes follow a Poisson distribution of same firing rate. An example is sketched in Fig. 13A depicting the original activity of N processes containing correlations of order $\omega = 3$ (gray processes). The measures of synchronization we study here are two standard methods for establishing the significance of synchronous firing –the normalized correlation coefficient (CC) and the unitary event (UE) analysis (Perkel et al., 1967a,b; Grün et al., 2002a,b). Both these measures rely on the count of the number of coincidences occurring among subsets of neurons. However, by looking at Fig. 13A it is visible that inserted triplets are undistinguishable from other spikes. A pattern of activity involving ξ neurons synchronously firing and $N - \xi$ not firing is said to have complexity ξ. This variable is therefore "experimental", i.e. lacking knowledge of the model that was used to generate the patterns. In the example of Fig. 13A, three patterns of complexity $\xi = 2, 3, 4$ respectively (right), and their occurrence in the processes (bottom) are shown.

We will show an analytical derivation of the number of predicted and empirical coincidences after sorting, as well as for the CC, and their relation to the original values (i.e. before sorting). Our results offer an analytical framework of the impact of sorting errors, that can be utilized for other data analysis measures as well. Furthermore, we show that sorting failures alter the processes' statistics, and affect not only the significance of the underlying correlations, but also of the correlations of other complexities and can strongly bias the results. Higher-order effects may come into play when studying correlation involving more than two neurons.

This article is organized as follows. Sections [7].2 and [7].3 introduces statistical models for sorting errors and for generation of correlated processes. In Section [7].4 we will introduce the expected and empirical number of coincidences as are the relevant measures

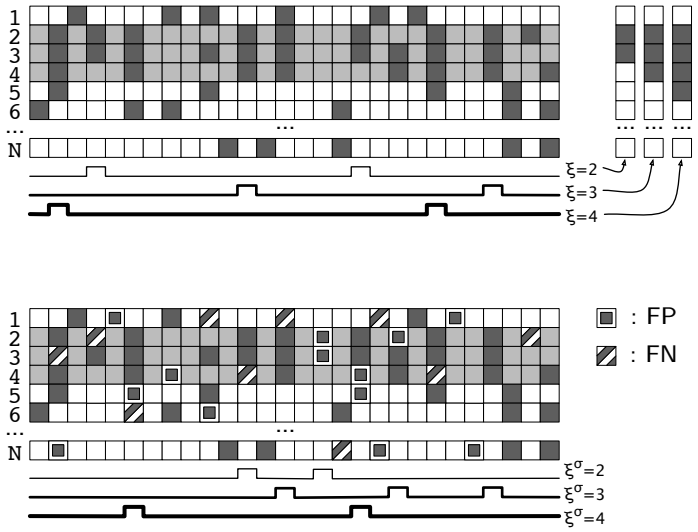

Figure 13: Activity of N simultaneous spike trains with correlation of order $\omega = 3$ inserted. A original activity; shadowed processes are correlated through inserted triplets, white processes are independent and colored squares represent spikes. Right, three patterns are shown of complexity $\xi = 2, 3, 4$ respectively. Bottom, the counting procedure of the patterns along the spike trains. B activity after spike sorting. The same processes as in A are distorted with insertion (FP, small squares) and deletion of spikes (FN, striped squares). Bottom, count of the same patterns as in A, now after spike sorting.

for our study, and derive their analytical expressions after having applied sorting failures. Cross-correlation function and unitary event analysis will be briefly introduced in Section [7].5. Results on the effects of spike sorting will then be discussed in detail in Secs. [7].5.1 and [7].5.2. Finally, Section [7].6 is dedicated to the discussion.

[7].2 Model of correlated point processes

Given a set of N simultaneously recorded neurons, we depict their firing activities in a certain time epoch as sequences of T time bins of length δ either containing a spike or being empty. We will assume in all of the following the time epoch to be short enough for the activity to be considered stationary. The probability of firing $p_i, i = 1, \ldots, N$, i.e. the bin occupation probability is defined as $p_i = \text{Prob}_i(\textbf{spike})$. Conversely, $1 - p_i = \text{Prob}_i(\textbf{no spike})$ is the probability that the bin contains no spike. Let us also define $n_{v^\xi}(\xi, N)$ as the number of coincidences of complexity $\xi \in \{2, ..., N\}$ of the pattern v^ξ. The latter is composed of ξ neurons firing and the remaining $N - \xi$ not firing. More specifically, v^ξ is one specific of the $\binom{N}{\xi}$ possible patterns obtained by permutations of the symbols **spike** and **no spike**. For example, on the bottom of Fig. 13A the counting procedure is shown for the three patterns $v^{2,3,4}$ (these are shown on the right). We will refer to $n_{v^\xi}(\xi, N)$ also as the *empirical number of coincidences* and often drop the index v^ξ. However it should be clear that we always refer to specific patterns of that complexity.

In order to construct processes containing correlations of order ω we firstly insert simultaneous spikes (i.e. in the very same time bin) into a subset of ω processes according

to a Poisson process with rate p_c. In the example shown in Fig. 13A correlations of order $\omega = 3$ are inserted, and the processes {2,3,4} contain six of such coincident triplets. Secondly, we also insert random spikes into the correlated processes, as "background" spikes, which occur also according to Poisson processes with rate p_i''. Thus these processes have total rate $p_i = p_i'' + p_c$ (where $i \in \{\text{correlated processes}\}$, $i = 2, 3, 4$ in the example shown in Fig. 13A). The remaining $N - \omega$ processes are independent realizations of Poisson processes of rate p_i', i.e. here the total rate is the background rate ($p_i = p_i'$, where $i \in \{\text{independent processes}\}$, $i \neq 2, 3, 4$ in the example of Fig. 13A). Our example illustrates that even if we would count the occurrences of the pattern v^ξ for which 1) $\xi = \omega$ and 2) neurons $i, i \in \{\text{correlated processes}\}$, the number of patterns will not match the number of inserted coincidences. Due to random firing of the independent neurons some of the inserted coincidences might end up in patterns of higher complexity (and thus be counted as different patterns). On the other hand the independent background firing in the correlated neurons might produce some ω-coincidences, which are indistinguishable from the inserted ones.

After spike sorting failures occur as FN and FP errors (see next section), a scenario as depicted in Fig. 13B results. Here, missed spikes (FN, striped) and falsely assigned spikes (FP, small squares) modify the processes. Furthermore, some of the coincidence patterns may thereby be modified, and as a consequence the number of patterns of a given complexity $n(\xi, N)$ may be affected. We define as $n^\sigma_{v^{\xi^\sigma}}(\xi^\sigma, N)$, or simply $n^\sigma(\xi^\sigma, N)$, the number of coincidences of complexity after sorting ξ^σ. The relationship between $n^\sigma(\xi^\sigma, N)$ and $n(\xi, N)$ will be derived in Sec. [7].4.1.1.

[7].3 Model of spike sorting errors

Here we formulate a stochastic model of spike sorting. Two basic assumptions are made in our model: 1) errors occur homogeneously along a spike train and 2) independently for each neuron. The latter assumption corresponds to saying that neurons whose correlations are analyzed are recorded on different electrodes, which is typically the case. Indeed, due to the difficulties to correctly identify and classify overlapping spikes, correlations between neurons recorded on the same electrode are often missed or strongly reduced.

The effect of applying our model is depicted on a single bin in Fig. 14. Here we see a tree view of the occupation (from top to bottom) of a bin belonging to neuron $i, i \in \{1, ..., N\}$. The initial state is an empty bin (top). An emitted spike (filled bin) has a chance to be missed as false negative (striped bin) or can "survive" spike sorting errors, i.e. be correctly classified. Conversely, a false positive (small square) may occur and occupy an empty bin. In our model, both error types can not occur at the same bin. Each arrow connecting two neuron states in Fig. 14 comes along with its transition probability. Thus the possible bin states are:

- the bin contains a spike, which was correctly detected and classified to neuron i (referred to as **spike**);
- the bin doesn't contain any spike, but it used to contain one. The spike is a false negative, i.e. a spike that was not assigned correctly to the neuron under consideration, but either to another neuron or discarded as noise (**FN**);

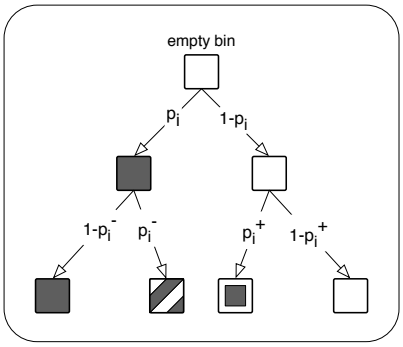

Figure 14: Statistical model of spike sorting errors. Flowchart of occupation process of a single bin i and effects of sorting errors on the bin. Arrows are associated with the corresponding conditional probability of transition from source to target bin. Top row: initially empty bin. Middle row: original activity; bin is occupied by a spike (with probability of firing p_i) or is empty ($1 - p_i$). Bottom row: possible experimental states of the bin; given a spike, it is missed as FN (correctly classified) with probability $p_i^- \cdot (1-p_i^-)$. Given no spike, a FP occurs with probability p_i^+ and the bin stays empty with probability (p_i^+). The probabilities of the four experimental states can be calcutated by multiplying the conditional probabilities from top to bottom (see also text).

- the bin contains a spike, however not an original spike from neuron i, but a false positive spike (**FP**);
- the bin does not contain any spike because neuron i did not emit a spike, nor a FP spike is found here (**no spike**).

As introduced above, p_i is the original probability of firing of neuron i in a bin. We define $p_i^\sigma, i = 1, ..., N$ as the firing rates after sorting. To derive it we now introduce two further conditional probabilities: the probability p_i^+ that given an originally empty bin is now occupied by a FP, and the probability p_i^- that given a spike it is now missed as FN. More formally:

$$P_i(\textbf{FP}|\textbf{no spike}) = p_i^+ \ , \tag{7.1}$$
$$P_i(\textbf{FN}|\textbf{spike}) = p_i^- \ , \tag{7.2}$$

where $i = 1, ..., N$ are the neuron ids. From here follow the conditional probabilities of firing (not being missed as FN) or not firing (nor being FP), respectively:

$$P_i(\textbf{no FN}|\textbf{spike}) = 1 - p_i^- \ , \tag{7.3}$$
$$P_i(\textbf{no FP}|\textbf{no spike}) = 1 - p_i^+ \ . \tag{7.4}$$

To obtain now the total probabilities to obtain one of the final states, we simply multiply the branches shown in Fig. 14 that lead to that specific state. We obtain:

$$P_i(\textbf{spike}) = P_i(\textbf{no FN}, \textbf{spike}) = P_i(\textbf{no FN}|\textbf{spike}) \cdot p_i = (1 - p_i^-) \cdot p_i, \tag{7.5}$$
$$P_i(\textbf{FN}) = P_i(\textbf{FN}, \textbf{spike}) = P_i(\textbf{FN}|\textbf{spike}) \cdot p_i = p_i^- \cdot p_i \tag{7.6}$$
$$P_i(\textbf{FP}) = P_i(\textbf{FP}, \textbf{no spike}) = P_i(\textbf{FP}|\textbf{no spike}) \cdot (1 - p_i) = p_i^+ \cdot (1 - p_i) \tag{7.7}$$
$$P_i(\textbf{no spike}) = (\textbf{no FP}, \textbf{no spike}) = P_i(\textbf{no FP}|\textbf{no spike}) \cdot (1 - p_i) = (1 - p_i^+) \cdot (1 - p_i) \tag{7.8}$$

The firing rate of neuron i after sorting p_i^σ is given by the probability of firing on the basis of the bin occupation after sorting. To obtain this we introduce the error rates for FN σ_i^+ and for FP errors σ_i^-, where $\sigma_i^+ = p_i^+ \frac{1-p_i}{p_i}$ and $\sigma_i^- = p_i^-$. Substituting these variables in Eqs. 7.5-7.8, we finally obtain:

$$\begin{aligned} P_i(\textbf{spike}) &= (1-\sigma_i^-)\cdot p_i, && (7.9)\\ P_i(\textbf{FN}) &= \sigma_i^- \cdot p_i && (7.10)\\ P_i(\textbf{FP}) &= \sigma_i^+ \cdot p_i && (7.11)\\ P_i(\textbf{no spike}) &= 1-(1+\sigma_i^+)\cdot p_i && (7.12) \end{aligned}$$

Using Eqs. 7.9-7.12, we finally obtain for the rate after sorting:

$$\begin{aligned} p_i^\sigma &= P_i(\textbf{spike}) + P_i(\textbf{FP}) = (1-\sigma_i^-)\cdot p_i + \sigma_i^+ \cdot p_i = p_i - \sigma^- p_i + \sigma^+ p_i \\ &= (1-\sigma^- + \sigma^+)\cdot p_i. && (7.13) \end{aligned}$$

[7].4 Analytical Results

We will assume in the following all processes to have the same original probability of firing, $p_i = p\ \forall i$, and the same error rates $\sigma_i^- = \sigma^-, \sigma_i^+ = \sigma^+$. The purpose is to keep the mathematical formalism more readable, burt can easily be extended to the non-homogeneous case. As prescribed by our correlation model, let us say that a correlation of order ω involves neurons $i_1, i_2, ..., i_\omega$. Thus, $p_{i_{1,...,\omega}} = p'' + p_c = p$ for the correlated processes, and $p_{i \neq i_{1,...,\omega}} = p' = p$ for the independent processes (cf. Sec. [7].2). This implies also that $p'' < p'$, due to the constraint that the processes have the same total rate p.

We are interested in the number of occurrences of patterns involving ξ neurons, for pattern complexities degree ξ that are equal or differ from the correlation degree ω, i.e. $\xi \gtreqless \omega$. For $\xi = \omega$, using the knowledge of our correlation model, we consider among the possible patterns of complexity ξ the jointly firing of neurons $i = i_1, ..., i_\omega$, that is the pattern $v^{\xi=\omega}$ for which the correlated neurons fire and the others do not, $v^{\xi=\omega} = i = i_{1,...,\omega} = 1, i \neq i_{1,...,\omega} = 0$. For $\xi > \omega$ the patterns of interest involve the synchronous firing of neurons $i = i_1, ..., i_\omega$ *and* $\xi - \omega$ independent neurons (that are statistically identical). For $\xi < \omega$, the ξ-patterns will involve spikes from a subset of the correlated neurons, that is with $i \in \{i_1, ..., i_\omega\}$. These are depicted on the right side of Fig. 13A for the case $\omega = 3$ and $\xi = 2, ..., 4$.

Let us define $x(\xi, N)$ as the number of coincidences of complexity ξ to be expected based on the hypothesis that the neurons are firing independently, also referred to as *predicted number of coincidences*. Assuming the processes to be independent, the probability of a coincidence pattern composed of ξ **spike** and $N - \xi$ **no spike** is:

$$P_\xi = p^\xi \cdot (1-p)^{N-\xi}. \qquad (7.14)$$

Given the assumption of stationarity in the time window under consideration containing T bins, the original predicted number of coincidences in this window is:

$$x(\xi, N) = P_\xi \cdot T = p^\xi \cdot (1-p)^{N-\xi} \cdot T \quad , \quad \xi = 2, ..., N \quad . \tag{7.15}$$

Application of the model of spike sorting errors introduced in Sec. [7].3 gives us the predicted number of coincidences for a specific pattern of complexity after sorting ξ^σ as a function of the original firing and the sorting error rates:

$$\begin{aligned} x^\sigma(\xi^\sigma, N) &= (p^\sigma)^{\xi^\sigma} \cdot (1-p^\sigma)^{N-\xi^\sigma} \cdot T = \\ &= \left[(1-\sigma^- + \sigma^+)p\right]^{\xi^\sigma} \cdot \left[1-(1-\sigma^- + \sigma^+)p\right]^{N-\xi^\sigma} \cdot T \,; \quad \xi^\sigma = 2, ..., N \,. \end{aligned} \tag{7.16}$$

We notice that the predicted number of coincidences is affected by FN and FP errors in a symmetric way. Indeed, the two variables σ^- and σ^+ compensate each other in the right-hand side of Eq. 7.16, thereby partly canceling their individual effects.

[7].4.1 Empirical number of coincidences

If some correlation is present among the ξ neurons, the empirical count $n(\xi, N)$ of occurrence of ξ-patterns will differ from the predicted number of coincidences $x(\xi, N)$. Indeed, the empirical number of coincidences $n(\xi, N)$ is the result of two separated contributions. A first term is the number of chance coincidences due to background spikes $n_{\text{chance}}(\xi, N)$, corresponding to the predicted number of coincidences $x(\xi, N)$. The second is given by the correlated patterns $n_{\text{correlated}}(\xi, N)$. To compute the term $n_{\text{chance}}(\xi, N)$ we have to take ξ times the probability of **spike** multiplied by $N-\xi$ times the probability of **no spike** and by the number of bins, thus

$$n_{\text{chance}}(\xi, N) = \begin{cases} (p'')^\omega (p')^{\xi-\omega}(1-p')^{N-\xi}T & \text{if } \xi \geq \omega \\ \\ (p'')^\xi (1-p'')^{\omega-\xi}(1-p')^{N-\omega}T & \text{if } \xi < \omega \quad , \end{cases} \tag{7.17}$$

where the correlated neurons have background rate p'' and the others p' and $\xi = 2, ..., N$. $n_{\text{chance}}(\xi, N)$ differs from $x(\xi, N)$ because now not just the total rate p, but the background rates p'' and p' need to be considered. The second contribution $n_{\text{correlated}}(\xi, N)$ is given by the coincidence rate of neurons $i = i_{1,...,\omega}$ times the rate of $\xi - \omega$ independent neurons, times the probability that the remaining $N-\xi$ neurons are silent in that instant of time,

$$n_{\text{correlated}}(\xi, N) = \begin{cases} p_c \cdot (p')^{\xi-\omega}(1-p')^{N-\xi}T & \text{if } \xi \geq \omega \\ \\ 0 & \text{if } \xi < \omega \quad , \end{cases} \tag{7.18}$$

Obviously, for complexity $\xi < \omega$ no additional patterns than those due to chance occur. Summing these two terms yields the original number of patterns of complexity ξ,

$$\begin{aligned} n(\xi, N) &= n_{\text{chance}}(\xi, N) + n_{\text{correlated}}(\xi, N) = \\ &= \begin{cases} \left((p'')^\omega + p_c\right)(p')^{\xi-\omega}(1-p')^{N-\xi}T & \text{if } N \geq \xi \geq \omega \\ \\ (p'')^\xi (1-p'')^{\omega-\xi}(1-p')^{N-\omega}T & \text{if } 2 \leq \xi < \omega \quad . \end{cases} \end{aligned} \tag{7.19}$$

[7].4.1.1 Effect of spike sorting failures

The co-occurrence of background spikes –some of which are missed as FNs– and of FP spikes gives rise to combinatorial factors contributing to the empirical number of coincidences after sorting $n^{\sigma}(\xi^{\sigma}, N)$. For example, a coincidence after sorting of complexity ξ^{σ} may be formed, say, by an amount A of original spikes of rate p'', B spikes of rate p', C FPs, such that $A+B+C=\xi^{\sigma}$. The complexity degree of an original pattern corresponds to the simultaneous occurrence of **spike** and **FN**, to which we associate the indices ξ and ξ' respectively. Thus $\xi+\xi'$ is the original complexity value of a pattern. The complexity degree of a pattern after sorting is given by **spike** and by **FP**: these will be represented by the indices ξ and $\xi^{\sigma}-\xi$ respectively (cf. Eq. 7.22 below). For a pattern of complexity $\xi+\xi'$ with i spikes from correlated neurons and $\xi+\xi'-i$ spikes from the remaining, independent neurons and $\{\xi^{\sigma}, \omega, N\}$ the complexity after sorting, the correlation order and the number of neurons respectively, we define the factor Φ_i as the product of the binomial factors to be considered,

$$\Phi_i = \Phi_i\left(\xi, \xi', \xi^{\sigma}, \omega, N\right) = \begin{cases} \binom{\omega}{i}\binom{\xi^{\sigma}-\omega}{\xi-i}\binom{N-\xi^{\sigma}}{\xi'} & \text{if } N \geq \xi^{\sigma} \geq \omega \\ \binom{\xi^{\sigma}}{\xi}\binom{\omega-\xi^{\sigma}}{i-\xi}\binom{N-\omega}{\xi+\xi'-i} & \text{if } 2 \leq \xi^{\sigma} < \omega \ . \end{cases} \tag{7.20}$$

The interpretation of Φ_i is quite straightforward, deriving for $\xi^{\sigma} \geq \omega$ from the obvious constraint for the correlated processes $i \in \{i_1, ..., i_{\omega}\} \Rightarrow i < \omega$. The remaining $\xi - i$ original spikes are recruited among $\xi^{\sigma} - \omega$ choices, and the FNs can be in any of the $N - \xi^{\sigma}$ positions. For $\xi^{\sigma} < \omega$ the considerations are analogous.

The spike sorting errors model yield to further combinatorial effects and to a more complex formalism for the original number of chance coincidences $n_{\text{chance}}(\xi, N)$, which simplify to Eq. 7.17 for $\sigma^- = \sigma^+ = 0$. In order to avoid confusion, we term this value $\mathcal{X}_{\xi+\xi'} \cdot T$ in this Section. In addition we define the new variable $n^{\star}_{\xi+\xi'}$, that represents the original number of coincidences $n(\xi, N)$ but also includes a further factor, therefore simplifying the formalism. The first of these new variables is given by

$$\begin{aligned} \mathcal{X}_{\xi+\xi'} &= \sum_{i=i_{\min}}^{i_{\max}} \Phi_i \cdot (p'')^i (p')^{\xi+\xi'-i} (1-p'')^{\omega-i} (1-p')^{N-\omega-(\xi+\xi'-i)} = \\ &= \sum_{i=i_{\min}}^{i_{\max}} \Phi_i \cdot (p'')^i (1-p'')^{\omega-i} (p')^{\xi+\xi'-i} (1-p')^{N-\omega-(\xi+\xi'-i)} = \\ &= \sum_{i=i_{\min}}^{i_{\max}} \Phi_i \cdot \mathcal{B}(p''; i, \omega) \mathcal{B}(p'; \xi+\xi'-i, N-\omega) \ , \end{aligned} \tag{7.21}$$

where the constraints given by the complexity after sorting ξ^{σ} for N neurons give $i_{\min} = \max(\xi, \xi+\xi'-(N-\omega))$ if $\xi^{\sigma} < \omega$ and $i_{\min} = \max(0, \xi-(\xi^{\sigma}-\omega))$ if $\xi^{\sigma} \geq \omega$, $i_{\max} = \min(\xi, \omega)$.

The number of coincidences after sorting $n^{\sigma}(\xi^{\sigma}, N)$ is composed of patterns of ξ original and well sorted spikes (having probability $(1-\sigma^-)^{\xi}$), ξ' FNs (probability $(\sigma^-)^{\xi'}$), and $\xi^{\sigma}-\xi$

FPs (probability $(\sigma^+)^{\xi^\sigma-\xi}$). The original complexity $\xi+\xi'$, is therefore partly decreased because of the ξ' FNs and then increased by $\xi^\sigma-\xi$ FPs, resulting in the correct value for the total complexity after sorting $(\xi+\xi')-\xi'+(\xi^\sigma-\xi)=\xi^\sigma$. The above considerations yield the set of equations (for $\xi^\sigma=2,...,N$)

$$n^\sigma(\xi^\sigma,N) = \sum_{\xi=0}^{\xi^\sigma}\tau_-^{\xi}(\sigma^+)^{\xi^\sigma-\xi}\sum_{\xi'=0}^{N-\xi^\sigma}(\sigma^-)^{\xi'}\varepsilon_{\xi+\xi'}^{N-\xi^\sigma-\xi'}\pi_{\xi+\xi'}^{\xi^\sigma-\xi}\cdot n^\star_{\xi+\xi'} \tag{7.22}$$

$$n^\star_{\xi+\xi'} = \begin{cases} p^{\xi^\sigma}T & \text{if } \xi+\xi'=0,1 \\ \mathcal{X}_{\xi+\xi'}T & \text{if } \xi+\xi'=2,...,\omega-1 \\ \mathcal{X}_{\xi+\xi'}T+p_c\cdot(p')^{\xi+\xi'-\omega}(1-p')^{N-(\xi+\xi')}T & \text{if } \xi+\xi'=\omega,...,N \end{cases}, \tag{7.23}$$

$$\tau_- = 1-\sigma^-$$

$$\pi_{\xi+\xi'} = \begin{cases} 1 & \text{if } \xi+\xi'=0 \\ \xi+\xi'\cdot p^{1/\xi^\sigma} & \text{if } \xi+\xi'=1 \\ p/(1-p) & \text{if } \xi+\xi'=2,...,N \end{cases} \tag{7.24}$$

$$\varepsilon_{\xi+\xi'} = \begin{cases} (1-p^+)(1-p) & \text{if } \xi+\xi'=0,1 \\ (1-p^+) & \text{if } \xi+\xi'=2,...,N \end{cases}. \tag{7.25}$$

For no errors, i.e. $\sigma^-=\sigma^+=0$, $n^\sigma(\xi^\sigma,N)$ equals the original number of coincidences of complexity ξ, $n(\xi,N)$, as it can be easily derived from Eqs. 7.21-7.25 by setting $\sigma^-=\sigma^+=0$, $\xi=\xi^\sigma$, $\xi'=0$, and $i=\min(\xi,\omega)$.

Let us examine in more details the effect of the different contributions in $n^\sigma(\xi^\sigma,N)$. For this purpose, in all the following we will consider the case ($\omega=3, i_{1,...,\omega}=i_{1,2,3}$) evaluating the following patterns: $v^{\xi^\sigma=3}=\{i=i_{1,2,3}=1, i\neq i_{1,2,3}=0\}$ ("direct case"), $v^{\xi^\sigma=2}=\{i=i_{1,2}=1, i\neq i_{1,2}=0\}$ and $v^{\xi^\sigma=4}=\{i=i_{1,2,3}, i^*=1, i\neq i_{1,2,3}, i^*=0\}, i^*\notin\{i_{1,...,\omega}\}$ ("cross-cases"). Figs. 15A-C depict the empirical number of coincidences of patterns of different complexities as a function and for different levels of FNs and FPs. Increasing the FP error rate and keeping the FN rate constant leads not surprisingly to an increase of the number of coincidences (light gray solid lines). As a FP spike occupies a formerly empty bin, the complexity of the pattern occurring amongst the neuron at that time step is increased, and this holds for each complexity degree. Therefore FPs affect the coincidence count by adding chance coincident patterns. On the other hand, keeping the FP rate fixed and increasing the number of false negative spikes (dark gray solid lines) destroys both, chance coincidences and synchronous patterns of complexity ξ^σ. One (or more) FNs occurring in a bin cause a pattern to decrease the value of its complexity degree by one (or more). As a counter-effect patterns of complexity higher than ξ^σ contribute to the complexity ξ^σ after sorting because of FNs and thus increase them. However, this phenomenon does not dominate as 1) it occurs at every complexity and 2) higher complexity patterns are more

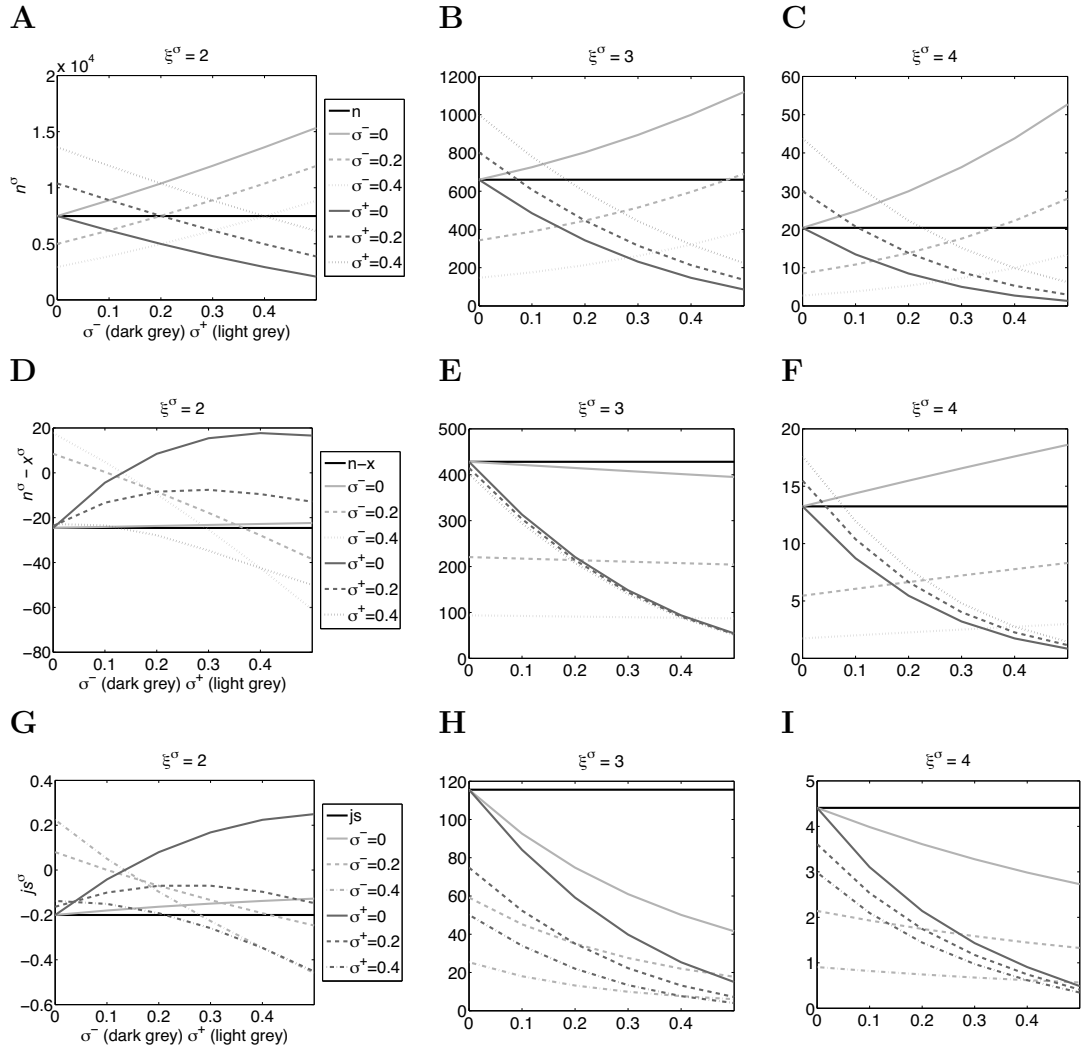

Figure 15: Empirical number of coincidences, number of excess coincidences and joint-surprise as a function of sorting errors. A-C: empirical number of coincidences; D-F: excess coincidences; G-H: joint-surprise. Left column: patterns of complexity $\xi^\sigma = 2$; middle column: $\xi^\sigma = 3$; right column: $\xi^\sigma = 4$. Black: original; dark gray: as a function of FNs for no FPs (solid), 20% FPs (dashed), 40% FPs (dotted); light gray: as a function of FPs for no FNs (solid), 20% FNs (dashed), 40% FNs (dotted). Parameters: $N = 8$, $T = 10^7$, $\omega = 3$, $p = 0.03$, $p_c = 5 \cdot 10^{-5}$, $\delta = 1$ ms.

uncommon than lower complexity patterns. However, the simultaneous occurrence of FN and FP spikes counterbalances their individual effects in a non-linear fashion (dashed and dotted curves in Figures 15A-C). In general, the impact of false negatives is stronger in destroying coincidences than that of false positives in creating them.

In order to compare the empirical and predicted number of coincidences (Eqs. 7.16 and 7.22) we plotted in Fig. 15D-F their difference $n^\sigma(\xi^\sigma, N) - x^\sigma(\xi^\sigma, N)$ for different values of complexity after sorting ξ^σ, that is the "excess coincidences". For pairs of neurons (Fig. 15D) the excess coincidences increase when FN errors only are applied (dark gray solid line). The reason why the initial value is negative is that no injected coincidences were inserted with order $\omega = 2$, and therefore with no errors the computed number of patterns is smaller than expected due to the smaller background rate p'' as

compared to p'. However, deletion of spikes due to FN errors leads to an increase of pairs, as some of the inserted triplets become pairs. When FPs only are applied, we notice a small increase of excess coincidences; indeed, in this case both $n^\sigma(\xi^\sigma, N)$ and $x^\sigma(\xi^\sigma, N)$ increase (light gray solid line). Interestingly, when both errors are applied (dashed and dotted lines) depending on their relative amount even a decrease of excess coincidences may be observed. In particular, for fixed but positive values of FNs the excess coincidences decrease with increasing FPs (light gray dashed and dotted lines). However, for fixed and non-zero values of FPs, the behavior of $n^\sigma(\xi^\sigma, N) - x^\sigma(\xi^\sigma, N)$ is parabolic with negative convexity, and decreasing absolute amounts with more and more FPs (dark gray lines). The explanation for this behavior can be seen in the opposite and conter-intuitive effects of errors on pairs: FNs make higher-order patterns degrade to pairs, whereas FPs contaminate the patterns of complexity 2 with spurious spikes, thus making them to get missed. FPs errors have small impact on excess coincidences of complexity 3, as shown in Fig. 15E (cf. slope of light gray lines). The reason for this is that although the empirical coincidences are increased by FPs (cf. Fig. 15B), a stronger increase is expected based on the rates, which are obviously also affected by FPs. Although this type of error leads thus to a small decrease of excess coincidences, on the contrary the deletion of spikes caused by FNs results in the correlation to be strongly reduced. This effect can be seen both in the dependence of $n^\sigma(\xi^\sigma, N) - x^\sigma(\xi^\sigma, N)$ on FNs with no or fixed FPs (dark gray lines) and in the progressively negative shift introduced by the fixed value of σ^- on the FP-dependence (cf. zero-value of light gray lines) in Fig. 15E. As a result, overall sorting failures result in a reduction of excess coincidences of complexity matching the initially inserted correlation (direct case). Fig. 15F shows how for complexity degrees higher than the order of injected correlation the excess coincidences reflect the behavior of both, the empirical and the predicted number of coincidences (cf. Fig. 15C and Eq. 7.16 respectively). Thus here FPs lead to an increase of excess coincidences and FNs to a decrease (see also discussion relative to Fig. 15C).

The dependence of the number of coincidences $n(\xi, N)$ before and after errors $n^\sigma(\xi^\sigma, N)$ as a function of the number of neurons N is shown in Fig. 16A,B. Black lines represent the original number of coincidences $n(\xi, N)$, dashed curves show cases where sorting errors were injected. All curves show a slight decrease for increasing N. The reason for that can be understood by looking at Eq. 7.19. For a fixed value of the probabilities of firing and the complexity degree ξ, the original empirical number of coincidences $n(\xi, N)$ decreases with N because of the term $(1-p')^{N-\xi}$ (or $(1-p')^{N-\omega}$) in Eq. 7.19. That is the pattern composed by ξ neurons firing and $N-\xi$ ($N-\omega$) neurons not firing becomes more and more unlikely with increasing N. As expected adding FPs results in an increase of the coincidence count (light gray lines), whereas FNs lead to a decrease of $n^\sigma(\xi^\sigma, N)$ (dark gray lines). For complexities higher than 2, the effects of sorting errors are stronger than the negative trend with N. Overall, the results discussed above for the case $N = 8$ are confirmed for populations of different numbers of neurons.

In Fig. 17A-C the dependance of $n^\sigma(\xi^\sigma, N)$ on the firing rate p/δ (in Hz) is shown for complexity after sorting $\xi^\sigma = 2$ (Fig. 17A), $\xi^\sigma = 3$ (Fig. 17B) and $\xi^\sigma = 4$ (Fig. 17C) and inserted triplets. In all cases $n^\sigma(\xi^\sigma, N)$ does not decrease with increasing firing rate, but it is either almost constant or increases. For complexity after sorting $\xi^\sigma = 3$ the number of coincidences $n^\sigma(3, 8)$ the correlated patterns dominate up to values of about

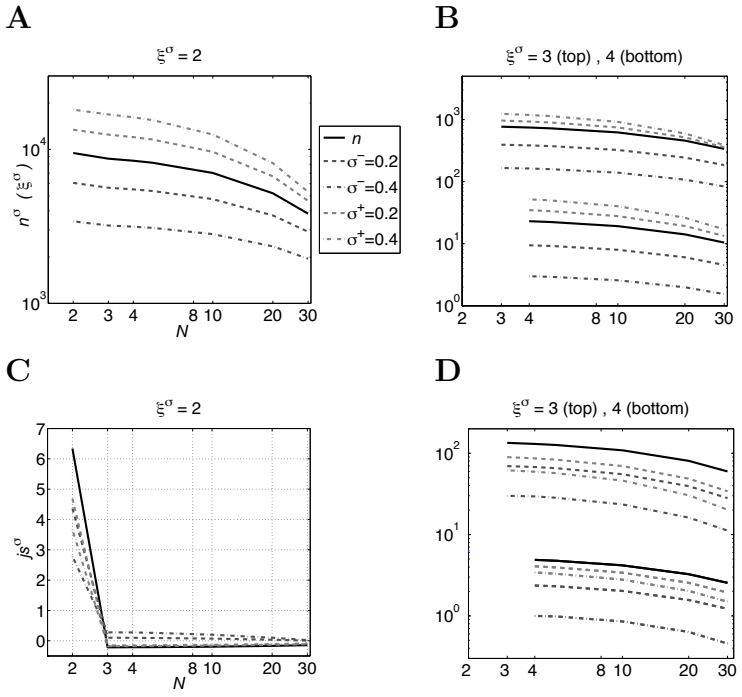

Figure 16: Empirical number of coincidences and joint-surprise as a function of the number of neurons. A,B: empirical number of coincidences; C,D: joint-surprise. Left: patterns of complexity $\xi^\sigma = 2$; right: patterns of complexity $\xi^\sigma = 3$ (top curves), $\xi^\sigma = 4$ (bottom curves). Black: original; dark gray: for 20% FNs (dashed) and 40% FNs (dotted); light gray: for 20% FPs (dashed) and 40% FPs (dotted). For $N = 2$ correlation order $\omega = 2$. Otherwise parameters as in Fig. 15.

$p/\delta \sim 1$ Hz (Fig. 17B). The effect of FPs is in this range negligible, whereas moderate levels of FNs destroy many of the 3-patterns. For higher rates the number of coincidences increase exponentially with the background rate, and the errors have the usual effect of (slightly) increasing the pattern count with FPs and decreasing with FNs. Indeed, for high-firing rates the effects of errors are "diluted". For $\xi^\sigma = 2$ the original number of coincidences increases exponentially with the rate (Fig. 17A, black). However, we can notice an interesting effect in the presence of FNs (Fig. 17A, dark gray). Here, for low rates $n^\sigma(2, 8)$ is much higher than the original value (solid curve). This is due to the fact that the triplets are partially destroyed by FNs, and "become" pairs. However, for higher rates, the value of the number of coincidences after FNs is fairly quickly back to below the original value. For complexity after sorting $\xi^\sigma = 4$ (Fig. 17C) the increase of the number of patterns seems to have two distinct exponential regimes, i.e. at low and at high rates. Here only the effect of FNs is pronounced in the low rate regime.

[7].5 Perturbation of the Significance of Correlation Measures

In the following sections we will briefly discuss the cross-correlation function (Perkel et al., 1967a,b; Aertsen et al., 1989) and the unitary event analysis (Grün et al., 2002a,b) since we want to evaluate the impact of spike sorting on the analysis results using these methods..

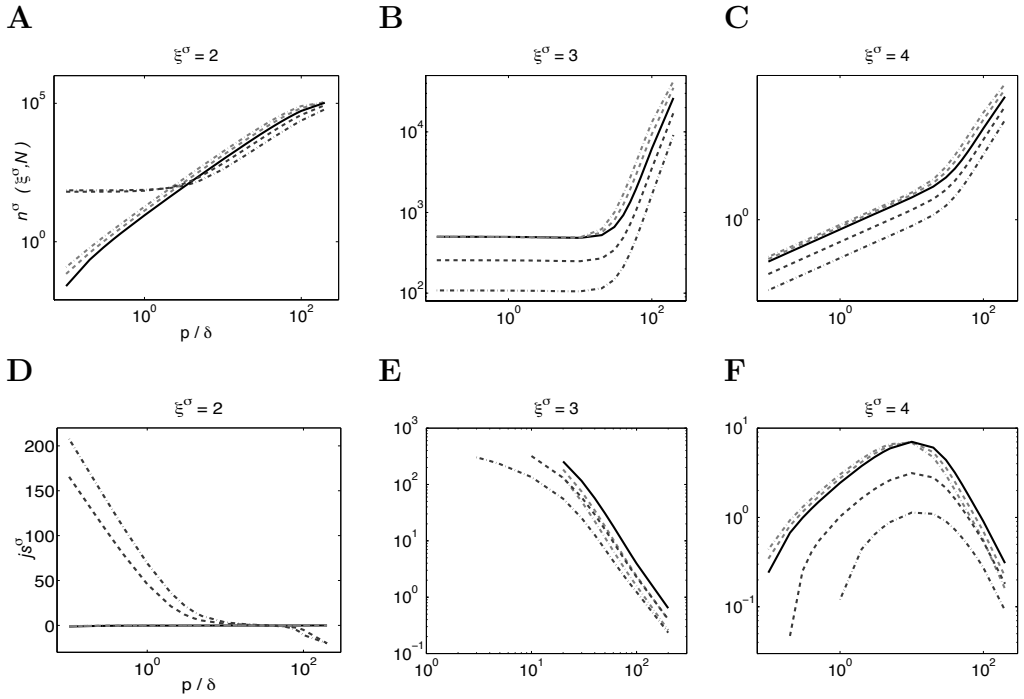

Figure 17: Empirical number of coincidences and joint-surprise as a function of the rate of the processes p/δ = [Hz]. A-C: empirical number of coincidences; D-F: joint-surprise. Left column: patterns of complexity $\xi^\sigma = 2$; middle column: $\xi^\sigma = 3$; right column: $\xi^\sigma = 4$. Black: original; dark gray: for 20% FNs (dashed) and 40% FNs (dotted); light gray: for 20% FPs (dashed) and 40% FPs (dotted). Parameters as in Fig. 15.

For details please refer to the respective original works.

[7].5.1 Cross-correlation

The cross-correlation analysis enables to measure the correlations between two point processes r_i and r_j, $i, j = 1, \ldots, N$, where the expected value of the single processes corresponds to their rates, i.e. $E[r_i] = p_i, E[r_j] = p_j$. The raw cross-correlation function for stationary processes is defined as:

$$CCF^{\text{raw}}_{i,j}(\tau) = E[r_i(t), r_j(t-\tau)] \ . \tag{7.26}$$

It yields the number of empirical coincidences as a function of delay τ. To obtain the covariance function, i.e. a measure corrected for the mean firing rates of the processes, one has to subtract the "Predictor", i.e. the product of the mean probabilities of firing $E[r_i(t)] \cdot E[r_j(t-\tau)] = p_i \cdot p_j$. Because we are interested here in exact coincidences (i.e. synchronous spikes occurring in the very same bin) we focus on the central peak of these functions.

In our framework, the value on the right-hand side of Eq. 7.26 corresponds to the original empirical number of coincident patterns involving neurons i and j, $n(2,2)$ (Eq. 7.19). As in the previous sections we assume homogeneity across neurons,i.e. $p_i = p_j = p$. This yields for the covariance

$$\begin{aligned} CCF_{i,j}(\tau) &= CCF^{\text{raw}}_{i,j}(\tau) - E[r_i(t)] \cdot E[r_j(t-\tau)] = \\ &= Cov[r_i(t), r_j(t-\tau)] = \begin{cases} n(2,2)/T - p^2 & |\tau| \leq 1 \text{ bin} \\ 0 & |\tau| > 1 \text{ bin} \end{cases} \end{aligned} \tag{7.27}$$

Clearly, the result of Eq. 7.27 will be influenced by spike sorting errors. According to our model, the probabilities of firing and the number of coincidences after sorting are for the two neurons p^σ and $n^\sigma(2,2)/T$, respectively (see Sections [7].3 and [7].4). This leads for the covariance to:

$$CCF^\sigma_{i,j}(\tau) = \begin{cases} n^\sigma(2,2)/T - (p^\sigma)^2 & |\tau| \leq 1 \text{ bin} \\ 0 & |\tau| > 1 \text{ bin} \end{cases} \tag{7.28}$$

where $n^\sigma(2,2)$ is the empirical number of coincidences of complexity after sorting $\xi^\sigma = 2$ for the two specific neurons i, j. The value on the right-hand side of Eq. 7.28 is non-zero for time shift $\tau = 0$, i.e. in correspondence to the central peak of the cross-correlation function. If we substitute $N = \xi^\sigma = 2$ in Eq. 7.22 we obtain:

$$n^\sigma(2,2) = \left(1 - \sigma^-\right)^2 \cdot n_2 + \left[2\sigma^+(1-\sigma^-) + (\sigma^+)^2\right] \cdot x_2 \quad . \tag{7.29}$$

Using Eqs. 7.15 and 7.16 gives for the central peak of the cross-correlation function after sorting:

$$CCF^\sigma_{i,j}(0) = n^\sigma(2,2) = \left(1 - \sigma^-\right)^2 \cdot [n_2 - x_2] \,. \tag{7.30}$$

The cross-correlation coefficient CC^σ equals $CCF^\sigma_{i,j}(0)$ divided by the standard deviation of the processes[6]. As shown in Fig. 18 spike sorting errors lead to an underestimation of the cross-correlation coefficient. Indeed, increasing both error types leads to a decrease of the cross-correlation coeffient, which is more pronounced for FP errors (dark gray line) than for FPs (light gray). This is due to the fact that sorting errors lead to a variation of the estimated rate p^σ, but do not explicitly introduce any correlations. Intuitively, in Eq. 7.28 above, the coincidences introduced by sorting errors in the term $n^\sigma(2,2)$ are exclusively due to chance (FPs spikes occurring synchronously to original spikes or to other FPs), and the second term $(p^\sigma)^2$ takes care of this already. Therefore, the increased empirical firing probability measured after FP errors is not accompanied by a corresponding amount of novel coincidences, and the correlation coefficient CC^σ is weakened.

On the other hand, FNs delete original spikes (and thus coincidences) in a systematic way, i.e. both from $n^\sigma(2,2)$ and $(p^\sigma)^2$ in a (statistically) identical amount. This fact, due to the properties of the Poisson distribution (but this holds for more regular processes as well, see Pazienti and Grün, 2006) leads to a stronger decrease of CC^σ as compared to FPs. Summarizing, in case of false negative spikes some of the correlated spikes are deleted; in case of false positives no additional coincidences are created than expected by the predictor (Pazienti and Grün, 2006).

[6] In case of Poisson processes these would be simply $\sqrt{p^\sigma}$.

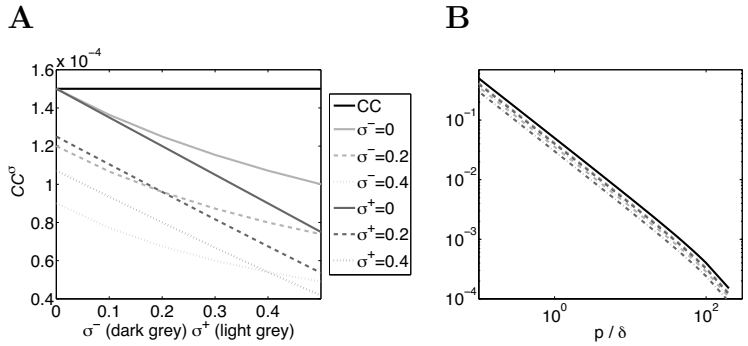

Figure 18: Correlation coefficient before and after spike sorting. A: CC and CC^σ as a function of sorting errors. Black: original; dark gray: as a function of FNs for no FPs (solid), 20% FPs (dashed), 40% FPs (dotted); light gray: as a function of FPs for no FNs (solid), 20% FNs (dashed), 40% FNs (dotted). B: as a function of the rate of the processes (in Hz). Black: original; dark gray: for 20% FNs (dashed) and 40% FNs (dotted); light gray: for 20% FPs (dashed) and 40% FPs (dotted). Parameters as in Fig. 15 with $\xi^\sigma = 2$.

Fig. 18B depicts the behavior of the correlation coefficient CC^σ for a wide range of firing rates $p/\delta = [\text{Hz}]$. Here the total number of spikes increase with the rates but the coincidence rate was kept constant. Therefore the coincident patterns are "diluted" in the firing activity of the neurons, and the cross-correlation coefficient decrease exponentially. The results shown in Fig. 18A are manifestly not affected by changes in the rates. Indeed, the curves of CC^σ, shown for different amount of errors, follow the decaying of the original cross-correlation coefficient in the whole range of rates, and always underestimate it.

[7].5.2 Unitary events

Unitary event analysis measures the significance of joint-spike events occurring amongst multiple, simultaneously recorded neurons (Grün et al., 2002a,b). When their synchronization exceeds the chance level by a significant amount, the coincident patterns are called unitary events. UE analysis evaluates the significance based on the null-hypothesis of independent firing. In the case of poissonian spike trains, the probability distribution of the number of coincident patterns can be analytically derived. For spike trains deviating from Poisson or non-stationary data we suggested methods for correction (Grün et al., 2003b; Pipa et al., 2003; Pipa and Grün, 2003). Here we restrict ourselves to the assumptions of stationary and Poissonian spike trains, i.e. the situation described in (Grün et al., 2002a,b), which we briefly introduce below. Under the null-hypothesis of statistically independent firing of the neurons, the probability of a pattern of complexity ξ amongst the N neurons to occur is $P_\xi = p^\xi(1-p)^{N-\xi}$ (cf. Eq. 7.14). The probability for such a high dimensional pattern to occur exactly n times can be approximated by a Poisson distribution (for a derivation see (Grün et al., 2002a)):

$$\psi(n; P_\xi; T) = \frac{(P_\xi T)^n}{n!} \cdot e^{-P_\xi T} \quad . \tag{7.31}$$

Here, $P_\xi \cdot T$ is the rate parameter of the Poisson distribution, that is the expected number of coincidences given the firing rates $x(\xi, N)$ already derived in Sec. [7].4:

$$x(\xi, N) = P_\xi \cdot T = p^\xi \cdot (1-p)^{N-\xi} \cdot T. \tag{7.32}$$

The empirical number of coincidences of complexity ξ, $n(\xi, N)$, is then compared to the predicted value $x(\xi, N)$ using the Poisson distribution (Eq. 7.31). Significant deviation from the expected value is estimated by the joint-p-value, i.e. the cumulative probability of having $n(\xi, N)$ or more coincident events (see Grün et al., 2002a for details) The significance is expressed as a non-linear (log-)transformation of the joint-p-value Ψ, resulting in the significance measure *joint-surprise* $js(\Psi_\xi)$:

$$js(\Psi_\xi) = js_\xi\left(n(\xi, N)|x(\xi, N)\right) = log\frac{1-\Psi_\xi}{\Psi_\xi} \quad , \tag{7.33}$$

with

$$\Psi_\xi\left(n(\xi, N)|x(\xi, N)\right) = \sum_{n=n(\xi,N)}^{\infty} \frac{[x(\xi, N)]^n}{n!} e^{-x(\xi,N)} \quad . \tag{7.34}$$

When the value of js_ξ exceeds an a priori threshold, i.e. $js_\xi(n(\xi, N)|x(\xi, N)) \geq js_\alpha$, the synchrony is considered significant.

If we now use x^σ and n^σ (Eqs. 7.16 and 7.22 respectively) instead of $x(\xi, N)$ and $n(\xi, N)$ we obtain the joint-surprise after sorting for complexity ξ^σ, defined as $js^\sigma_{\xi^\sigma} \equiv js_{\xi^\sigma}(n^\sigma(\xi^\sigma, N)|x^\sigma(\xi^\sigma, N))$. Figs. 15G,H,I show the typical dependance of the significance measure on the error rates σ^- and σ^+. Here triplets were inserted into a subset of three out of $N = 8$ neurons (cf. Sec. [7].4) and the complexities after sorting $\xi^\sigma = 2-4$ are investigated. For the "direct case" ($\omega = 3, \xi^\sigma = 3$) (Fig. 15H) the significance after sorting (gray lines) is lower than the original (black line) for any error types, i.e. the correlation is always underestimated. When only one kind of errors is applied (solid gray lines) the joint-surprise equals for no errors the original value js, and then decreases with opposite curvature with σ^- (dark gray) and σ^+ (light gray). FP errors have therefore a smaller impact on the significance in this case, leading to a less pronounced loss of significance. Increasing errors leads to a further reduction of significance (dashed lines). These reduction of the joint-surprise exceeds the effects on the excess coincidences shown in Fig. 15E.

For the "cross-case" $\xi^\sigma < \omega$ (Fig. 15G) we observe a very different phenomenon, now leading to an overestimation of the significance. For $\sigma^- > 0$ (dark gray solid line) the significance measure increases with the FN rate. The reason for that is that introducing FNs (i.e. deleting spikes) causes some of the triplets to change their complexity to the value $\xi^\sigma = 2$. The resulting excess coincidences (cf. Fig. 15D) may lead to a overestimation of the significance for experimental data where a consistent amount of FN errors were made (for example by too "conservative" spike sorting). We also observe a slight increase in significance when applying FPs spikes only (solid light gray line), explainable again by the effects on the excess coincidences. For $\xi^\sigma > \omega$ (Fig. 17C) instead, in contrast with what was observed for the excess coincidences (Fig. 15F), the significance is always underestimated as compared with the original (shown in black). In this case FNs errors have again a stronger effect than FPs. We would like to notice here, that the correlation of the quadruplets is significant for low or no errors, due to inserted triplets and background

firing. However, the effect of errors (more strongly of FNs) leads eventually to a loss of the significance.

Fig. 16C,D show the value for the joint-surprise as a function of the number of processes. For $\xi^\sigma < \omega$ the significance is overestimated in case of FNs for any N above 2 (Fig. 16C). Here higher-order effects of spike sorting are therefore especially noticeable. Indeed, for $N = 2$ the significance after sorting js^σ underestimates the original (black line), but as soon as $N > 2$ the overestimation of the significance already discussed in Fig. 15G comes into play. FP errors (light gray lines) do not have a strong effect and lead for $N > 2$ to a value of js fairly similar to the original one. For complexities equal or higher than 3 underestimation of the synchronization is observed for any N (Fig. 16D), and the errors have a stronger impact than the number of processes. Overall, the dependance of the joint-surprise on the number of processes confirms the results discussed above for the case $N = 8$ (Figs. 15G-I, cf. also (Pazienti and Grün, 2006)).

The dependance of the joint-surprise measure on the firing rate (p/δ, in Hz) of the neurons is shown in Fig. 17D-F for different levels of sorting errors and complexities after sorting $\xi^\sigma = 2$ (Fig. 17D), $\xi^\sigma = 3$ (Fig. 17E) and $\xi^\sigma = 4$ (Fig. 17F). For $\xi^\sigma = 2$ the effect of FN errors discussed above is very prominent. Here, the insterted triplets are turned into pairs by FN errors, leading the joint-surprise to high significance values. However, for increasing rate the joint-surprise tends to the original value, that is the effect of errors is progressively reduced, as the correlated spikes are more and more diluted in the background. FP errors do not introduce any strong rate-dependent effect. For the direct case $\xi^\sigma = \omega = 3$ the significance after sorting is always underestimated (Fig. 17E). For complexity 4 the reduction due to FN spikes is very pronounced (Fig. 17F, dark gray lines). This is the case for complexity higher than 4 as well: the more we get far from the order of original correlation ($\omega = 3$ in this case), the more the significance is underestimated with FN errors. However for FPs we observe an interesting phenomenon. For rates up to about 10 Hz false positive errors elicit an overestimation of the joint-surprise, although too small to produce erroneously significant results for the correlation of quadruplets. However, for higher firing rate the trend changes and the significance is underestimated. Thus, this higher-order effect is firing rate-dependent.

[7].6 Discussion

We studied the effects of imperfect spike sorting on two correlation methods: cross-correlation function and unitary event analysis. These methods are designed to estimate the correlation structure of multiple single-unit neuronal processes from multi-site recordings. The central peak of the cross-correlation function measures correlation between neuron pairs, whereas the joint-surprise measure can deal with N-dimensional patterns. Both methods correct for random coincidences due to independent firing. However, the influence of manipulated spike trains on these methods is still uncertain.

We presented a model that introduces "failures" (i.e. false negatives and false positive spikes) into point processes. Our model does neither modify the higher-order correlation structure nor the working hypotheses of the analysis methods investigated. No higher-order patterns are systematically introduced and their timing is unaffected. We only assume that each neuron suffers errors independently of others, i.e. we concentrate on the

study of the synchronization of neurons recorded on different electrodes.

Our approach is general in two respects. On the one hand our model of sorting errors can be seen as a simple way of modifying point processes (not only spike trains) by introducing failures and therefore modifying their statistics. Thus, the model is applicable in other contexts than electro-physiological data as well, i.e. in any analysis of point processes. On the other hand, the model can be applied to other neuro-physiological data measures other than cross-correlation function and unitary event analysis. Indeed, the simplicity of the model together with its analytical description would easily allow to gain insights into the effects of sorting on any methods of data analysis. This may give hints about the robustness of the results against spike sorting errors and possibly lead to adjustments of the spike sorting algorithms and strategies. This work is intended as an illustrative approach to the study of the effects of spike sorting algorithms on data analysis.

Effects of sorting errors on correlation analyses

For both analysis measures the effect of sorting errors leads in most of the cases to a reduction of the significance (cf. Figure 17). False negative errors have in general a more severe influence on the significance estimation of sorted data than false positives. The reason is that unlike false positives, which may generate "chance" coincidences only, FNs directly affect the correlated firing of the neurons by destroying a fraction of the higher-order correlation patterns. This suggests that too conservative sorting strategies (not classifying spikes located at the "outer regions" of the clusters in the feature space for example) not only lead (locally, at the level of the nearby neurons) to missing overlapping spikes, but also negatively affect (globally, at the assembly level) the measured synchronization among neurons located further away (i.e. $100\mu m$ or more, minimal inter-electrode distance for most setups).

For the central peak of the normalized cross-correlation function, both error types always lead to an underestimation, the effect being stronger in case of FNs. Let us mention that the central peak of the cross-correlation function may overestimate the synchronization, reflecting an underlying correlation of higher-order. This happens e.g. when a correlation is present among a population of neurons that involves the considered pair. Previous studies about the effect of imperfect sorting on cross-correlation measures showed that the results may be strongly biased by spurious spike trains (Bedenbaugh and Gerstein, 1997; Gerstein, 2000; Bar-Gad et al., 2001a,b). This overestimation of the significance is unavoidable when using the cross-correlation function, which is not designed to measure higher-order correlations. Here, we showed that sorting errors do not worsen further this effect. In case of the unitary event analysis, in some cases higher-order effects due to sorting play a role. We distinguished between direct cases (in which the complexity degree equals the order of correlation, $\xi^{\sigma} = \omega$) and cross-cases ($\xi^{\sigma} \neq \omega$) and presented analytical results and a case study (Figs. 15G-I, 16C,D and 17D-F). The effects of sorting is for direct cases an underestimation of the joint-surprise. In this domain the unitary event analysis appears robust against sorting errors, confirming previous results (Pazienti and Grün, 2006). For cross-cases there is under some circumstances erroneous overestimation of the significance, e.g. with false negative errors for $\xi^{\sigma} < \omega$ (Fig. 15G)

and with false positive errors for $\xi^\sigma > \omega$ (Fig. 15H). However, the latter effect is rather small and belongs to fairly extreme ranges of physiological parameters. The documented effects occur for amount of errors in the range of the ones documented in the literature (see Introduction).

There is another fundamental difference of approach between cross-correlation function and unitary event analysis. In the first method the correlation of a single pair of neural signal is analyzed, and the activity of other neurons is discarded[7]. The latter method, on the other hand, while allowing for higher complexities, is restricted to exact patterns of firing/not firing, i.e. N-dimensional strings of zeros and ones[8]. The drawback in this case is that if e.g. within a neuron population some neurons fail to fire the –strictly spaking– new pattern will be classified as different. This is reflected in our results, where we observed a certain sensibility of the UE analysis to complexity "migration" of synchronization patterns.

On the assumption of Poisson processes

Our results do not depend on the assumption of using Poisson processes. Simulations using processes with different statistical properties (such as more regularity than for Poisson processes, not shown here) confirmed the validity of our results and our conclusions. The motivation for our model of correlation (Sec. [7].2) is exclusively to allow an analytical study of the effects of spike sorting errors. This choice allowed us to present closed form relations for the firing rates and the pattern counts after spike sorting (p^σ, x^σ and n^σ, see Eqs. 7.13, 7.16 and 7.22 respectively) and to make theoretical predictions about the effects of spike sorting. We believe that this choice makes our analysis and the results more robust and, as already mentioned, easily extendable to other possible applications.

To summarize, the effect of spike sorting can strongly bias the results of correlation analysis, even under realistic parameter settings (firing rate, analysis time window, etc.) and with previously reported amount of sorting errors. Furthermore, in case of many simultaneous recordings higher-order effects come into play and may affect the results. The choice of the appropriate spike sorting technique and strategy appear as a crucial step and it is too often an underestimated and undocumented step. It is of pressing importance to document more extensively the spike sorting methods utilized and to incorporate objective quality controls of the outcomes. Furthermore, detailed investigations on the employed analysis method would allow the disentanglement of wrong interpretations and the comparability of the results.

Acknowledgments

Supported in part by the Volkswagen Foundation, the "Stifterverband für die Deutsche Wissenschaft" and the BMBF Bernstein Center for Computational Neuroscience Berlin (grant 01GQ0413).

[7]This implies also that part of the advantages of recording with arrays of electrodes is lost.

[8]The unitary event analysis in its later version gives the ability to set "wild cards", i.e. to discard the activity of other neurons when analyzing certain patterns (unpublished).

8 Bounds of the Ability to Destroy Precise Coincidences by Spike Dithering

Antonio Pazienti, Markus Diesmann and Sonja Grün

This section is published with the same title as

Pazienti A, Diesmann M, Grün S (2007)
Advances in Brain, Vision, and Artificial Intelligence,
Lecture Notes in Computer Science, chap. 41, pp. 428-437, Springer Berlin / Heidelberg.

Abstract

Correlation analysis of neuronal spiking activity relies on the availability of distributions for assessing significance. At present, these distributions can only be created by surrogate data. A widely used surrogate, termed dithering, adds a small random offset to all spikes. Due to the biological noise, simultaneous spike emission is registered within a finite coincidence window. Established methods of counting are: (i) partitioning the temporal axis into disjunct bins and (ii) integrating the counts of precise coincidences over multiple relative temporal shifts of the two spike trains. Here, we rigorously analyze for both methods the effectiveness of dithering in destroying precise coincidences. Closed form expressions and bounds are derived for the case where the dither range equals the coincidence window. In this situation disjunct binning detects half of the original coincidences, the multiple shift method recovers three quarters. Thus, only a dither range much larger than the detection window qualifies as a generator of suitable surrogates.

[8].1 Introduction

The only way to identify information processing in biological neuronal networks is to simultaneously record from many neurons at a time. Nowadays multi-channel recordings are a standard technique in electrophysiological laboratories. Correlation analysis of such data has demonstrated that neurons exhibit correlated spiking activity on a fine temporal scale (ms precision) and in relation to the experimental protocol (Riehle et al., 1997; Nowak et al., 1995). This has been interpreted as indicative for an involvement of correlated spiking activity in brain processing.

However, the presence of correlated spiking activity is not obvious from visual inspection. At first sight, the data appear to originate from a stochastic process with large variability in the number and the timing of spikes in responses to an identical stimulus. Furthermore, the rate of spike emission typically exhibits a complex temporal profile. Clearly, spike coincidences with millisecond precision can also occur as chance events. Thus, the empirical number of joint-spike events needs to be compared to the distribution

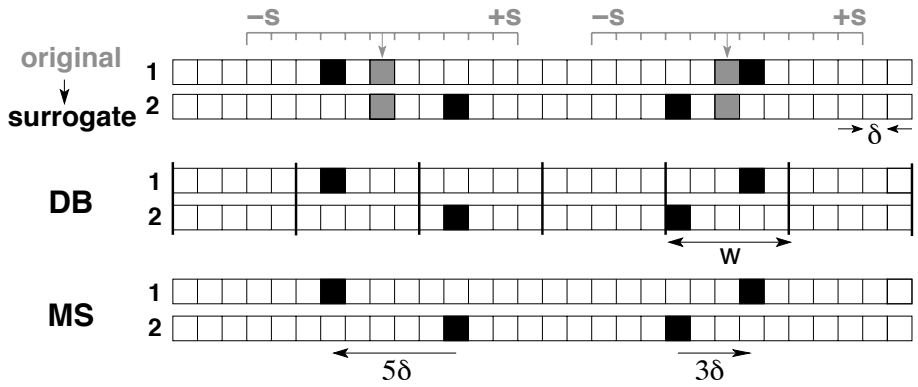

Figure 19: Spike dithering and two methods of coincidence detection. Filled bins indicate spike occurrence, the width of the bins indicates the time resolution δ (typically 1 ms). Top: Generation of surrogate data. Original simultaneous spike data (grey bins) of neuron 1 and 2. Coincidences are assumed to be precise (within the same bin). In surrogate spike trains (black bins) all original spikes are independently dithered with uniform probability in the range $\pm s$ (in units of δ). Middle: In the disjunct binning (DB) method coincidences are detected in exclusive windows of width w to allow a temporal jitter of the spikes. Only spikes within the same window (between thick vertical lines) are counted as a coincidence. Bottom: In the multiple shift (MS) method spike coincidences are detected if the distance between spikes is smaller than or equal to an a-priori parameter (see Sec. [8].3).

of coincidence counts resulting from independent spike trains. This distribution can only be derived using strong assumptions about the statistics of the spike trains (Grün et al., 2002a) typically not fulfilled by electrophysiological data. Therefore, Monte-Carlo methods are widely used to construct the distribution of coincidence counts from surrogate data (Pipa and Grün, 2003) that maintain certain statistical properties of the original data but do not include correlations (Ikegaya et al., 2004).

Various methods are in use for the generation of surrogate data (Hatsopoulos et al., 2003; Pipa et al., 2003; Pipa and Grün, 2003; Grün et al., 2003a; Pipa et al., 2007). All of them fulfill the condition to destroy the correlation, but also have the drawback to simultaneously destroy one or the other statistical feature of the data (Grün et al., 2003b; Davies et al., 2006), e.g. the Poissonian nature or the exact spike counts. Date and colleagues proposed the method of spike dithering to generate surrogates which currently best meets the criterion to destroy the correlation between spike trains and simultaneously to maintain as many statistical properties of the data as possible (Date et al., 1998). The approach is to randomly re-place each spike within a small time window around its original position, thereby almost perfectly preserving the other statistical features of the single neuron data. Meanwhile, the method is in routinely use in the correlation analysis of neuronal spike trains (Abeles and Gat, 2001; Maldonado et al., 2005). Strategies have been developed to reduce the perturbation of the inter-spike interval statistics for moderate dithers (Davies et al., 2006; Gerstein, 2004).

However, it is not well understood how much dither is required to destroy the spike correlation, in particular if joint-spike events are allowed to have a temporal jitter. Here we study the decay rate of the number of coincidences as a function of the dither width and as a function of allowed temporal jitter of the coincidences. In particular we answer the question to which degree coincidences are destroyed, if the dither width corresponds

to the allowed temporal jitter of the joint-spike events. Intuition says that coincidences should then be reduced by 50%. This needs to be analyzed in the context of the chosen method of coincidence detection since it critically influences the result: we concentrate on the disjunct binning method (DB) and the multiple shift method (MS) of coincidence detection (Grün et al., 1999) (cf. Fig. 19 middle and bottom, respectively).

In the following we treat the two methods in two subsequent sections, in each of which we briefly introduce the respective method, and derive analytically the probability of detecting coincidences given originally precise coincidences as a function of dither and of the allowed coincidence width. The results section compares the two methods for the particular case of the applied dither being equal to the allowed coincidence width. We show that the probability of detection decays with increasing dither, however much faster for DB as compared to the MS method. We also compare to the case where only one spike train is dithered.

[8].2 Disjunct Binning

The original spike data are discretized into bins of width δ, such that the total duration T of the recording is divided into N bins ($T = \delta \cdot N$). Each bin is assumed to contain at most one spike. As a result the activity of each neuron is represented by a binary sequence (Fig. 19) of zeros (no spikes) and ones (spikes). We define coincident events (or simply coincidences) as the joint firing of the two neurons within a coincidence window of w bins, thereby allowing coincidences to have a certain temporal jitter. In order to detect the total number of coincident events, the DB method sections T into disjunct, adjacent time segments (coincidence windows) $W_k, k = 1, ..., \lceil N/w \rceil$ each containing w bins of width δ. With bins numbered from 1 to N, the first coincidence window W_1 is composed of bins $\{1, 2, ..., w\}$, the second W_2 of $\{w + 1, w + 2, ..., 2w\}$, and so on.

We assume the original coincidences (i.e., before dithering) to be perfectly synchronous joint-events, i.e., both neurons have a spike in the very same bin. Due to an applied dither in the range of $[-s, s]$ bins a spike may trespass the border of a coincidence window and fall into another coincidence window. The *dither factor* $D = \lceil \frac{s}{w} \rceil$, i.e., the next integer larger than (or equal to) $\frac{s}{w}$, defines in how many coincidence windows the spike may fall and thus how many borders it might cross.

Next we are interested in the probability to detect a coincidence after dithering. The result depends on whether dithering is applied to both neurons (*2-neuron dithering*) or only one neuron (*1-neuron dithering*). The approaches are treated separately in the next two sections.

[8].2.1 2-neuron dithering

In 2-neuron dithering each spike of both spikes trains is randomly displaced in the range of $[-s, s]$ bins with uniform probability.

In order to calculate the probability that a coincidence after dithering is still detected as a coincidence, we need to consider all coincidence windows W_k into which the dithered spikes may be scattered. The number of windows is given by the dither factor D. If we assume the original coincidence to be in window W_0, spikes may be dithered into

coincidence windows W_k with $k = 0, \pm1, \pm2, ..., \pm D$. Therefore, the probability is the sum of the probabilities that the spikes fall into the same window W_k.

The probability to detect a coincidence within a particular coincidence window W_k depends on the number of bins that may be reached from the original coincidence position given a particular dither s. The probability to fall in a single bin δ within the dither interval $[-s, +s]$ is $1/(2s+1)$. Depending on the initial position $\alpha = 1, 2, ..., w$ of a spike in the coincidence window, a different number of bins is reachable in the surrounding coincidence windows. In the coincidence windows where all w bins can be reached ($k \in [-D+2, \ldots, D-2]$), the probability of a spike to fall into the window is $\Delta w_k^\alpha \cdot \frac{1}{2s+1}$, with $\Delta w_k^\alpha = w$. In the remote windows $\{W_{-D}, W_{-D+1}, W_{D-1}, W_D\}$, the probability corresponds to the number of reachable bins, i.e., $\Delta w_{k'}^\alpha \cdot \frac{1}{(2s+1)}$ with $k' = -D, -D+1, D-1, D$, respectively.

Because the two coincident spikes are dithered independently, the joint probability of both spikes being in window W_k is the product of the probabilities ($\Delta w_k^\alpha \cdot \frac{1}{2s+1}$) for the individual spikes. Then the total probability to detect the coincidence after dithering is given by the sum of the joint probabilities across all reachable coincidence windows:

$$P_\alpha^{[2-\mathrm{n}]}(w, s) = \sum_{k=-D}^{k=D} \left(\frac{\Delta w_k^\alpha}{2s+1} \right)^2 . \tag{8.1}$$

The closure relation is given by the condition that the total dither involves $2s+1$ bins:

$$\sum_{k=-D}^{k=D} \Delta w_k^\alpha = 2s+1 \quad \Rightarrow \quad \sum_{k=-D}^{k=D} \frac{\Delta w_k^\alpha}{2s+1} = 1 . \tag{8.2}$$

Fig. 20A,B show the coincidence detection probability $P_\alpha^{[2-\mathrm{n}]}(w, s)$ as a function of the initial position α of the spikes in the coincidence window, for different values of the dither s. Surprisingly, the probability of detection $P_\alpha^{[2-\mathrm{n}]}(w, s)$ depends on the distance of the initial coincidence from the borders of the coincidence window. For $s = w$ (Fig. 20A) the probability $P_\alpha^{[2-\mathrm{n}]}(w, s)$ reaches its minimum if the initial coincidence is in the center of the window, and is maximal when the initial coincidence is just at the window border. This counterintuitive result holds true for all values of w. However, it can be understood by considering that if spikes were originally in the proximity of the border of the coincidence window the number of destination windows is generally smaller than for originally centered spikes. As a consequence, spikes fall in larger stretches of successive bins, and thus the probability for the fission of coincidences by the borders of the coincidence windows is reduced. The total probability $P_\alpha^{[2-\mathrm{n}]}(w, s)$, which is constrained by Eq. 8.2, is maximized if few increments Δw_k^α are large and is minimal if all increments have intermediate values. In other words, the number of ways of arranging the two spikes in a destination window increases quadratically with the number of involved bins (cf. Eq. 8.1), hence the α-dependance observed in Fig. 20A.

As shown in Fig. 20B, the overall probability $P_\alpha^{[2-\mathrm{n}]}(w, s)$ progressively increases with decreasing s from $s > w$ to $s < w$, shown here for a fixed w. For decreasing s the spikes have a decreasing chance to trespass the window border and to escape from their original window. In extreme, for $s \ll w$ the spikes may not reach any other windows and thus

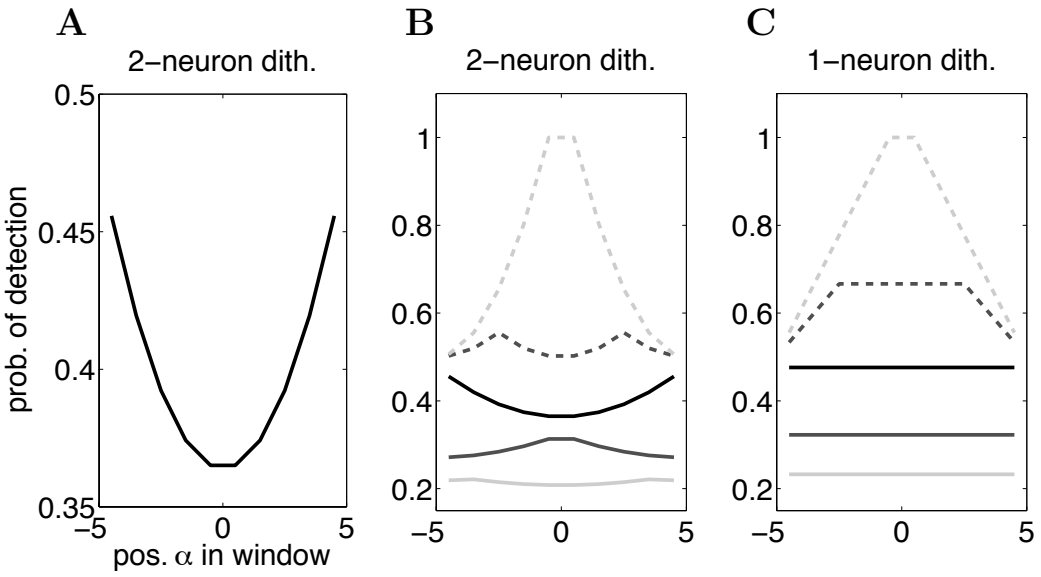

Figure 20: Probability of detecting coincidences after dithering for DB as a function of the position α of the original coincidences measured from the center of the coincidence window W_0. A,B: For 2-neuron dithering. C: For 1-neuron dithering. Black curves: case $w = s$ (enlarged ordinate in A), solid grey curves: $w < s$, dashed grey curves: $w > s$. Parameter values: $w = 10$, $s = 15$ (solid, dark grey), $s = 21$ (solid, light grey), $s = 7$ (dashed, dark grey), and $s = 4$ (dashed, light grey).

stay coincident. In contrast, for $s > w$ the coincidence has an increasing probability to be destroyed because of the large number of potential destination windows. The probability $P_\alpha^{[2-\mathrm{n}]}(w, s)$ shows different shapes depending on the exact relationship between s and w.

[8].2.2 1-neuron dithering

In case only the spikes of one spike train are dithered (e.g. only the spikes of neuron 2, (Hatsopoulos et al., 2003)) the probability of detecting the coincidences after dithering only depends on the new positions of the spikes of train 2. This method leads to a total probability

$$P_\alpha^{[1-\mathrm{n}]}(w, s) = \begin{cases} w/(2s+1) & \text{if } s \geq w-1 \\ \Delta w_k^\alpha/(2s+1) & \text{if } s < w-1\,, \end{cases} \tag{8.3}$$

where we assumed the initial coincidence window to be W_k and Δw_k^α to be the associated number of bins reachable by a spike from neuron 2. Again, this number depends on the initial position α of the spike.

For $s \geq w - 1$ both sides of the dither window $[-s, s]$ are larger than the coincident window W_k and thus the probability for the two original spikes to stay coincident after dithering depends on the probability for the dithered spike to stay in that window. Its probability is given by the number of bins in the window w relative to the total number of possible bins, i.e., $2s + 1$, the spike may be dithered into (upper relation in Eq. 8.3). This obviously does not depend on the initial position α of the coincidence.

If both sides of the dither window are smaller than the coincident window ($s < w-1$), only a fraction of the bins may receive a spike after dithering and depends on the original position α of the spike (Fig. 20C). For $s < w-1$ the probability of detecting the coincidence

after dithering increases progressively as s decreases, with a maximum at the central bins of the window. The maximal detection probability $w/(2s+1)$ is attained if the whole dither window $[-s, s]$ is included in the coincidence window W_k.

[8].3 Multiple Shift

This method provides a different way of counting coincident spikes of two neurons, avoiding the arbitrarily located "hard" borders. The multiple shift method defines a maximum allowed shift b. Assuming again the spike trains to have resolution δ, the procedure begins with counting all precise coincidences. Then spike train 2 is shifted with respect to spike train 1 by δ and again all precise coincidences are counted. The procedure continues for all positive shifts $2\delta, 3\delta, .., b\delta$ and for the negative shifts $-\delta, -2\delta, ..., -b\delta$. Consequently, spikes with a distance of up to $\pm b$ bins are counted as coincident. The parameter b is analogous to the coincident width w, however with the substantial difference that there are no fixed borders and the initial position of the coincidence α is meaningless.

Consider both spikes constituting a coincidence to be dithered in the range $\pm s$ and the origin of the temporal axis to be located at the position of the initial coincidence. After dithering the probability to find spike 2 at distance k from spike 1 is given by the probability to find 1 at i times the probability to find 2 at $k+i$ summed over all possible positions i:

$$J(k,s) = \frac{1}{2s+1} \sum_{i=-s}^{s} p(k+i) \; . \tag{8.4}$$

However, $p(k+i)$ is subject to further constraints. If e.g. spike 1 is at $-s$, spike 2 can only be coincident or to the right of spike 1, requiring $p(k-s)$ to vanish for negative k. Therefore, the effective limits of the sum also depend on k, collapsing Eq. 8.4 to

$$J(k,s) = \begin{cases} 1/(2s+1) & \text{for } k = 0 \\ \frac{2s+1-|k|}{(2s+1)^2} & \text{for } |k| \leq 2s \\ 0 & \text{for } |k| > 2s \; . \end{cases} \tag{8.5}$$

The probability of dithering two initially coincident spikes to a distance $|k|$ reaches its maximum at zero offset and decreases linearly with $|k|$ before it drops to zero at $\pm 2s$.

In the MS method all spikes dithered up to a distance $k = \pm b$ are classified as coincident. To obtain the probability to detect an initially coincident event after dithering $P^{[\mathrm{MS}]}(b,s)$ we have to sum the probabilities $J(k,s)$ of all possible dithering results for k in the range $-b, ..., b$

$$\begin{aligned} P^{[\mathrm{MS}]}(b,s) &= \begin{cases} 1/(2s+1) & \text{for } b = 0 \\ \frac{1}{2s+1} + \sum_{k=-b}^{b} \frac{2s+1-|k|}{(2s+1)^2} & \text{for } b \leq 2s \\ 1 & \text{for } b > 2s \end{cases} \\ &= \begin{cases} \frac{2b+1}{2s+1} - \frac{b(b+1)}{(2s+1)^2} & \text{for } b \leq 2s \\ 1 & \text{for } b > 2s \; . \end{cases} \end{aligned} \tag{8.6}$$

[8].4 Results

In this section we will derive the expected probability of detecting a coincidence after dithering given a large number of coincidences occurring in the spike trains at random times.

In the disjunct binning framework the assumption of many coincidences occurring at random times implies that the original coincident events will cover, in expectation, all possible initial positions $\alpha \in [1, ..., w]$. Therefore we have to average the results of Secs. [8].2.1 and [8].2.2 (Eqs. 8.1, 8.3) over α. For 2-neuron dithering this yields

$$\langle P_\alpha^{[2-\mathrm{n}]}(w,s)\rangle_\alpha \;=\; \frac{1}{w}\sum_{\alpha=1}^{w}\sum_{k=-D}^{k=D}\left(\frac{\Delta w_k^\alpha}{2s+1}\right)^2 . \tag{8.7}$$

Using similar arguments we derive the expected probability for the case of DB after 1-neuron dithering utilizing Eq. 8.3:

$$\langle P_\alpha^{[1-\mathrm{n}]}(w,s)\rangle_\alpha = \begin{cases} w/(2s+1) & \text{if } s \geq w-1 \\ \Delta w_k^\alpha/(2s+1) & \text{if } s < w-1\,, \end{cases} \tag{8.8}$$

whereas in the case of the MS method there is no α-dependence of the probability. For convenience however we also rewrite Eq. 8.6:

$$\langle P^{[\mathrm{MS}]}(b,s)\rangle = \begin{cases} \frac{2b+1}{2s+1} - \frac{b(b+1)}{(2s+1)^2} & \text{for } b \leq 2s \\ 1 & \text{for } b > 2s\,. \end{cases} \tag{8.9}$$

Fig. 21A shows $\langle P_\alpha^{[2-\mathrm{n}]}(w,s)\rangle_\alpha$, $\langle P_\alpha^{[1-\mathrm{n}]}(w,s)\rangle_\alpha$ and $\langle P^{[\mathrm{MS}]}(b,s)\rangle$ as functions of the dither s and for three different values of allowed coincidence width. The expected probability declines with increasing dither in all cases. Detecting only precise coincidences ($w = 1$ or $b = 0$, respectively) the dither has a strong effect and destroys coincidences already at small values of s.

With increasing coincidence width the different cases deviate from each other, the 2-neuron dithering being the more effective way of destroying coincidences. For $w = b = 10$ the 2-neuron dithering destroys about 80% of the original coincidences for dither values of about $s = 20$. In this situation, the 1-neuron dithering leads to similar but slightly higher probabilities of detection, whereas for a similar loss of detected coincidences with the MS method a dither of about $s = 50$ is required.

Let us now investigate the special case in which the dither equals the coincidence width, i.e., $s = w$, in order to obtain closed form expressions and limits. For the 2-neuron dithering setting $w = s$ and dither factor $D = 1$ reduces Eq. 8.7 to

$$\begin{aligned} \langle P_\alpha^{[2-\mathrm{n}]}(w=s)\rangle_\alpha &= \frac{1}{w}\sum_{\alpha=1}^{w}\sum_{k=-1}^{k=1}\left(\frac{\Delta w_k^\alpha}{2s+1}\right)^2 \\ &= \frac{1}{3} + \frac{s(s-1)}{3(2s+1)^2}\,. \end{aligned} \tag{8.10}$$

For non-zero values of dithering Eq. 8.10 assumes values between 1/3 (for $s, w = 1$) and $\frac{1}{3} + \frac{1}{12}$ (for $s, w \gg 1$), that is $\frac{1}{3} \leq \langle P_\alpha^{[2-\mathrm{n}]}(w=s)\rangle_\alpha < 0.41\bar{6} = P_{\mathrm{lim}}^{[2-\mathrm{n}]}$. Therefore $P_{\mathrm{lim}}^{[2-\mathrm{n}]}$ is

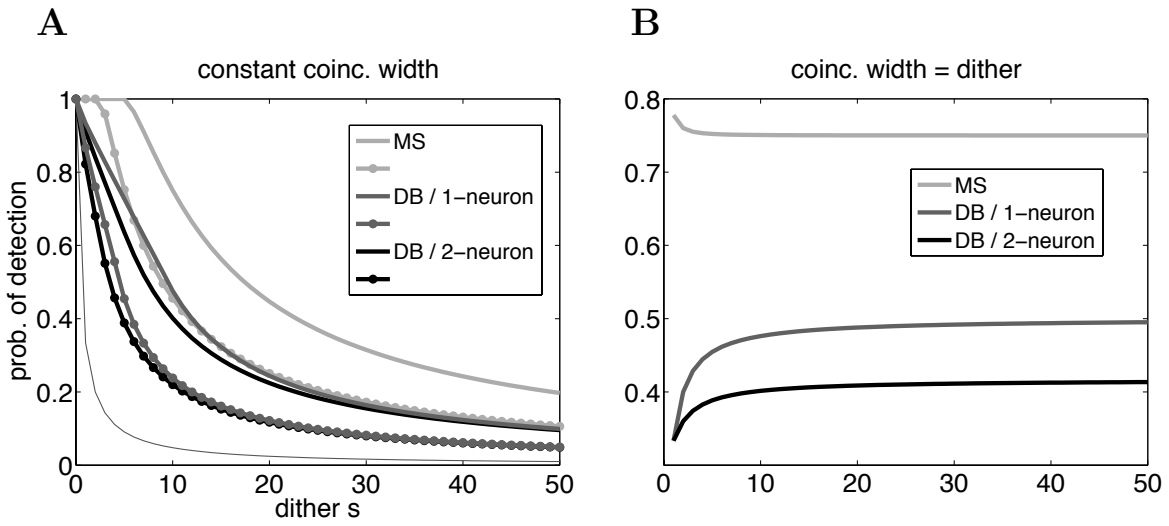

Figure 21: Expected probability of detecting coincidences with DB and MS as a function of dither range. $\langle P^{[\mathrm{MS}]}(b,s)\rangle$ (light grey), $\langle P_\alpha^{[1-\mathrm{n}]}(w,s)\rangle_\alpha$ (dark grey), $\langle P_\alpha^{[2-\mathrm{n}]}(w,s)\rangle_\alpha$ (black). A: Three values of constant coincidence width. Thin curve: $b=0, w=1$ (MS and 1-/2-neuron, respectively), thick curves with knobs: $w=b=5$, thick curves: $w=b=10$. B: Bounds for coincidence width corresponding to dither width, $w=s$ and $b=s$ respectively.

the maximum probability of detecting a 2-neuron dithered coincidence with the disjunct binning method when the dither equals the coincidence width.

For 1-neuron dithering Eq. 8.8 with $w=s$ is just

$$\langle P_\alpha^{[1-\mathrm{n}]}(w=s)\rangle_\alpha = \frac{s}{2s+1}\ , \tag{8.11}$$

where the probability is larger than $1/3$ $(s, w=1)$ and tends to $P_{\mathrm{lim}}^{[1-\mathrm{n}]}=0.5$ for $s, w \gg 1$.

Finally for the MS method replacing $b=s$ in Eq. 8.9 yields

$$\langle P^{[\mathrm{MS}]}(b=s)\rangle = 1 - \frac{s(s+1)}{(2s+1)^2}\ , \tag{8.12}$$

bounded between $1-2/9=0.\bar{7}$ $(b, w=1)$ and $P_{\mathrm{lim}}^{[\mathrm{MS}]}=0.75$ (for $b, s \gg 1$), the difference being only about 4%. The above results are visualized in Fig. 21B.

[8].5 Discussion

In this contribution we have rigorously analyzed the effectiveness of 2-neuron dithering for the disjunct binning and the multiple shift detection methods and for comparison also 1-neuron dithering for DB. The analysis is restricted to precise coincidences. Further studies are required to investigate the biologically more relevant case of jittered (i.e., imprecise) coincidences (Grün et al., 1999), the presence of background activity, and processes with a biologically realistic inter-spike interval statistics (Davies et al., 2006). Nevertheless, the present study provides detailed new insight in the dithering process. After uniform 2-neuron dithering of coincident spikes, the distribution of spike distances $|k|$ is not uniform,

favoring the survival of coincidences. Furthermore, in DB the probability of detection after dithering depends on the initial location of the coincidence in a complex manner.

We provide analytic expressions for the expected probability of detection in the different scenarios. In DB and MS the expressions reduce to simple closed forms for $w = s$ and $b = s$, respectively. Under these constraints we obtain in the limit $s \to \infty$ the bounds $P_{\text{lim}}^{[2-\text{n}]} = 0.41\overline{6}$, $P_{\text{lim}}^{[1-\text{n}]} = 0.5$, and $P_{\text{lim}}^{[MS]} = 0.75$. These asymptotic values are monotonically approached. Thus, for 1-neuron dithering analyzed by DB the intuition that a dither width equal to the coincidence window destroys 50% of the coincidences is confirmed. For 2-neuron dithering the rate of destruction is slightly larger. Counter to intuition, for MS the effect is much less pronounced. At $b = s$ still 3/4 of the coincidences survive. For example, with $b = 10$ and $s = 50$ the probability of detection still is at $P^{[MS]}(b, s) \simeq 0.2$. Thus, for detection methods like MS which essentially evaluate the central peak of the cross-correlation, a dither width much larger than the detection window is required to destroy a relevant fraction of the coincidences.

Acknowledgements.

We enjoyed inspiring discussions with George Gerstein during his stay in our laboratory at RIKEN BSI. Partially funded by BMBF Grant 01GQ0413 to the BCCN Berlin, the Stifterverband für die deutsche Wissenschaft, DIP F1.2, and EU Grant 15879 (FACETS).

Acknowledgments

I would like to thank Prof. Kurths for having been the supervisor of my PhD. He has always been extremely friendly and helpful with me during these years. But above all he has always found some time for me, despite all things that keep him busy. I appreciated.

My great gratitude goes to Sonja Grün. I was happy to accompany her in the great and adventurous journey from the "Villa" to Wako-shi. Now she has a big nice group, but I remember with a lot of pleasure also our *tête-à-tête* for lunch during my first months in Berlin. Sonja has always believed in me (I remember the first time she told me: "Look, of COURSE this is a result!"), and I feel we built up over the time a relationship based on trust and respect. But most of all, she showed me what doing science really means.

I would like to thank also the other people I have had the pleasure to work with.
Markus Diesmann for his laptop, the nice discussions, and having written the quickest paper ever.
Benjamin "Kapaiko" Staude for the cross-correlations between Berlin and Tokyo, Werder and AS Roma, a garden on the river and a balcony on the cherry trees.
Michael "Hello Kitty" Denker for keeping me in phase with a beer at the party and a computer tip.
Martin "tiefgefrorene-Pizza" Nawrot for the crucial help with the german, and for being louder than I in the lab.
And Clemens Boucsein, Stefan Rotter, "The Potjansen", Abigail Morrison, Saskia....

It would be too long to thank all the other people that supported me during these years in Rome, Berlin, and even Tokyo. I just thank all of them.

A special acknowledgment goes to Denise, who is here next to me.

Finally, all this wouldn't be worth it without Massimo, Rita, Allegra and the newcomers Lucetta and Pietrino. I'm proud to have made it also for you.

References

Abeles M (1991) Corticonics: Neural Circuits of the Cerebral Cortex. 1st edn., Cambridge University Press, Cambridge.

Abeles M, Gat I (2001) Detecting precise firing sequences in experimental data. J Neurosci Methods 107(1–2): 141–154.

Aertsen AM, Gerstein GL, Habib MK, Palm G (1989) Dynamics of neuronal firing correlation: modulation of "effective connectivity". J Neurophysiol 61(5): 900–917.

Bar-Gad I, Heimer G, Ritov Y, Bergman H (2003) Functional correlations between neighboring neurons in the primate globus pallidus are weak or nonexistent. J Neurosci 23(10): 4012–4016.

Bar-Gad I, Ritov Y, Bergman H (2001a) The neuronal refractory period causes a short-term peak in the autocorrelation function. J Neurosci Methods 104(2): 155–63.

Bar-Gad I, Ritov Y, Vaadia E, Bergman H (2001b) Failure in identification of overlapping spikes from multiple neuron activity causes artificial correlations. J Neurosci Methods 107(1-2): 1–13.

Bar-Hillel A, Spiro A, Stark E (2006) Spike sorting: Bayesian clustering of non-stationary data. J Neurosci Methods 157(2): 303–316.

Bedenbaugh P, Gerstein GL (1997) Multiunit normalized cross correlation differs from the average single-unit normalized correlation. Neural Comput 9(6): 1265–1275.

Brillinger DR (1988) Maximum likelihood analysis of spike trains of interacting nerve cells. Biol Cybern 59(3): 189–200.

Brody C (1998) Slow covariations in neuronal resting potential can artefactually fast cross-correlations in the spike trains. J Neurophysiol 80: 3345–3351.

Brown EN, Kass RE, Mitra PP (2004) Multiple neural spike train data analysis: state-of-the-art and future challenges. Nat Neurosci 7(5): 456–461.

Buzsáki G (2004) Large-scale recording of neuronal ensembles. Nat Neurosci 7(5): 446–451.

Buzsáki G, Draguhn A (2004) Neuronal oscillations in cortical networks. Science 304(5679): 1926–1929.

Câteau H, Reyes AD (2006) Relation between single neuron and population spiking statistics and effects on network activity. Phys Rev Lett 96(5): 058101.

Cox D (1962) Renewal theory. Science paperbacks.

Cox D, Lewis P (1966) The Statistical Analysis of Series of Events. London: Chapman and Hall.

Daley D, Vere-Jones D (2003) An Introduction to the Theory of Point Processes. Springer.

Date A, Bienenstock E, Geman S (1998) On the temporal resolution of neural activity. Tech. rep., Divison of Applied Mathematics, Brown University.

Davies RM, Gerstein GL, Baker SN (2006) Measurement of time-dependent changes in the irregularity of neuronal spiking. J Neurophysiol 96: 906–918.

Dayan P, Abbott L (2001) Theoretical Neuroscience. The MIT Press, Cambridge, Massachusetts London, England.

Efron B, Tibshirami RJ (1993) An Introduction to the Bootstrap. Chapman & Hall/CRC.

Eggermont JJ (1990) The Correlative Brain, vol. 16 of Studies of Brain Function. Springer-Verlag, Berlin.

Engel AK, Fries P, Singer W (2001) Dynamic predictions: oscillations and synchrony in top-down processing. Nat Rev Neurosci 2(10): 704–716.

Fano M (1947) Active stabilization of electrodes for intracellular recording in awake behaving animals. Neuron 27: 461–468.

Fee MS, Mitra PP, Kleinfeld D (1996) Variability of extracellular spike waveforms of cortical neurons. J Neurophysiol 76(6): 3823–3833.

Georgopoulos AP, Schwartz AB, Kettner RE (1986) Neuronal population coding of movement direction. Science 233(4771): 1416–1419.

Gerstein GL (2000) Cross-correlation measures of unresolved multi-neuron recordings. J Neurosci Methods 100(1-2): 41–51.

Gerstein GL (2004) Searching for significance in spatio-temporal firing patterns. Acta Neurobiol Exp (Wars) 64(2): 203–207.

Gerstein GL, Bedenbaugh P, Aertsen MH (1989) Neuronal assemblies. IEEE Trans Biomed Eng 36(1): 4–14.

Grün S, Diesmann M, Aertsen A (2002a) Unitary events in multiple single-neuron spiking activity: I. Detection and significance. Neural Comput 14(1): 43–80.

Grün S, Diesmann M, Aertsen A (2002b) Unitary events in multiple single-neuron spiking activity: II. Nonstationary data. Neural Comput 14(1): 81–119.

Grün S, Diesmann M, Grammont F, Riehle A, Aertsen A (1999) Detecting unitary events without discretization of time. J Neurosci Methods 94(1): 67–79.

Grün S, Riehle A, Aertsen A, Diesmann M (2003a) Temporal scales of cortical interactions. Nova Acta Leopoldina NF88, Nr. 332: 189–206.

Grün S, Riehle A, Diesmann M (2003b) Effect of cross-trial nonstationarity on joint-spike events. Biol Cybern 88(5): 335–351.

Harris K, Henze D, Csicsvari J, Hirase H, Buzsáki G (2000) Accuracy of tetrode spike separation as determined by simultaneous intracellular and extracellular measurements. J Neurophysiol 84(1): 401–414.

Harris KD (2005) Neural signatures of cell assembly organization. Nat Rev Neurosci 6(5): 399–407.

Hatsopoulos N, Geman S, Amarasingham A, Bienenstock E (2003) At what time scale does the nervous system operate? Neurocomputing 52-54(52–54): 25–29.

Hazan L, Zugaro M, Buzsáki G (2006) Klusters, NeuroScope, NDManager: a free software suite for neurophysiological data processing and visualization. J Neurosci Methods 155(2): 207–216.

Hebb DO (1949) Organization of behavior. A neurophysiological theory. John Wiley & Sons, New York.

Horton PM, Nicol AU, Kendrick KM, Feng JF (2007) Spike sorting based upon machine learning algorithms (soma). J Neurosci Methods 160(1): 52–68.

Hubel DH, Wiesel TN (1968) Receptive fields and functional architecture of monkey striate cortex. J Physiol 195(1): 215–243.

Hyvärinen A, Oja E (2000) Independent component analysis: algorithms and applications. Neural Networks 13(4-5): 411–430.

Ikegaya Y, Aaron G, Cossart R, Aronov D, Lampl I, Ferster D, Yuste R (2004) Synfire chains and cortical songs: temporal modules of cortical activity. Science 5670(304): 559–564.

Kass RE, Ventura V (2001) A spike-train probability model. Neural Comput 13(8): 1713–1720.

Lewicki MS (1998) A review of methods for spike sorting: the detection and classification of neural action potentials. Network 9(4): R53–78.

Lindner B (2006) Superposition of many independent spike trains is generally not a poisson process. Phys Rev E Stat Nonlin Soft Matter Phys 73(2 Pt 1): 022901.

Maldonado P, Babul C, Singer W, Rodriguez E, Berger D, Grün S (2005) Dissociation between discharge rates and synchrony in primary visual cortex of monkeys viewing natural images, (Submitted).

Mountcastle VB (1957) Modality and topographic properties of single neurons of cat's somatic sensory cortex. J Neurophysiol 20(4): 408–434.

Nawrot MP (2003) Ongoing Activity in Cortical Networks: Noise, Variability and Context. Ph.D. thesis, Albert-Ludwigs-Universität Freiburg, Germany.

Nawrot MP, Boucsein C, Rodriguez Molina V, Riehle A, Aertsen A, Rotter S (2007) Measurement of variability dynamics in cortical spike trains. J Neurosci Methods doi:10.1016/j.jneumeth.2007.10.013.

Nowak LG, Munk MH, Nelson JI, James A, Bullier J (1995) Structural basis of cortical synchronization. i. three types of interhemispheric coupling. J Neurophysiol 74(6): 2379–2400.

Pazienti A, Grün S (2006) Robustness of the significance of spike synchrony with respect to sorting errors. J Comput Neurosci 21(3): 329–342.

Perkel DH, Gerstein GL, Moore GP (1967a) Neuronal spike trains and stochastic point processes. I. The single spike train. Biophys Journ 7(4): 391–418.

Perkel DH, Gerstein GL, Moore GP (1967b) Neuronal spike trains and stochastic point processes. II. Simultaneous spike trains. Biophys Journ 7(4): 419–440.

Pipa G (2001) Entwicklung und Untersuchung einer nicht-parametrischen Methode zur Schätzung der Signifikanz zeitlich koordinierter Spike-Aktivität. Diploma thesis, physics, J-W Goethe Univ, Frankfurt/M, Germany.

Pipa G (2006) The neuronal code: Development of tools and hypotheses for understanding the role of synchronization of neuronal activity. Ph.D. thesis, Technische Universität, Berlin.

Pipa G, Diesmann M, Grün S (2003) Significance of joint-spike events based on trial-shuffling by efficient combinatorial methods. Complexity 8(4): 79–86.

Pipa G, Grün S (2003) Non-parametric significance estimation of joint-spike events by shuffling and resampling. Neurocomputing 52-54: 31–37.

Pipa G, Riehle A, Grün S (2007) Validation of task-related excess of spike coincidences based on neuroxidence. Neurocomputing (in press).

Pouzat C, Delescluse M, Viot P, Diebolt J (2004) Improved spike-sorting by modeling firing statistics and burst-dependent spike amplitude attenuation: a Markov chain Monte Carlo approach. J Neurophysiol 91(6): 2910–2928.

Pouzat C, Mazor O, Laurent G (2002) Using noise signature to optimize spike-sorting and to assess neuronal classification quality. J Neurosci Methods 122(1): 43–57.

Quian Quiroga R, Nadasdy Z, Ben-Shaul Y (2004) Unsupervised spike detection and sorting with wavelets and superparamagnetic clustering. Neural Comput 16(8): 1661–1687.

Quirk MC, Wilson MA (1999) Interaction between spike waveform classification and temporal sequence detection. J Neurosci Methods 94(1): 41–52.

Reich DS, Mechler F, Victor JD (2001) Independent and redundant information in nearby cortical neurons. Science 294(5551): 2566–2568.

Riehle A, Grammont F, Diesmann M, Grün S (2000) Dynamical changes and temporal precision of synchronized spiking activity in monkey motor cortex during movement preparation. J Physiol Paris 94(5-6): 569–582.

Riehle A, Grün S, Diesmann M, Aertsen A (1997) Spike synchronization and rate modulation differentially involved in motor cortical function. Science 278(5345): 1950–1953.

Schmitzer-Torbert N, Jackson J, Henze D, Harris K, Redish AD (2005) Quantitative measures of cluster quality for use in extracellular recordings. Neuroscience 131(1): 1–11.

Shadlen MN, Movshon JA (1999) Synchrony unbound: a critical evaluation of the temporal binding hypothesis. Neuron 24(1): 67–77, 111–25.

Singer W, Engel AK, Kreiter AK, Munk MHJ, Neuenschwander S, Roelfsema PR (1997) Neuronal assemblies: necessity, signature and detectability. Trends in Cognitive Sciences 1(7): 252–261.

Smith LS, Mtetwa N (2007) A tool for synthesizing spike trains with realistic interference. J Neurosci Methods 159(1): 170–180.

Takahashi S, Anzai Y, Sakurai Y (2003a) Automatic sorting for multi-neuronal activity recorded with tetrodes in the presence of overlapping spikes. J Neurophysiol 89(4): 2245–2258.

Takahashi S, Anzai Y, Sakurai Y (2003b) A new approach to spike sorting for multi-neuronal activities recorded with a tetrode–how ICA can be practical. Neurosci Res 46(3): 265–272.

Takahashi S, Sakurai Y, Tsukada M, Anzai Y (2002) Classification of neuronal activities from tetrode recordings using independent component analysis. Neurocomputing 49(1-4): 289–298.

Vaadia E, Haalman I, Abeles M, Bergman H, Prut Y, Slovin H, Aertsen A (1995) Dynamics of neuronal interactions in monkey cortex in relation to behavioural events. Nature 373(6514): 515–518.

Ventura V, Cai C, Kass RE (2005) Statistical assessment of time-varying dependency between two neurons. J Neurophysiol 94(4): 2940–2947.

von der Malsburg C (1981) The correlation theory of brain function. Internal report 81-2, Max-Planck-Institute for Biophysical Chemistry, Göttingen, FRG.

Wang GL, Zhou Y, Chen AH, Zhang PM, Liang PJ (2006) A robust method for spike sorting with automatic overlap decomposition. IEEE Trans Biomed Eng 53(6): 1195–1198.

Wehr M, Pezaris JS, Sahani M (1999) Simultaneous paired intracellular and tetrode recordings for evaluating the performance of spike sorting algorithms. Neurocomputing 26-27: 1061–1068.

Wood F, Black MJ, Vargas-Irwin C, Fellows M, Donoghue JP (2004) On the variability of manual spike sorting. IEEE Trans Biomed Eng 51(6): 912–918.

Zhang PM, Wu JY, Zhou Y, Liang PJ, Yuan JQ (2004) Spike sorting based on automatic template reconstruction with a partial solution to the overlapping problem. J Neurosci Methods 135(1-2): 55–65.